UNIVERSITA' DEGLI STUDI DI PADOVA

DEPARTMENT OF INDUSTRIAL ENGINEERING DII

Master's Degree in Energy Engineering

"*Assessment of Utility-scale Hybrid Systems, based on Wind and PV plants, and mapping of potential installation sites in Spain*"

Supervisor:

Prof.ssa Anna Stoppato

Traineeship Tutors:

Dr. Javier Dominguez

Luis Arribas

Candidate:

Michael Borsato

Student ID 2045261

Academic Year

2023/2024

Abstract

In a global context characterized by a rapid shift from an energy production based mainly on fossil fuels to the exploitation of renewable energy sources, interest in hybrid systems based on wind and PV plants has arisen, thanks to their benefits concerning cost reduction and improvement of the generation profile. Along with this increasing interest, a proper assessment of suitable sites for hybrid systems installation is necessary for the optimal utilization of renewable sources. In this thesis, to perform an assessment of co-located utility-scale PV-Wind hybrid plants in Spain, a map of suitability is created; to build it, an approach based on Geographic Information Systems (GIS), relying on Boolean and Fuzzy Logic, is employed using a GIS software. Then, a model for the evaluation of the profitability of a PV-Wind hybrid system is defined; this model is based on identifying the optimal capacity of a PV-Wind hybrid plant in a single site and on evaluating its Internal Rate of Return (IRR). Finally, a map of profitability in Spain for this type of system is created through the implementation of the model in a GIS software that allows to evaluate the IRR of every suitable site. The result is based on initial assumptions and on the values of the parameters employed in the model; this allows to perform a sensitivity analysis on the main parameters. The results indicate that 24% of the studied area in Spain is suitable for PV-Wind hybrid systems; in this suitable territory, the most profitable sites are located in northern regions such as Galicia and Aragon, and in some areas of Castile-Leon, Castile-La Mancha and Andalusia. Finally, the results of the sensitivity analysis show that, according to the implemented model, an increase in the electricity price set by a simple Power Purchase Agreement for the sale of energy corresponds to an increase in the IRR of the hybrid system that produces and sells the energy. At the same time, an increase in the evacuation capacity of the electrical grid connected to the plant leads to an increase in the hybrid system IRR and a reduction in the number of suitable sites.

Sommario

In un contesto globale caratterizzato da un rapido cambiamento dalla produzione energetica basata principalmente sui combustibili fossili allo sfruttamento delle fonti di energia rinnovabile, è sorto un interesse per i sistemi ibridi basati su impianti eolici e fotovoltaici, grazie ai loro benefici riguardanti la riduzione dei costi e il miglioramento del profilo di generazione. Insieme a questo crescente interesse, è necessaria una valutazione adeguata dei siti idonei per l'installazione di sistemi ibridi in modo da permettere un utilizzo ottimale delle fonti rinnovabili. In questa tesi, per eseguire una valutazione dei siti idonei per impianti ibridi fotovoltaico-eolici di scala industriale co-localizzati in Spagna, viene creata una mappa di idoneità; per costruirla, viene impiegato un approccio basato su Geographical Information Systems che utilizza la Boolean Logic e la Fuzzy Logic grazie a un software GIS. Successivamente, viene definito un modello per la valutazione della redditività di un sistema ibrido fotovoltaico-eolico; questo modello si basa sull'identificazione della capacità ottimale di un impianto ibrido fotovoltaico-eolico in un singolo sito e sulla valutazione del suo Tasso Interno di Rendimento (TIR). Infine, viene creata una mappa di redditività in Spagna per questo tipo di sistema, attraverso l'implementazione del modello in un software GIS che consente di valutare l'IRR di ogni sito idoneo. Il risultato si basa su ipotesi iniziali e sui valori dei parametri impiegati nel modello; ciò consente di effettuare un'analisi di sensibilità sui principali parametri. I risultati indicano che il 24% dell'area studiata in Spagna è idonea per sistemi ibridi eolico-fotovoltaico; in questo territorio idoneo, i siti più redditizi sono situati nelle regioni settentrionali come la Galizia e l'Aragona, e in alcune aree di Castiglia e León, Castiglia-La Mancia e Andalusia. Infine, i risultati dell'analisi di sensibilità mostrano che, secondo il modello implementato, un aumento del prezzo dell'elettricità fissato da un semplice Power Purchase Agreement per la vendita di energia corrisponde a un aumento del TIR del sistema ibrido che produce e vende l'energia. Allo stesso tempo, un aumento della capacità di evacuazione della rete elettrica collegata all'impianto porta a un aumento del TIR del sistema ibrido e a una riduzione del numero di siti idonei.

Table of contents

List of figures

List of tables

Nomenclature

Abbreviations

WTG – Wind Turbine Generator

MITECO - Ministerio para la Transición Ecológica y el Reto Demográfico

RES - Renewable Energy Sources

PV – Photovoltaic

HPP – Hybrid Power Plant

GIS – Geographical Information System

PoCs – Points of connections

MNRE - Ministry of New and Renewable Energy

AEE - Asociación Empresarial Eólica

AHP - Analytic Hierarchy Process

BWM - Best Worst Method

CIEMAT - Centro de Investigaciones Energéticas Medioambientales y Tecnológicas

WRF - Weather Research and Forecasting

IBA - Áreas Importantes para la Conservación de las Aves y la Biodiversidad en España

ZEPIM - Zonas Especialmente Protegidas de Importancia para el Mediterráneo

MaB - Reservas de la Biosfera

LIG - Lugares de Interés Geológico

MCDM - Multi-criteria decision making method

DEM - Digital Elevation Model

STC - Standard Condition

PPA – Power Purchase Agreement

NREL – National Renewable Energy Laboratory

IGN - Instituto Geográfico Nacional

IEA - Internation Energy Agency

NCAR - National Center for Atmospheric Research

EEA - European Enviroment Agency

Symbols

H - Global daily irradiation on a horizontal plane [kWh/m^2/day]

v - Wind speed at 100 m [m/s]

μ - Fuzzy membership function [-]

γ - Constant to define the type of operation performed by the fuzzy overlay [-]

PSH - Peak Sun Hours [h/day]

PR – Performance Ratio [-]

G_{stc} - Global Irradiance at Standard Condition [kW/m^2]

Y_f - Final PV system yield [kWh/kW]

Y_r - Reference yield [kWh/kW]

E_w - Wind turbine produced energy [GWh]

$P_{eol,max}$ - Maximum wind power installable in 1 km^2 [MW/km^2]

$P_{pv,max}$- Maximum PV power installable in 1 km^2 [MW/km^2]

P_{turb} - Power of a single turbine [MW]

E_{load} - Average energy consumption of a load [kWh/day]

PR_{load} – Performance ratio of a load [-]

DED - Daily Eolic Density [kWh/m^2/day]

η_{eol} - efficiency of the aerogenerator [-]

A_{eol} - Wind turbine swept area [m^2]

P_{pv} - Photovoltaic plant power [MW]

P_{eol} – Wind plant power [MW]

$E_{in,max}$ - Maximum energy injected in the grid [MW]

E_{in} – Energy injected in the grid [MWh/day]

$P_{in,max}$ – Maximum evacuation capacity of the grid [MW]

f - Fraction of energy effectively injected in the grid [%]

E_{prod} - Daily total energy production [MWh/day]

n - project life [years]

CAPEX - Capital Expenditures [M€]

OPEX - Operating Expense [M€]

LCOE – Levelized Cost of Electricity [€/MWh]

τ - Capital recovery factor [-]

r - Discount rate [%]

NPV – Net Present Value [M€]

C - Cash flow [M€]

R_{hyb} – Revenues [M€]

p – Energy price set by the PPA [€/MWh]

IRR - Internal Rate of Return [%]

1. Introduction

The energy sector is undergoing a rapid change from a production based mainly on fossil fuels to the exploitation of renewable energy sources (RES). At the COP28 climate change conference, held in Dubai, United Arab Emirates, in 2023, more than 130 national governments agreed to triple the world's installed renewable energy capacity by 2030, while under existing policies and market conditions, global renewable capacity is forecast to reach 7300 GW by 2028 [1]. In 2023, 473 GW of renewable power were added to the global energy mix, representing 87% of the new installed capacity, with solar energy accounting for 73% of this growth [2]. In 2022, wind and solar power generation amounted to a 12% share of the global total, and solar photovoltaic (PV) and wind are forecast to account for 95% of global renewable expansion by 2028, benefiting from lower generation costs than both fossil and non-fossil fuel alternatives [3]. Indeed, in 2023, spot prices for solar PV modules declined by almost 50% year-on-year, and an estimated 96% of newly installed, utility-scale solar PV and onshore wind capacity had lower generation costs than new coal and natural gas plants [1].

In this global context, an interest in hybrid power plants (HPP) has arisen. In particular, HPP composed of wind turbines and PV modules can represent a valuable future market [4], reflecting the growth in the capacity installed that these two technologies are expected to have in the near future. Hybrid systems, which can be composed also of energy technologies that differ from wind and PV plants, are characterized by benefits that can justify the research efforts, aimed at a profitable installation and operation of the plants themselves.

Focusing on the installation aspect, a consistent literature production related to the assessment of suitable sites for RES has flourished in the last decades, as demonstrated by the reviews performed in [5] and [6]; the main goal of this field of research is the identification of a reliable scientific method for detecting of sites where the properties of the territory, the presence of natural resources, and the accessibility to human infrastructure lead to renewable energy installations with the maximum profitability and the minimum environmental and social impact. This thesis fits in this research field, aiming to investigate a methodology to identify the most profitable sites on a defined territory for the

implementation of utility-scale PV-Wind Hybrid Systems, a technology that could represent an important share of the future new renewable energy installed capacity.

In this first chapter, a general definition of hybrid power plant is given; an overview of the state of the art of this kind of technology is presented, pointing out its main benefits and the context in which its development is carried out. In the second part of the introduction, the focus is set on the assessment of suitable RES installation sites, presenting the main concepts related to Geographic Information Systems (GIS) and examples of methodologies already investigated in the literature. Finally, the main goals of the thesis are stated.

1.1 PV-Wind Hybrid Power Plants – State of the art

A hybrid system is "a power-generating facility that converts primary energy into electrical energy" with "more than one power-generating module connected to a network at one connection point. These might also include different forms of energy storage" [4]. This definition can be associated with many types of configurations, including traditional energy systems working on fossil fuels, renewable energy sources, and storage technologies. Moreover, these systems can be utility-scale systems connected to the grid, or stand-alone systems, dedicated to self-consumption of energy; in the case of utility-scale systems, the plants can be installed onshore or offshore, as demonstrated by the case of the wind-wave system [7].

Due to the broadness of the definition, it is necessary to better specify the boundaries within which this research will work. According to the taxonomy proposed in [8] for Hybrid Power Plants, if different energy technologies are locationally linked, but their operations remain mainly independent, the HPP falls under the category of "co-located resources"; if an HPP consists of energy technologies coordinated in their operations, but not locationally linked, it falls under the category of "virtual power plant"; finally, if multiple energy technologies are both locationally and operationally linked, the HPP is included in the full hybrid category. This work will focus on full hybrid systems, composed only of two technologies: solar PV and wind systems. In particular, the considered system will be an onshore utility-scale one, with a capacity in the order of MW. In the following paragraphs, the different configurations that a PV-Wind HPP can present are analysed, along with its main benefits.

1.1.1 PV-Wind HPP configurations

Considering a PV-Wind Hybrid System, as stated in [9], different configurations to connect a wind plant, a PV plant and potentially a storage system can be employed, depending on the business case. Three common solutions for integration in a co-located HPP are:

a) Co-located HPP with individual point of connection solution.

   In this solution, all the technologies have individual Points of Connection (PoCs), but at the same time they are connected to the same substation, which serves as the interconnection point between HPP and external grid. To integrate each technology, a global plant controller is needed, so that the entire system can be considered as a single power plant from the grid perspective. Today's wind plant controllers already provide this capability. However, for a co-located HPP, they require more advanced functionalities to also accommodate solar PV and potentially a storage system alongside the wind turbines. Two schemes of the plant, with and without energy storage, are shown in *Figure 1.1*.
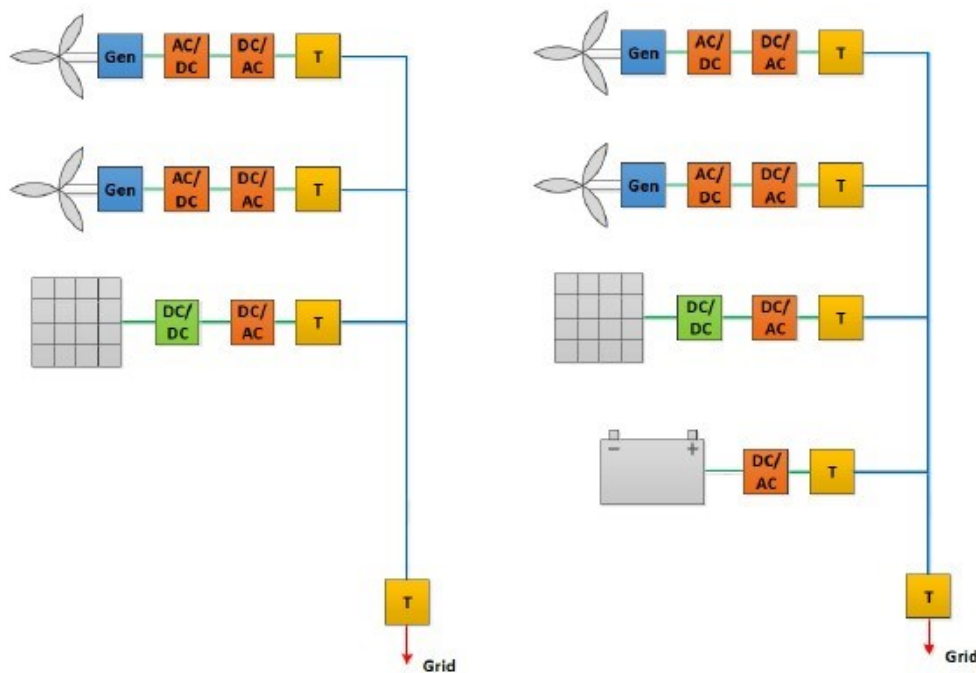
Figure 1.1 - Co-located HPP with individual point of connections solution, without (on the left) and with (on the right) energy storage [9].

b) Wind Turbine Generator (WTG)-coupled solution.

   A WTG-coupled system takes advantage of the existing conversion equipment inside the WTG. Several coupling options are possible. An example is a DC-coupled system, where all the technologies are connected to a common DC-link. This can be achieved by connecting the PV and the energy storage system to the

power converter of the WTG. In this system, the WTG controller needs to be capable of controlling both the PV and the energy storage, so that the entire system can be considered as a single generating plant from the grid perspective. Another example is a case of a power plant consisting of multiple WTG-coupled hybrid systems connected to an AC collector system; in this case, the global plant controller needs to consider the capabilities and functionalities of the individual technologies. Two schemes of the plant, with and without energy storage are shown in *Figure 1.2*.
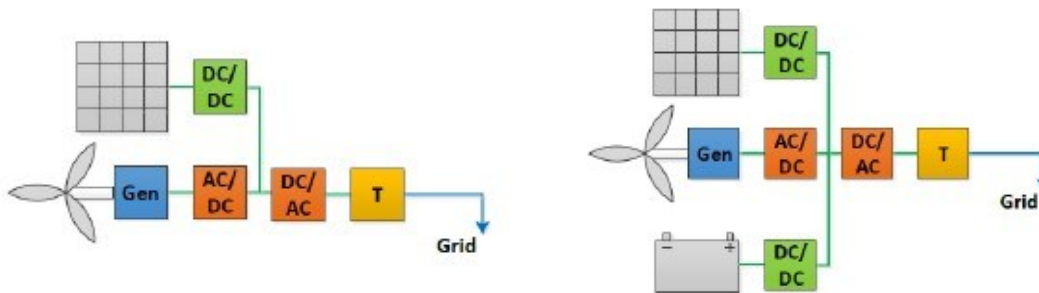
Figure 1.2 - Wind Turbine Generator (WTG)-coupled solution, without (on the left) and with (on the right) energy storage [9].

c) DC-coupled HPP solution.

In a DC-coupled system the collector system at grid level is based on DC technology. Indeed, the individual technologies are connected to a DC collector system. Different control schemes at plant level are required compared to traditionally AC connected plants. Moreover, additional grid components within the HPP need to be integrated into the plant controller. In the case of High Voltage AC connected systems, a grid-side DC/AC inverter represents the interface between plant and grid, while in High Voltage DC connected systems, a DC/DC converter is required to couple the plant with the grid. For larger High Voltage AC connected HPP, two variants of schemes are possible: AC aggregation, where several DC feeders are connected to the grid AC bus through individual DC/AC inverters; otherwise, DC aggregation where feeders are connected to a common DC bus and then converted to AC power through one large DC/AC inverter. The control schemes and functionalities of the plant controller depend on the selected topology. Four schemes of the plant, with a High Voltage AC connection or with a High Voltage DC connection, and with or without energy storage are shown in *Figure 1.3*.
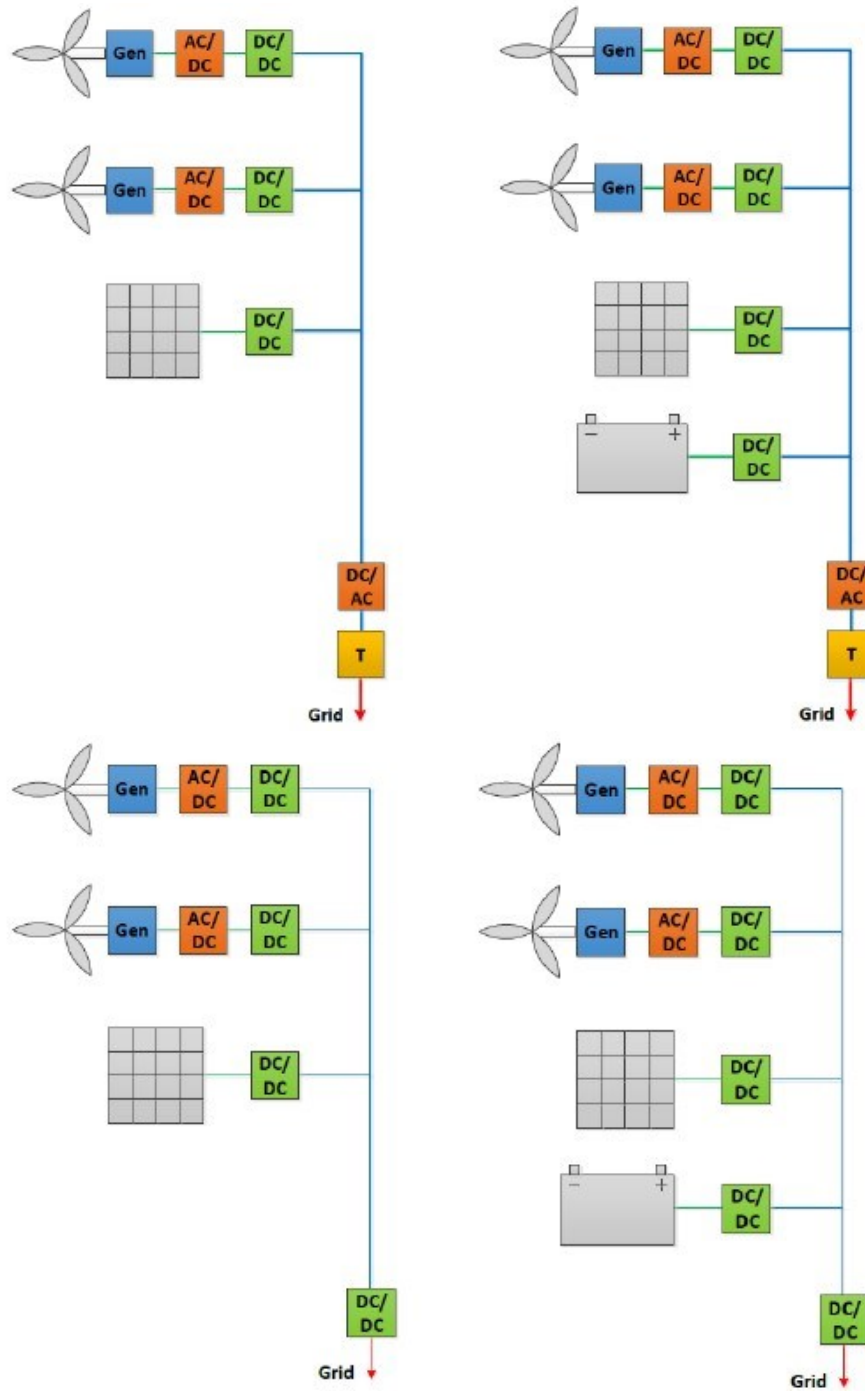
Figure 1.3 - DC-coupled HPP solution, with AC connection and without energy storage (top-left), with AC connection and energy storage (top-right), with DC connection and without energy storage (bottom-left), with DC connection and energy storage (bottom-right) [9].

A review on solar and wind power solutions, along with their challenges and opportunities, is presented in [10].

All the configurations presented offer benefits that justify their employment compared to a standalone PV or wind system; these advantages are discussed in the following paragraph.

1.1.2 PV-Wind Hybrid System benefits

The interest in HPP systems is due to their benefits; the main ones, investigated in [9] and in [11], are listed below:

a) Increased Annual Energy Production and capacity factor.
   Combining technologies with varying power generation patterns can improve the overall combined HPP capacity factor and increase the overall energy output, as demonstrated in [11]. Specifically, when combining PV and wind power production systems in regions with high diurnal or seasonal complementarity of wind and PV power, a higher degree of capacity is achievable in presence of grid connection limitations. An example of complementarity assessment between wind and photovoltaic generation is shown in [12]: the assessment is carried out in the Brazilian Northeast and demonstrates how this complementarity, together with energy storage technologies, can mitigate the shortcomings imposed by the intermittent nature of solar and wind energy sources.

b) Improvement of the utilization rate of the plant infrastructure.
   Similar to the previous case, the negative correlation of wind and solar resources leads to higher utilisation of the converter, transformer and connection capacity due to a higher number of full-load hours compared to a pure wind or solar installation.

c) Reduced power fluctuations and gradients.
   Merging wind and PV plants can attenuate their individual power fluctuations and decrease the gradient of the overall power plant output. In this way, the demand for energy storage systems is reduced and the grid requirement can be fulfilled with more simplified compensation equipment. Moreover, hybrid systems equipped with energy storage can act as grid stabilizers by supplying power during peak demand times, reducing grid congestion and enhancing overall stability.

d) Increase the predictability in the combined production.
   A more schedulable power dispatch can be achieved, contributing to meeting load demand even in areas where the power grid is too weak to provide reliable power supply. Overall, business case certainty is improved. Deviations from committed day-ahead forecasts can be reduced, along with associated penalties; the correlation between production and demand is improved.

e) CAPEX reduction.
   Combining wind and solar power enables an optimal utilization of their electrical infrastructure, reducing the cost of developing the HPP infrastructure itself. Further cost reductions can be achieved by installing storage systems and PV units in existing wind power plants; in this way, it is possible to reduce the land use, and to employ the same electrical infrastructure (converters, substation, grid connection) and public infrastructure (access roads). However, overplanting by adding new

generation and storage units to existing infrastructure can overload the point of common connection. To avoid this, a deep understanding of electrical infrastructure, site conditions, grid restrictions, and interdependencies between wind and solar capacity is necessary during HPP development.

f) OPEX reduction.

During their lifetime, wind and PV systems are subject to maintenance work that requires complete shutdowns for certain periods leading to power production losses. With energy storage systems, these operational costs can be reduced to some extent through optimized scheduling, allowing the HPP to deliver requested power despite shutdowns of wind or PV plants. Moreover, for PV, wind and energy storage systems a similar power electronic maintenance expertise is required; therefore, the maintenance can be performed by the same technicians, reducing the OPEX cost.

g) Increase in ancillary services capability.

The presence of batteries provides the opportunity to access new markets, facilitating additional revenue streams. In addition, with the decrease of subsidies for wind and solar, optimizing HPPs to participate in ancillary services markets becomes crucial for plant operators and developers. Examples include providing reactive power control, black start capability when storage is integrated, and voltage control services.

1.1.3 Worldwide PV-Wind Hybrid system projects

Worldwide various co-located PV-Wind Hybrid plants are already in operation; a database concerning PV-Wind HPPs, with or without storage systems, and wind systems in combination with storage can be found in [13]. In 2023, a total of fifteen PV-Wind HPPs are operational worldwide; five of them feature an energy storage system. In the following table, a list of the operational projects installed worldwide can be found:

Project	Wind capacity [MW]	Solar capacity [MW]	Storage capacity [MW]/[MWh]	Status
Minnesota, USA	2	0.50	0 / 0	Operational
Tacaratu, Pernambuco, Brazil	80	11	0 / 0	Operational
Bahia, Brazil	22	5	0 / 0	Operational
Antofagasta, Chile	0.03	0.21	0.25 / 0.80	Operational
Azores, Portugal	5	1	6 / 3.20	Operational
South West Wales, UK	4	4.95	0 / 0	Operational
Zaragoza, Spain	1	0.25	0.43 / 0.50	Operational
Albacete, Spain	2	1.12	0 / 0	Operational
Louzes. Greece	24	1	0 / 0	Operational
Tilos Island, Greece	1	0.16	0.80 / 2.40	Operational
Kavithal, Karnataka, India	50	28.80	0 / 0	Operational
Tamil Nadu, India	2	0.20	0 / 0	Operational
Coober Pedy, Australia	4	1	1 / 0.50	Operational
Southern Tablelands, Australia	166	10	0 / 0	Operational
New England Tablelands, Australia	175	20	0 / 0	Operational

Considering the plants in operation, as shown in *Table 1.1*, one has a summed capacity under 1 MW, seven have a capacity between 1 MW and 10 MW, five between 10 MW and 100 MW, two between 100 MW and 1000 MW and none over 1000 MW; therefore, most of the plants in operation have a capacity between 1 MW and 10 MW.

Concerning storage systems, out of all the plants only five HPP storage systems are operational; four of them have a capacity under 1 MW, while only one over 1 MW; two

storage systems can store more than 1 MWh, while the other three can store less than 1 MW.

In the future however, larger power plants are expected to be put into operation; some of the existent projects worldwide are shown in the table below:

Table 1.2 - List of PV-Wind hybrid existent projects worldwide (own elaboration based on data from [13]).

Project	Wind capacity [MW]	Solar capacity [MW]	Storage capacity [MW]/[MWh]	Status
Lexington, Oregon, USA	300	50	30 / 120	Contracted
Burgos, Spain	69	74	0 / 0	Under Commissioning [14]
Haringvliet, Netherlands	21	31	12 / -	Under Construction
Calabria, Italy	420	120	0 / 0	Under Development [15]
Agios Eustratios, Greece	1	0.10	0.72 / 3.60	Under Development
Megistis, Greece	1	0.86	1,44 / 7.20	Under licensing
Golmud, China	400	250	- / 100	Approved
Ramagiri, India	40	120	10	Approved
Andhra Pradesh, India	16	25	10 / 15	Contracted
Rajasthan, India	510	600	0 / 0	Contracted [16]
Gujarat, India	24.30	21.50	0 / 0	Contracted [17]
Cervantes, Australia	130	17.50	0 / 0	Under Development
Kondinin, Australia	120	50	- / -	Under feasibility study
Pilbara region, Australia	6000	5000	- / -	Under Development
Port Augusta, Australia	225	150	0 / 0	Under Development
Queensland, Australia	800	-	- / -	Under Feasibility Study

The majority of the upcoming plants in the list have a capacity in the range between 100 MW and 1000 MW. In addition, larger storage systems are expected to be developed.

Concerning the spatial distribution in the countries listed in *Table 1.1* and *Table 1.2*, as shown in *Figure 1.4*, Australia, Brazil and India represent the countries with the highest total capacity in operation, with projects having a combined of capacity of 377 MW, 118 MW and 81 MW, respectively. Australia and India, along with the USA and China, are among the most involved countries in the development of this type of systems, as shown in *Table 1.2*.
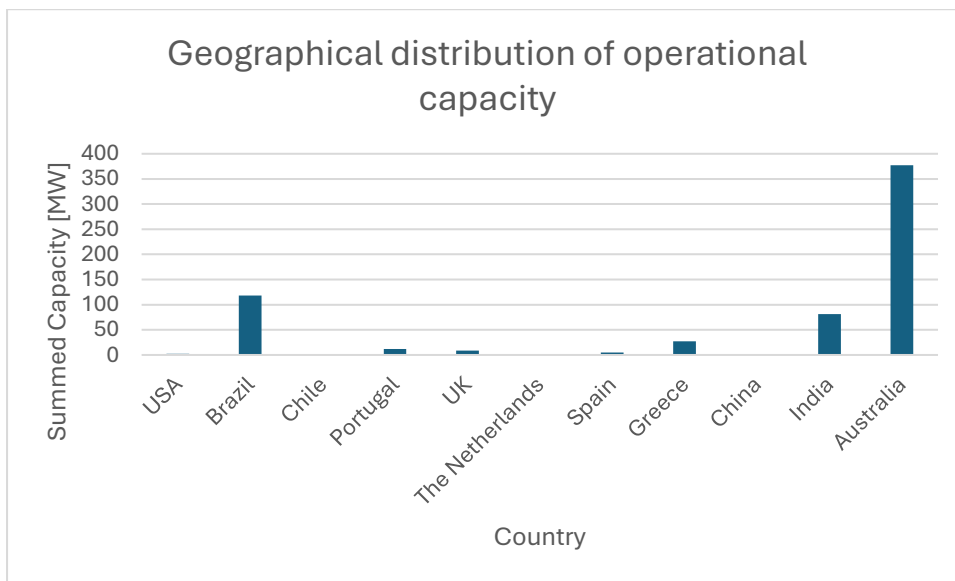
Figure 1.4 - Geographical distribution of operational capacity of PV-Wind hybrid systems (own elaboration).

In Spain, in 2023, two projects are operational, with a combined capacity of 1.67 MW and 3.12 MW respectively. A third project, with wind and PV capacities of 69 MW and 74 MW, has been commissioned by Iberdrola [14].

In Italy instead, no utility-scale PV-Wind hybrid plant projects are operational. However, in February 2024, a new collaboration agreement between SolarDuck, Green Arrow Capital and New Developments s.r.l. was signed for a utility-scale offshore hybrid wind-solar project in Calabria with a planned capacity of 540 MW [15]. This indicates that PV-Wind HPPs can represent an attractive solution even in countries where no HPPs have been developed. In addition, offshore solutions can represent a profitable alternative, eliminating the issue of the land occupation.

Globally, an example of operative policy regarding Solar-Wind Hybrid Systems has been developed in 2018 by the Ministry of New and Renewable Energy (MNRE) in India [18]. The objective of the policy is to provide a framework for the promotion of both new utility-

scale grid-connected Solar-Wind HPPs and the hybridization of existing wind and solar projects. The policy mandates the regulatory authorities to formulate standards and regulations for this kind of systems; moreover, it addresses the problem of defining a Solar-Wind HPP, allowing flexibility in the share of wind and solar components but introducing the condition that the rated power capacity of one resource must be at least 25% of the rated power capacity of the other source for the system to be recognized as hybrid project. Finally, the policy addresses the topic of procurement of power from a hybrid project, establishing a tariff-based transparent bidding process.

A policy of this type, which aims to reduce variability in renewable power generation and achieve better grid stability in a national grid, could promote the diffusion of PV-Wind Hybrid plants, helping the production of energy at competitive prices. For this reason, the "Asociación Empresarial Eólica" (AEE) developed in 2019 a regulatory proposal by the wind sector for the implementation of hybrid projects in Spain [19]. The proposal distinguishes the case of new HPPs and the case of the hybridization of existing wind plants. To promote them, issues regarding their definition, access and connection to the electrical grid permissions, the remuneration regime and participation in auctions must be addressed.

To promote the development of HPP projects, a proper assessment of suitable sites for their installation is necessary; indeed, the identification of areas with features suitable for an HPP allows for profitable installations with optimal utilization of renewable resources. In the next paragraphs this topic will be briefly discussed, analysing how this aspect can be tackled.

1.2 Assessment of suitable RES installation sites

With the increasing growth in renewable power production, the assessment of suitable sites for RES installation becomes crucial to optimally exploit the renewable potential. This topic has been discussed in the scientific literature, where various methods of tackling the problem have been identified. One effective approach involves the utilization of Geographic Information Systems (GIS), which consist of integrated hardware and software that allow to store, manage, analyse, and visualize geographic data, so that, it is possible to derive spatial information [20]. These systems were first developed between the 1960s and the 1970s and evolved into an industrial application in the 1980s. Subsequently, GIS established themselves as an "industry", spreading into new fields thanks, for instance, to their integration in the web and in decision support systems.

Among the many fields of application, GIS can be employed to study the renewable potential of an area, along with other relevant parameters for the development of RES. In

the following paragraph, a brief explanation of the main functionalities and features of a GIS is presented, along with an introduction to the software employed in this thesis to manage geographical data. Additionally, the development of GIS-based approaches in the scientific literature for assessing suitable sites for RES installation is discussed.

1.2.1 GIS and Digital Cartography

To understand how a GIS works, it is necessary to consider the elements that characterize it. In the first place, a GIS involves the use of maps: a map is a representation of the reality based on certain conventions. Since the considered reality is usually volumetric, the representation in a map requires a transformation from three to two dimensions; the third dimension can be represented with an "attribute". For instance, the peak of a mountain can be represented on a map in a position characterized by two coordinates of latitude and longitude and an attribute representing the altitude.

In addition, since the surface of the earth is spherical, to represent it in a plane surface like that of a map it is necessary the use of a "projection", to minimize the distortion. Many types of projections have been developed; they can be grouped into three categories: cylindrical, conic, and planar (*Figure 1.5*). In the first category, the projection plane is a cylindric tangent to the earth surface; in the second category, the projection plane is a tangent or secant cone. Lastly, in the third one, the projection plane is tangent to the earth surface in one point only.
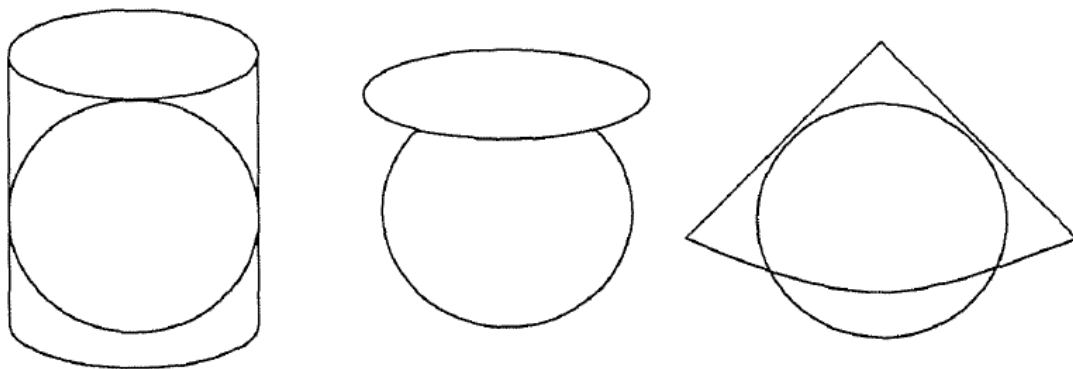
Figure 1.5 - Three categories of projections: cylindrical (on the left), planar (on the centre), conic (on the right) [20].

The third important aspect of a map is the "scale", that represents the relationship between the map and the reality, determining the level of detail of information in a map.

Typically, the information in a GIS can be represented in two structures: vectors and matrices. In the first case, spatial objects are represented through vectors that are localized in space by pairs of coordinates that coincide with the origin and the end point (*Figure 1.6*). The characteristics of the represented object are associated with the object itself in the form of attributes. If the origin point and the end point of a vector coincide, it is possible to represent a point; when more vectors are combined, it is possible to represent linear objects and surfaces. In the second case, the matrix, also known as "raster", is composed of cells or "pixels" that have a specific value and location (*Figure 1.6*). The value can be a binary value, representing the absence or presence of a determined spatial object (for instance, "0" can represent the absence of an object in a pixel, while "1" can indicate its presence). Alternatively, each pixel can have a decimal value when a continuous variable is represented. Finally, integer values can be associated with pixels to represent categories or thematic surfaces.
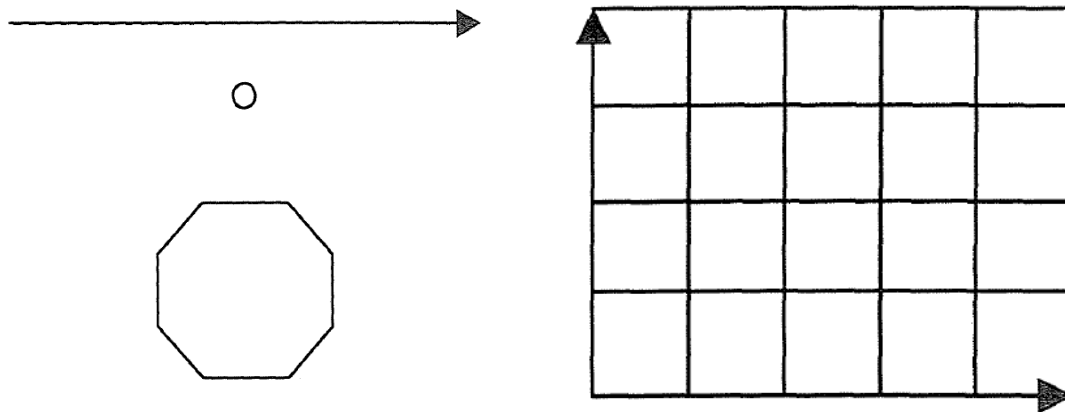
Figure 1.6 - Examples of spatial objects: on the left, a vector, a point and a surface, representing a polygonal object; on the right, a matrix, representing a raster [20].

Concerning the data, they can be managed in a GIS either in the graphic form, or in the form of tables. The first case includes cartography and products related to image generation (e.g., satellite images). The second case involves tabular data related to the territory and the previously mentioned graphic data. Moreover, the integration of data in a GIS is strictly related to the availability of information sources and the ability of minimizing the distortion of the sources during the integration process itself.

A significant aspect of a GIS is represented by the inclusion of aspects related to the "topology", i.e. the mathematical field that studies the relationships between elements in space. In systems with matrices, these relationships are generally represented as proximity analysis between cells, starting from a physical proximity or similarity of attributes between pixels. In a vectorial system instead, topology is defined by the directionality, connectivity, and proximity between vectors. The existence of these relationships allows for calculations

between variables to generate new data through spatial analysis tools. These tools are implemented in software that exploit all the potentiality of GIS in user-friendly interfaces. One of these software is ArcGIS Pro, which will be used in the analysis conducted in this thesis; a brief presentation of it is included in the next paragraph.

1.2.2 ArcGIS pro

ArcGIS Pro is a GIS software developed by Esri with multiple functionalities. In the first place, it allows to integrate data from multiple sources and datasets in multiple formats. In this thesis, most of the employed data are derived from previous research works. All data are collected in two types of formats: "raster files" and "shapefiles". Raster files represent data in matrix form, while shapefiles represent data in vector form, characterized by points, lines, and polygons. The software allows to visualize these data in a 2-D form by representing the information in "layers". Layers are maps with their own projection that can be superimposed on a "base map", representing a portion of the Earth surface. In this way, the parameters used in the following analysis can be associated with a layer, and their spatial distribution can be displayed in the software interface. In addition, a layer is characterized by a proper symbology, which can be modified to have a better visualization of the values of the variable in the interface. While a vectorial layer is characterized by a scale that represents its level of detail, a raster layer is characterized by a resolution that indicates the size of the cells composing the layer. Moreover, a vectorial layer or a raster layer that represents a variable with discrete values can be associated with an "attribute table", where information represented in the layer is categorized into "fields", in order to be visualized in tabular form. Eventually, the data represented in layers and attribute tables can be edited and analysed through a wide variety of tools, allowing for modifications, operations, calculations among variables, statistical analysis, and the storage of results in new maps or attribute tables.

Additionally, the workflow can be automated through the "ModelBuilder" tool or through the employment of Python. The first allows to connect various tools to create a workflow where each operation is performed step by step, giving the opportunity to perform a sensibility analysis on the variables employed. Similarly, the implementation of Python scripts in ArcGIS PRO allows to perform geographic data analysis, data conversion, data management, and map automation. This is possible thanks to ArcPy package, designed to integrate Python into the software.

In this thesis, Python will be employed to perform iterative calculations employing the tools available in the software. The advantage of this approach lies in the characteristics of this programming language, which is suited for interactive work and quick prototyping of "one-off" programs known as scripts, while also being powerful enough to write large applications. In addition, ArcGIS applications written with ArcPy can take advantage of additional Python modules and libraries developed for GIS and other fields of application.
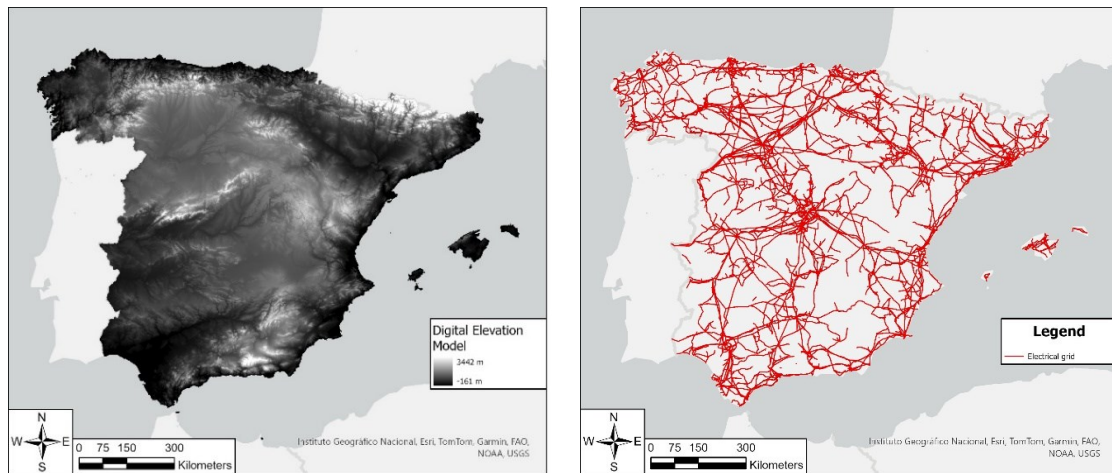
Figure 1.7 - Examples of raster layer (on the left) and polygon layer (on the right) (own elaboration).

	OBJECTID *	pointid	grid_code	P_fv	P_w	E_prod_1	E_prod_2	E_prod_3	E_prod_4	E_prod_5	E_prod_6	E_prod_7	E_prod_8	E_prod_9	E_prod_10
1	1	1	1	20	5	94,737	88,7035	120,574	136,319	106,416	138,318	131,39	119,038	112,313	129,579
2	2	2	1	20	5	106,079	100,542	131,201	150,173	119,882	159,339	148,586	141,72	124,196	141,706
3	3	3	1	20	5	92,5813	89,5163	119,952	141,375	111,361	151,203	136,466	133,588	114,308	129,027
4	4	4	1	20	5	104,568	99,8571	130,759	150,46	119,889	163,531	153,798	144,853	126,302	141,319
5	5	5	1	20	5	104,568	99,8571	130,759	150,46	119,889	163,531	153,798	144,853	126,302	141,319
6	6	6	1	20	5	104,784	100,563	132,13	152,216	121,175	161,971	150,966	144,577	127,061	141,51
7	7	7	1	20	5	103,352	97,8131	131,044	150,18	118,401	158,765	146,792	141,146	123,648	141,105
8	8	8	1	20	5	103,352	97,8131	131,044	150,18	118,401	158,765	146,792	141,146	123,648	141,105

Figure 1.8 - Example of attribute table associated to a polygon layer; in the table fifteen fields can be identified in fifteen columns, representing different indices or physical quantities; each object (listed in the first column) is associated to a row and to the data in the same row represented in the other columns (own elaboration).

1.2.3 GIS-based approach in the scientific literature

GIS has been studied and applied in various field of research. This thesis will focus on GIS-based approaches for, on one hand, evaluating suitable locations for installation of RES and, on the other hand, assessing the available renewable potential. In this perspective, GIS has proven to be a valuable tool thanks to its capability of managing georeferenced data.

Various GIS-based approaches have been studied in the literature; frequently, these are associated with Multi-Criteria Decision Making (MCDM). MCDM methods are decision support to solve complex problems where multiple factors affect a single result; they

provide a suitable option through the evaluation and comparison of the characteristic properties of different alternatives. Combining GIS and MCDM methods it is therefore possible to handle complex spatial planning problems.

Considering the assessment of suitable locations for RES, many studies that try to handle this problem can be found in the literature ([21], [22], [23], [24], [25], [26], [27], [28], [29], [30], [31]); most of the studies taken as reference in this thesis work present a methodology that is composed by the following step:

a) Identification of the main parameters that affect the choice of the installation site.
   The suitability of a site depends on various factors that are often classified in three categories: geotechnical, socio-environmental, and economic. Depending on the characteristics of the territory studied a parameter can be included or excluded from the analysis; georeferenced data about the variables are collected by means of different sources, as databases and atlases of national or international institutes.

b) Application of MCDM methodology.
   To compare variables belonging to categories of different nature, MCDM based approaches are used; two examples are the Analytic Hierarchy Process method (AHP) and the Best Worst Method (BWM). These methods assign weights to each parameter to determine its relative importance in the analysis.

c) Data processing in GIS and reclassification.
   Parameters and respective weights are processed in GIS software to visualize them in maps; first, each parameter is reclassified into "classes" to identify which values of the parameter are associated with a suitable or an unsuitable site; the various maps associated with each parameter are then "superimposed" by means of the software tools, taking into account the respective weight. A final map representing a suitability index is obtained; the values of the suitability index are eventually reclassified in classes that represent a certain level of suitability, from a "very suitable" to a "not suitable", to categorize each site of the studied area.

In this thesis, point a) and point c) are performed by means of a GIS-based approach that consists of a combination of a Boolean Logic approach and a Fuzzy Logic approach, as it will be explained in the next paragraphs. The step shown in point b) is omitted and it can represent a future development of this research in a following work. Therefore, all the parameters that will be taken into account will have the same weight, i.e. the same importance. Moreover, a further step will be considered: the identification of the hypothetical "optimal" size of a PV-Wind hybrid plant and the evaluation of its profitability will be performed. This approach allows to compare the territory considered site by site to identify which are the areas suitable for an installation of a plant with the highest profitability. This analysis represents a step forward in a more comprehensive analysis of the convenience of hybrid installations, based on an economical perspective.

1.3 Thesis outline and goals

As demonstrated, a consistent research work concerning the assessment of installation sites for RES has flourished in the scientific literature; as a consequence, also the increasing interest raised in PV-Wind Hybrid Systems is followed by the necessity of identifying the most appropriate sites for their installation. For this reason, the "Centro de Investigaciones Energéticas Medioambientales y Tecnológicas" (CIEMAT), within the framework of the Investment and Reform Plan for Economic Recovery proposed by the Ministry of Science and Innovation, has undertaken the challenge of generating a map of Spain for the hybridization of wind and solar energy, pointing out the sites where PV-Wind hybrid plants can be installed assuring their profitability. As the starting point of this project, the final master thesis "Elaboration of the Wind and Solar Energy Hybridization map in Spain" [5] has been developed in 2021. The final result of that work has been the generation of a cartography that shows the most suitable areas for the implementation of solar and wind hybrid technology, as well as the sites that should be excluded according to environmental, technological and socioeconomic criteria.

The current master thesis is developed in CIEMAT within the same framework, and it will consider as the initial point the precedent research work. In this thesis the same parameters and the same concept of suitability used in [5] will be employed, developing a new methodology to assess the suitability of PV-Wind HPP, and incorporating new concepts related to the profitability of a power plant.

According to this, the goals of this master thesis are:

a) Build a map of suitability for the installation of utility-scale PV-Wind hybrid power plants in Spain.
b) Build a model for the evaluation of the profitability of a utility-scale PV-Wind hybrid power plant, based on some assumptions.
c) Build a map of profitability for utility-scale PV-Wind hybrid power plants in Spain.
d) Perform a sensibility analysis on the main parameters of the developed model.

The methodology employed to achieve these goals will be discussed in the following three chapters:

- Chapter 2 deals with the suitability map generation; site selection criteria are identified for the suitability assessment; then, the software ArcGIS Pro is employed together with a GIS approach based on a combination of a Boolean Logic and Fuzzy Logic methods to create a suitability map; the results are validated by comparing them with the sites of real wind power plants.
- Chapter 3 deals with the model for the evaluation of HPP profitability; this model consists of a solar and wind resource evaluation for a particular site, a numerical

sizing method used to evaluate the optimal size of the PV-Wind HPP for each site, and a profitability evaluation of the optimal solution; the software Excel will be employed to validate the consistency of the model.

- Chapter 4 deals with the profitability map generation and the discussion of the final results; first, an algorithm that integrate the generated suitability map and the profitability model is written through Python programme language; then, the algorithm is implemented in ArcGIS Pro, to obtain the profitability map; the results are validated through the model implemented in Excel; eventually, a sensibility analysis on the main parameters of the model will be performed changing their values in the script employed for the profitability map generation.

A scheme of the followed methodology is shown in *Figure 1.9*. Once the goals are achieved, aspects worthy of a further in-depth study are highlighted in the final Chapter 5, along with the conclusions on the work performed.
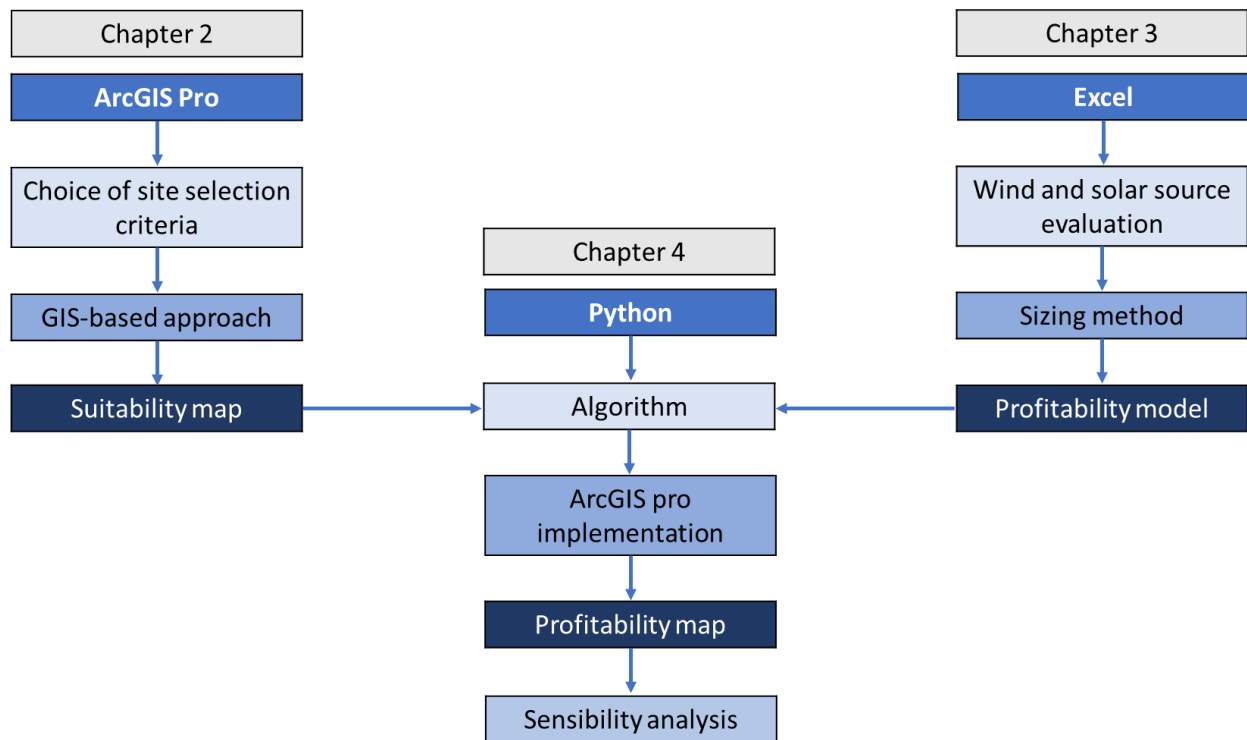
Figure 1.9 - Scheme of the general followed methodology (own elaboration).

2. Suitability assessment

As first step, a suitability assessment for PV-Wind hybrid system in Spain is conducted with the deployment of the software ArcGIS pro, to create a map of suitability that will provide the sites where a subsequent profitability analysis will be carried out. These sites indeed, will be the ones where, first, the regulation of a defined territory allows the installation and the operation of a PV-Wind HPP, and second, where the hypothetic installation is "recommendable" according to a series of parameters.

As stated in the introduction, numerous studies have been performed in the literature regarding this field of research. The methodology that will be used in this work refers directly to this scientific production, and it is schematically represented in *Figure 2.1*. As a first step, a series of parameters are chosen to represent the main factors that influence the assessment of a PV-Wind HPP. Second, these parameters are "reclassified" according to either the "Boolean logic" or the "Fuzzy logic"; finally, the reclassified parameters are combined to generate a suitability map for PV systems and one for wind systems; then, the latter are superimposed to create a suitability map for PV-Wind HPP. Each of these steps corresponds to the use of proper ArcGIS Pro tools and to the generation of raster or polygon layers, and the final result will be a raster layer where "suitable" and "not suitable" sites are represented. As reference for this map, a resolution of 1000 m X 1000 m and a projection "WGS 1984" will be considered.
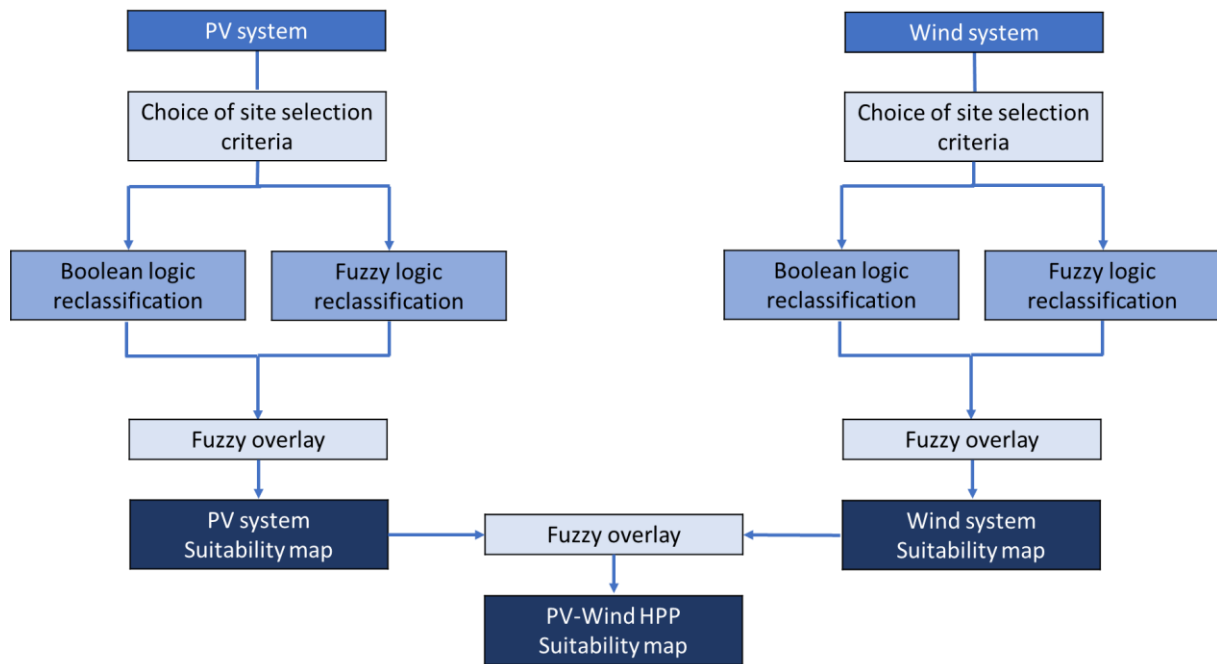
Figure 2.1 - Scheme of the followed methodology to create a PV-Wind HPP Suitability map (own elaboration).

2.1 Study area

The study area includes the whole Spanish peninsular territory, Balearic Islands, Ceuta and Melilla. The Canary Islands, which belong to Spain, are excluded from the analysis, due to lack of data regarding the wind resource. The total area of Spanish peninsular territory is 493491 km^2 while Balearic Islands, Ceuta and Melilla occupy respectively 4992 km^2, 19 km^2 and 13 km^2 [32]. The latitude of this surface extends from 35°53'45" N of Ceuta and 35°17'15" N of Melilla to 43°47'36" N of the north end of the Iberian Peninsula; the longitude of the peninsular territory extends from 9°17'46" W of the west end to 3°19'05" E of the east end; instead, the longitude of the Balearic Islands, extends from 1°12'05" E of the west end to the 4°19'29" E of the east end.

Figure 2.2 - Map representing the study area for the current thesis (IGN).

2.2 Selection of parameters

A correct selection of parameters that determines the pertinence of a site is the first important step for a creation of a map of suitability. In the literature analysed in *section 1.2.3*, each study presents its own list of considered factors. Since in this master thesis the considered power generation system is a hybrid system based on PV and wind plants, only the parameters relevant for these types of systems are considered. The multitude of parameters taken into account in each single study reflects the complexity of the process of site selection, where the availability of natural energy sources as wind energy, strictly correlated to the wind speed, and solar irradiation, are not the only important factors.

In general, three categories for the optimal site selection for wind and PV plants can be identified: geotechnical, socio-environmental, and economic variables. Following this categorization, based on [5] and on the previous studies presented in *section 1.2.3*, the following parameters are chosen for the creation of a suitability map:

Geo-Climatic

- *Solar irradiation [kWh/m2/day]*: solar irradiation is the incoming energy from the sun at a particular point of the earth surface, and it is responsible for the electrical energy output from PV farms.
- *Wind speed [m/s]*: average wind speed is correlated to the wind available energy for the electrical production of wind farms.
- *Elevation [m]*: a high elevation is generally not recommended in the literature, due to the association with high construction difficulty [33].
- *Slope [°]*: a high slope is generally not recommended in the literature, due to the association with high construction difficulty [33].

Socio-Environmental

- *Distance from airports [m]*: distance from airports is important due to the adverse effects of solar and wind farms on aviation activities as interferences to the aviation radar signals and distractions to the pilot's vision.
- *Distance from Rivers and surface water [m]*: to prevent possible pollution caused by the construction of wind and solar power plants for water bodies, it is necessary to maintain a proper distance from the water.
- *Environmental sensitivity*: to preserve the biodiversity, the installation of solar and wind farms should respect environmental constraints that determine the environmental sensitivity of an area.
- *Land use*: the land use imposes physical constraints on construction, or limitations due to the regulations adopted by governments or by economic effects.
- *Distance from the coastline [m]*: the distance from coastline creates issues like visual impacts on tourist activities, effect of salt on the life and efficiency of the equipment, and pollution-related incidents. Moreover, legislations might limit the use of coastal lands.
- *Distance from urban and rural residential areas [m]*: a proper distance from urban and rural residential areas is necessary to avoid inconvenience, visual intrusion in daylight, noise nuisance to human life, and for the future development of cities and rural activities.

Economic

- *Distance from transport network [m]*: a proper distance from transport network is necessary to avoid environmental damage and road construction costs.

> *Distance from electrical transmission grid [m]*: a proper distance from electrical transmission grid is necessary to minimize the construction cost, ecological damage, and energy losses.

> *Distance from electrical power plants and substations [m]*: a minimum distance from existing power plants and substation allows to minimize the infrastructure construction cost, ecological damage, and energy losses.

To perform a suitability analysis through the tools provided by the software ArcGIS PRO, each parameter should be associated with a raster or a polygon layer, containing the values that each parameter assumes in each site within the studied area or the category each site falls in. The layers needed to initialize the analysis were gathered or generated in previous works, presented in the following paragraphs.

2.2.1 Solar and Wind layers

The first layers considered in the analysis are the ones regarding the solar irradiation and the wind speed, that are correlated with the energy that can be produced by a PV plant and a wind plant respectively. As it will be explained in Chapter 3, the model developed for the profitability calculation is based on average monthly values of solar and wind resources; therefore, twenty-four layers were produced by CIEMAT to perform the analysis. Twelve of these layers represent Spain global monthly average daily irradiation on a horizontal plane, in $[kWh/km^2]$; these raster layers are obtained by means of the data contained in the web portal ADRASE[1], developed by CIEMAT. This project is part of a framework promoted by the World Bank in 2013, and it aims at raising awareness among governments and the private sector about renewable energy potential, particularly related to solar and wind sources, by creating high-quality national and regional solar resource atlases. The resolution of these raster layers is 5000 m X 5000 m, and their projection is "WGS 1984"; to obtain the desired resolution of 1000 m X 1000 m, the ArcGIS Pro tool "Project raster" is employed.

The other twelve layers represent Spain's monthly average wind speed, expressed in [m/s], at 100 m height; these raster layers are obtained by CIEMAT by means of the Weather Research and Forecasting Model (WRF)[2]. The resolution of these raster layers is 3000 m X 3000 m, and their projection is "WGS 1984"; to obtain the desired resolution of 1000 m X 1000 m, the tool "Project raster" is employed.

---

[1] The methodology followed to obtain the layers concerning the monthly average daily values of solar irradiation is not a subject of this thesis; more information can be found in [52].

[2] As for the solar irradiation layers, the methodology followed to obtain the average monthly values of wind speed is not a subject of this thesis; more information can be found in [53].

For the creation of the suitability map, the employed criteria are the global annual average daily solar irradiation on a horizontal plane and the annual average wind speed. The layers corresponding to these two parameters are generated by mean of algebraic operations performed with the "Raster calculator" tool, calculating for each site the average value of the correspondent twelve monthly layers:

$$H = \frac{\sum_{k=1}^{12} H_k}{12} \tag{2.1}$$

$$v = \frac{\sum_{k=1}^{12} v_k}{12} \tag{2.2}$$

With H global annual average daily irradiation on a horizontal plane [kWh/m^2/day], H_k global monthly average solar irradiation on a horizontal plane for month k [kWh/m^2/day], v annual average wind speed at 100 m [m/s], v_k monthly average wind speed for month k at 100 m [m/s].

The resulting layers are represented in *Figure 2.3* and *Figure 2.4*.
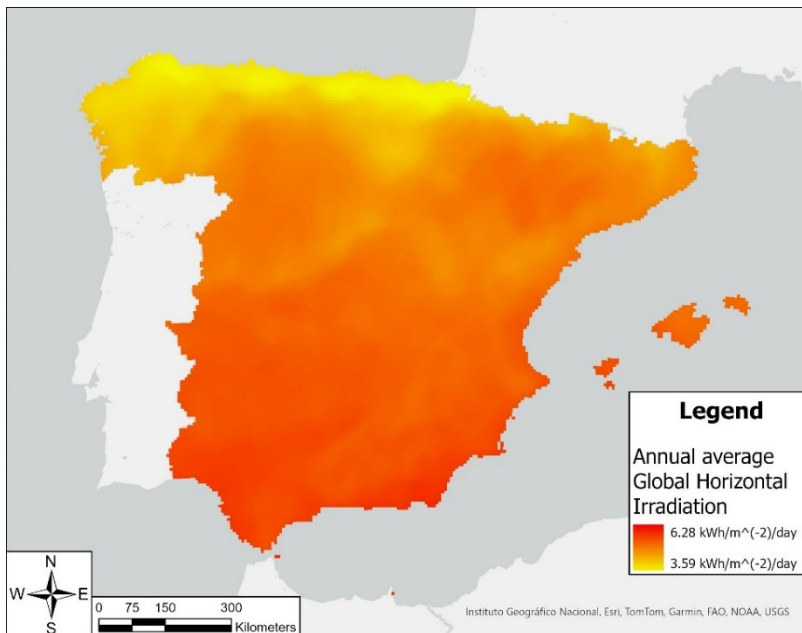
Figure 2.3 - Annual average Global Horizontal Irradiation on a daily basis (elaborated by CIEMAT [34]).

24
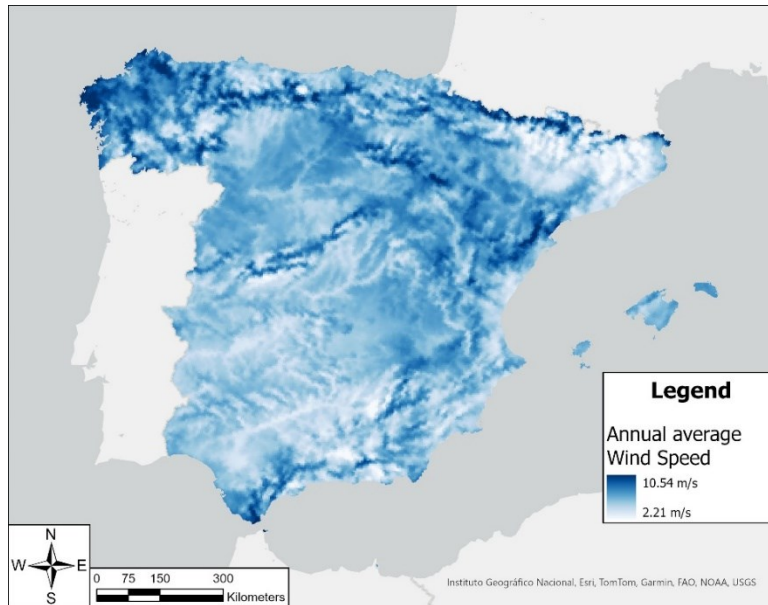
Figure 2.4 - Annual average Wind Speed (elaborated by CIEMAT [35]).

Considering the Global Horizontal Irradiation, the areas with the highest value of the parameters are the ones in the south of the Peninsula, especially along the coastline of Andalusia, as expected; the intensity of the irradiation subsequently decreases with the increase of the latitude, until the North Coast of Spain, where it assumes more moderate values.

Concerning the wind speed, high values can be found in: south part of Andalusia; Galicia, especially where the coastline faces the Atlantic Ocean; border between Castile and León and Asturias and Cantabria; area where Castile and León, La Rioja, Aragon and Navarra border with each other; the northern part of Aragon along the Pyrenees; the coastline between Catalonia and Valencian Community. Considering instead areas with low values of wind speed, they include: the continental part of Andalusia; a large territory between Extremadura and Castile and León, some internal parts of Galicia and Asturias; the territories of Aragon and Catalonia protected by the Pyrenees; some areas along the coastline of the Valencian Community and the Region of Murcia.

2.2.2 Environmental sensitivity layers

The first series of maps considered for the analysis have been created by the "Ministerio para la Transición Ecológica y el Reto Demográfico (MITECO)" of Spain, through the "Subdirección General de Evaluación Ambiental de la Dirección General de Calidad y Evaluación Ambiental" [34]. The latter indeed, in response to a call for an increase of

installations of wind farms and PV plants according to the "Plan Nacional Integrado de Energía y Clima y la Estrategia a Largo Plazo para una Economía Española Moderna, Competitiva y Climáticamente Neutra en 2050", has developed a tool that allows to identify the areas in the national territory of Spain that exhibit the most restricting environmental constraints. This tool is correlated to a territorial model that groups together the main environmental factors and returns as a result a partition of the territory based on the "environmental sensitivity" index. According to this index, the sites characterized by a high sensitivity represent areas unrecommended for a RES installation, while the ones that present a low value of sensitivity represent available sites.

To obtain the partition of the territory, the following parameters and correlated maps were taken into account:

- Urban residential areas
- Water bodies and flood zones
- Plans for the recovery and conservation of endangered species
- Protection zones for birds against collision and electrocution on high-voltage power lines
- Ecological connectivity
- Important Areas for the Conservation of Birds and Biodiversity in Spain "Áreas Importantes para la Conservación de las Aves y la Biodiversidad en España" (IBAs)
- Habitats of Community interest
- Network "Natura 2000"
- Natural Protected Areas
- RAMSAR wetlands
- Mediterranean protected areas "Zonas Especialmente Protegidas de Importancia para el Mediterráneo" (ZEPIM)
- Reserves "Reservas de la Biosfera" (MaB)
- Places of geological interest "Lugares de Interés Geológico" (LIG)
- Visibility
- "Camino de Santiago" (Way of St. James)
- Livestock trails
- Public Utility Mountains "Montes de Utilidad Pública"
- UNESCO World Heritage Sites

According to the methodology followed to obtain a map of environmental sensitivity of the territory, represented schematically in *Figure 2.5*, all the parameters are first associated with raster layers; the representation follows different criteria that are categorized as valid either for elements that affect wind plants or for elements that affect PV plants.
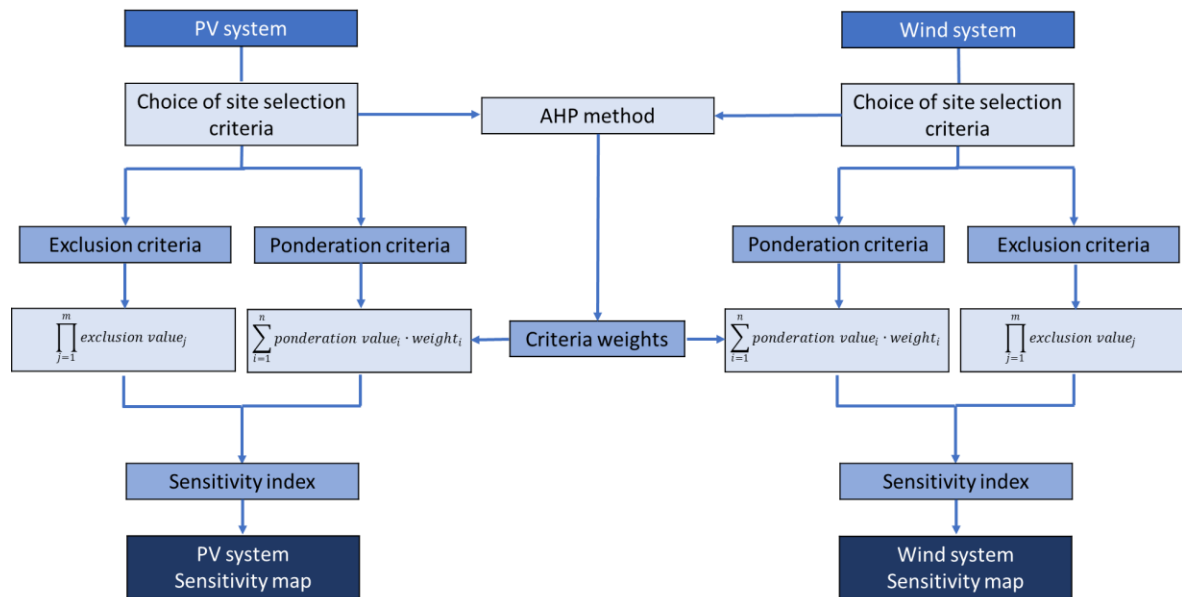
Figure 2.5 - MITECO methodology for the creation of an environmental sensitivity map (own elaboration).

Subsequently, these raster layers can be classified in ponderation layers and exclusion layers: the firsts correspond to parameters used to measure the level of sensitivity of an area between a maximum and a minimum value; the seconds, instead, correspond to parameters used only to identify the areas of maximum sensitivity, i.e. where RES installations are unrecommendable. In the ponderation layers, the elements that define "ponderation" zones correspond to pixels with a value of "1" for the presence and "0" for the absence; meanwhile, in the exclusion layers, the elements that define areas of maximum environmental sensitivity possess a value of "0" for the presence and "1" for the absence (*Figure 2.6*).
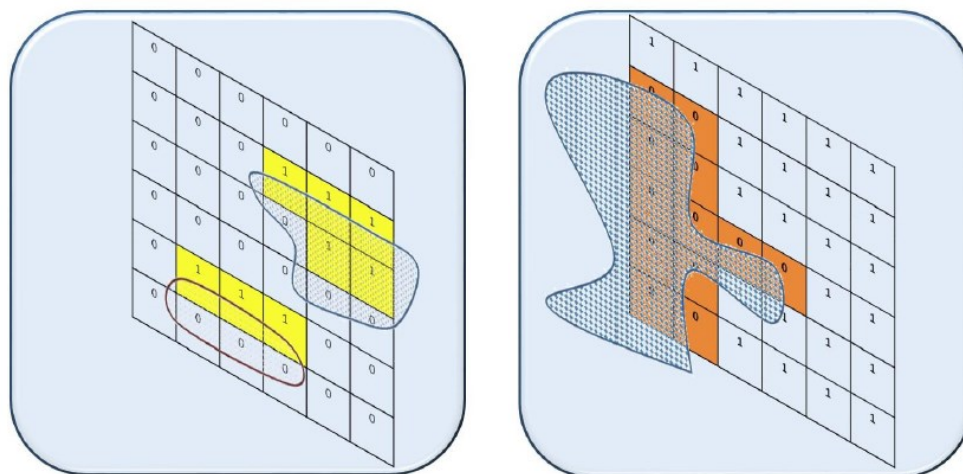
Figure 2.6 - Examples of ponderation layer (on the left) and of exclusion layer (on the right) [34].

Then, with a proper methodology based on the Analytic Hierarchy Process (AHP)[3] MCDM method, weights corresponding to each parameter are obtained; these weights are subsequently multiplied by the ponderation elements only through "map algebra" tools, which allow to perform algebraic operation pixel by pixel, so that all the pixels characterized by values of presence ("1") will have a value of importance ("$1 \cdot weight$").

At this point, each parameter is associated either with an exclusion layer, with values of "1" and "0", or with a ponderation layer, with values of "$1 \cdot weight$" or "0". Considering first the layers regarding PV plants and then the layers regarding wind plants, the exclusion layers are multiplied by each other, in order to obtain a final exclusion layer for PV systems and a final exclusion layer for wind systems. The layers are represented in *Figure 2.7* and *Figure 2.8*; as explained, the cells with a value of "1" are available for a RES installation, while the cells with a value of "0" are not recommended since they have a maximum value of sensibility.
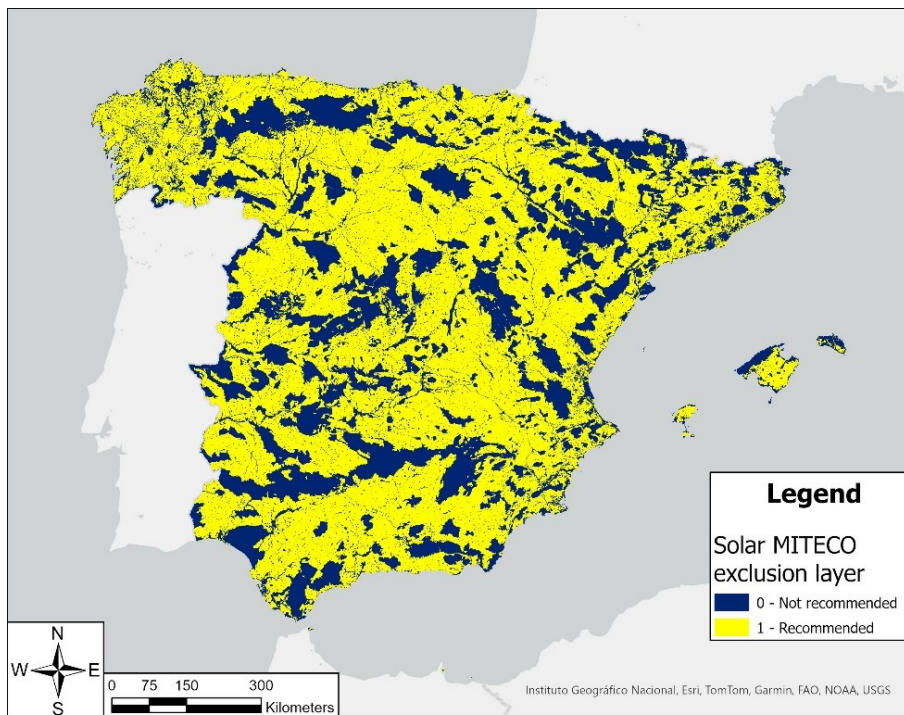
Figure 2.7 - Solar exclusion layer created by MITECO to generate an environmental sensitivity layer [36].

---

[3] As stated in the introduction, the MCDM method as the AHP are not a subject of this thesis; the explanation regarding the application of this method in the approach followed by the MITECO is left to [34] and [51].
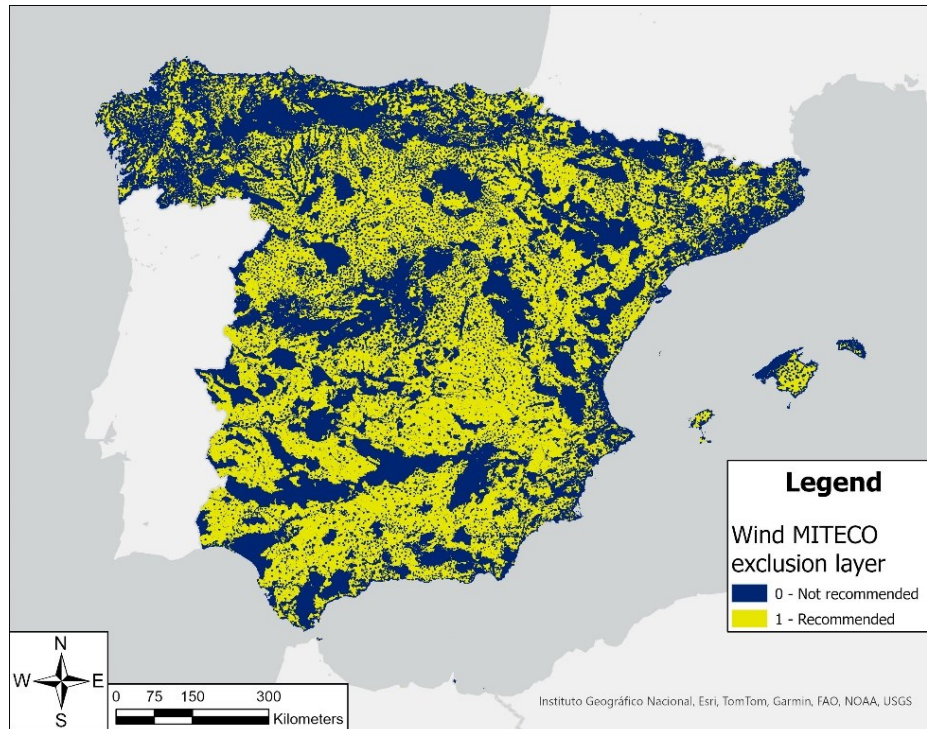
Figure 2.8 – Wind exclusion layer created by MITECO to generate an environmental sensitivity layer [36].

Considering the ponderation layers for PV systems and wind systems, they are superimposed by performing the following operation through the map algebra tools:

$$Sensitivity\ index\ (w/o\ excl.layers) = 1 - (\sum_{i=1}^{n} pond.value_i \cdot weight_i) \qquad (2.3)$$

The results of this operation are two maps, one concerning wind installations and the other PV installations; these two layers are used in the suitability analysis of the master thesis as ponderation layers regarding the parameter of the environmental sensitivity. These layers are represented in *Figure 2.9* and *Figure 2.10*; the scale of the sensitivity index is represented in order to have values between a minimum (1010 for the solar layer and 800 for the Wind layer) and a maximum (10000 for both layers); these values are a measure of the level of the importance of environmental constraints in the territory that affect the availability of the territory itself for a RES installation.
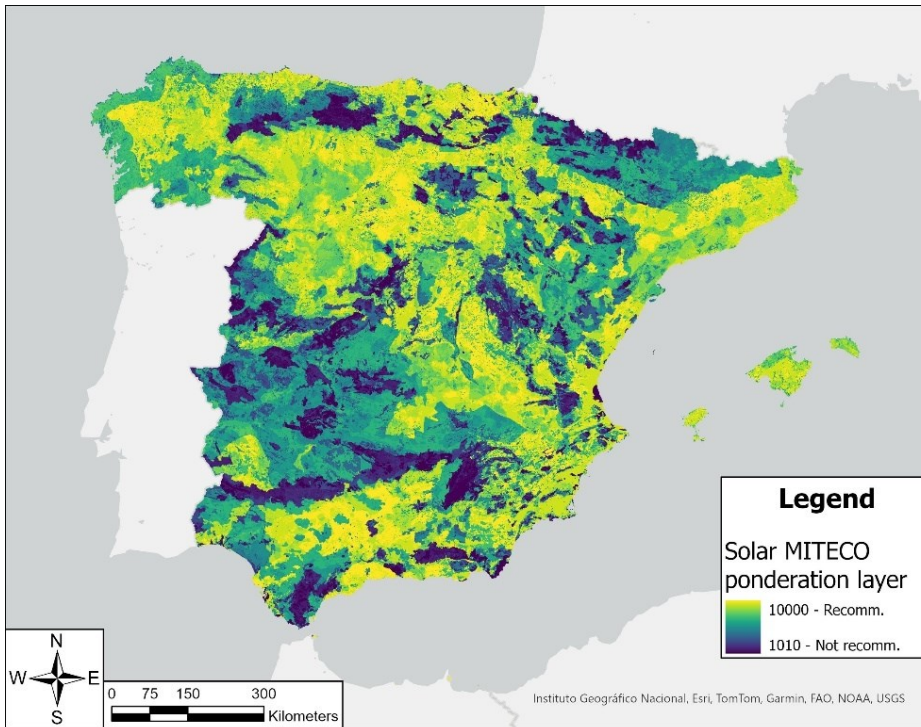
Figure 2.9 - Solar ponderation layer created by MITECO to generate an environmental sensitivity layer [36].
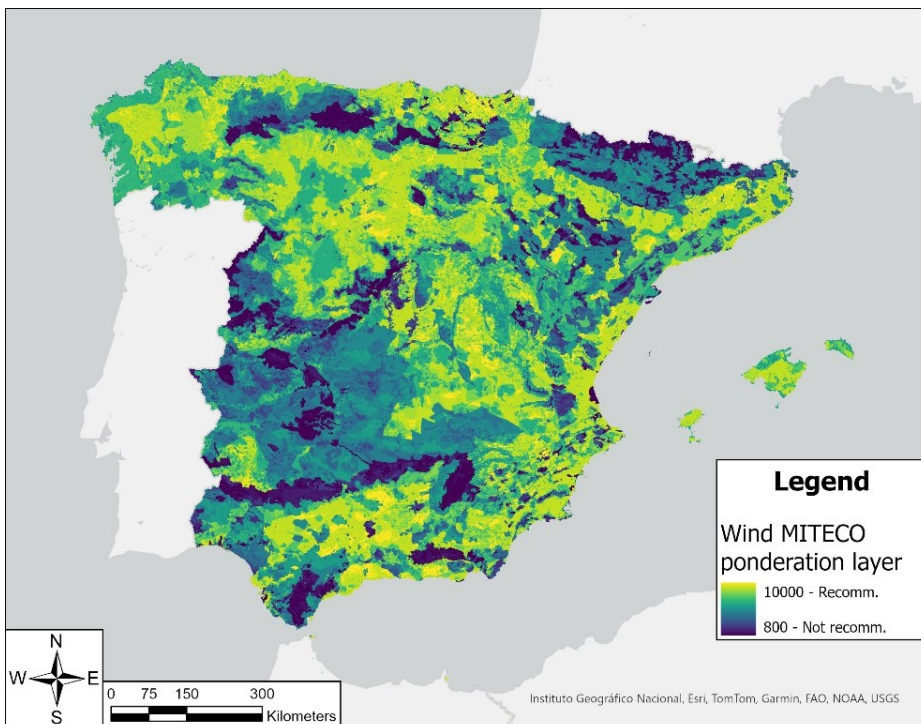
Figure 2.10 - Wind ponderation layer created by MITECO to generate an environmental sensitivity layer [36].

To conclude the analysis on the environmental sensitivity, through the map algebra, the following operation is carried out, to integrate the exclusion and the ponderation parameters obtaining a final environmental sensitivity map for Spain:

$$Sensitivity\ index\ =\ (1 - (\sum_{i=1}^{n} pond.value_i \cdot weight_i)) \cdot (\prod_{j=1}^{m} excl.value_j) \qquad (2.4)$$

This final representation, represented in *Figure 2.11* and *Figure 2.12*, will not be used in the suitability analysis; instead, the final exclusion and ponderation raster layers, two concerning wind systems and two concerning solar systems, will be employed.
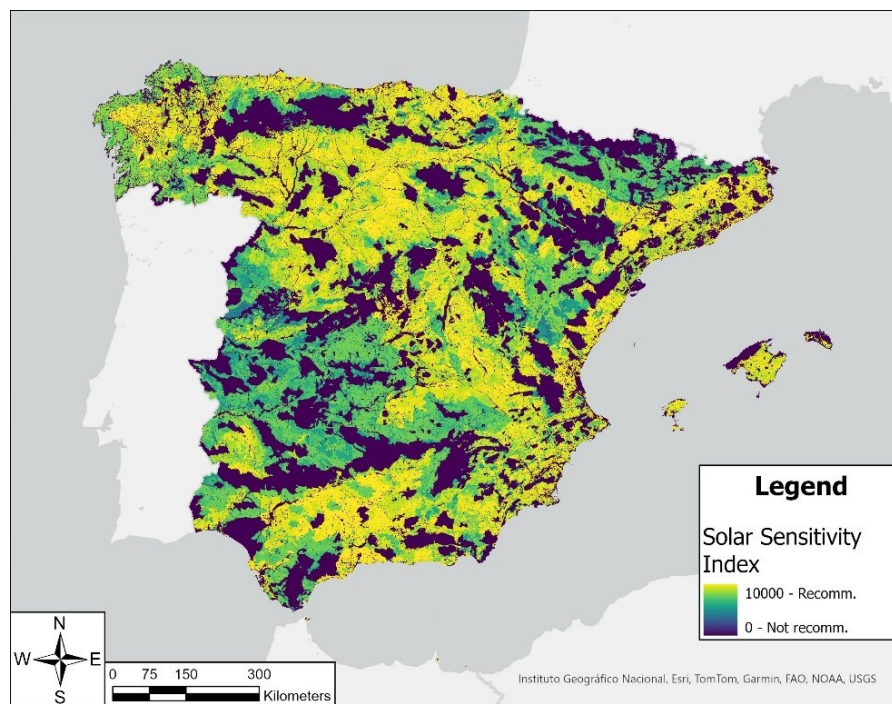
Figure 2.11 - Solar environmental sensitivity map [36].
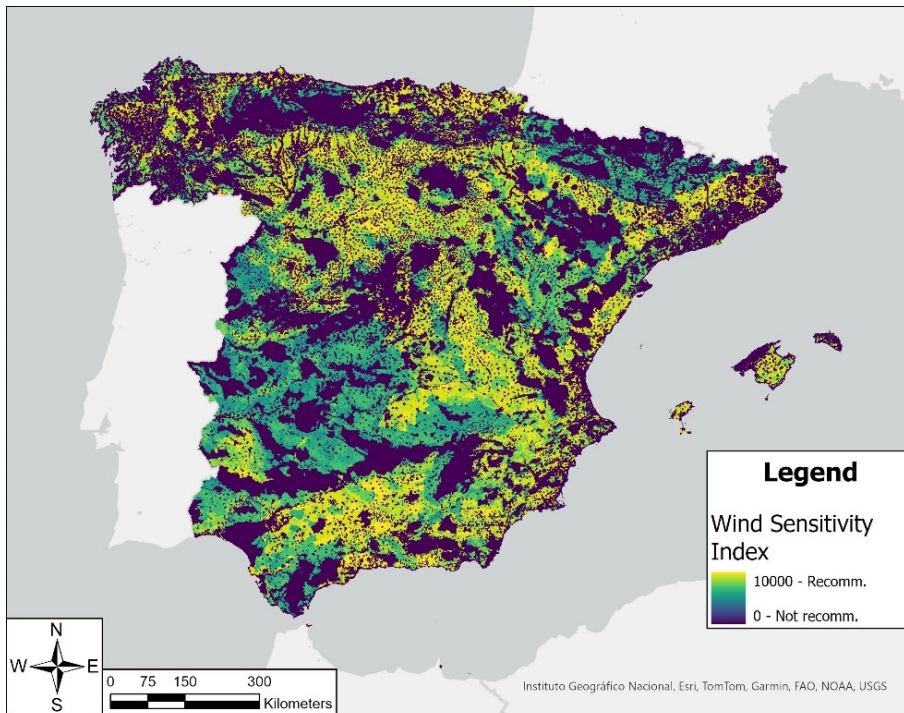
Figure 2.12 - Wind environmental sensitivity map [36].

Exclusion and ponderation layers have a resolution of 25m X 25m and they are represented with the "ETRS 1989" projection. Therefore, since the resolution and the projection of the final map will be respectively 1000 m X 1000 m and "WGS 1984", it is necessary to project the maps with the right resolution and projection to employ them correctly for the creation of the suitability map. To perform this operation, the tool "Project raster" of ArcGIS PRO is used.

2.2.3 Layers of the remaining parameters

The second series of maps considered by the analysis have been gathered in the realization of the master thesis "Elaboración del mapa de hibridación de energía eólica y solar en España" [5], carried out in CIEMAT. These maps, employed for a study of suitability for PV-Wind HPP in Spain, correspond to a selection of parameters resulting from an investigation work conducted in the scientific literature on the most influencing parameters for PV and wind plants site selection.

The list of maps is represented below, associated to the respective file format, source and resolution or scale:

Table 2.1 - List of remaining parameters and respective layers employed to create a suitability map (own elaboration).

Parameter	Type of file	Source	Resolution or scale
Ground elevation (Digital Elevation Model - DEM)	Raster	IGN[4]	200 m X 200 m
Ground Inclination	Raster	Generated from DEM	200 m X 200 m
Land Cover	Shapefile	IGN	1:100.000
Airports	Shapefile	AENA[5]	-
Electric Power Plant	Shapefile	IGN	1:100.000
Urban residential areas	Shapefile	IGN	1:100.000
Rural residential areas	Shapefile	IGN	1:100.000
Transport Network	Shapefile	IGN	1:100.000
Coastline	Shapefile	IGN	1:100.000
Electrical grid	Shapefile	IGN	1:100.000
Electrical substation	Shapefile	IGN	1:100.000

The layer of the ground inclination is generated through ArcGIS PRO tools, starting from the layer of the Digital Elevation Model (DEM). The DEM and the ground inclination are represented in [m]; their resolution is 200 m X 200 m while their projection is "WGS 1984". Thus, since the resolution chosen for the final suitability map is 1000 m X 1000 m, the tool "Resample" is used to obtain the correct resolution.

In addition, all the polygon layers associate with parameters of "distance" don't provide information about distances from themselves. Therefore, to represent the correct information, all the polygon layers are transformed in raster layers, associating each parameter to a map representing the Euclidean distance expressed in [m] from each polygon, by mean of the tool "Euclidean distance" in ArcGIS pro. An example of

---

[4] Instituto Geográfico Nacional, Madrid, Spain
[5] Aeropuertos Españoles y Navegación Aérea S.A., Madrid, Spain

representation of Euclidean distance is shown in *Figure 2.13*, taking into account the layer of the electrical grid in the territory.
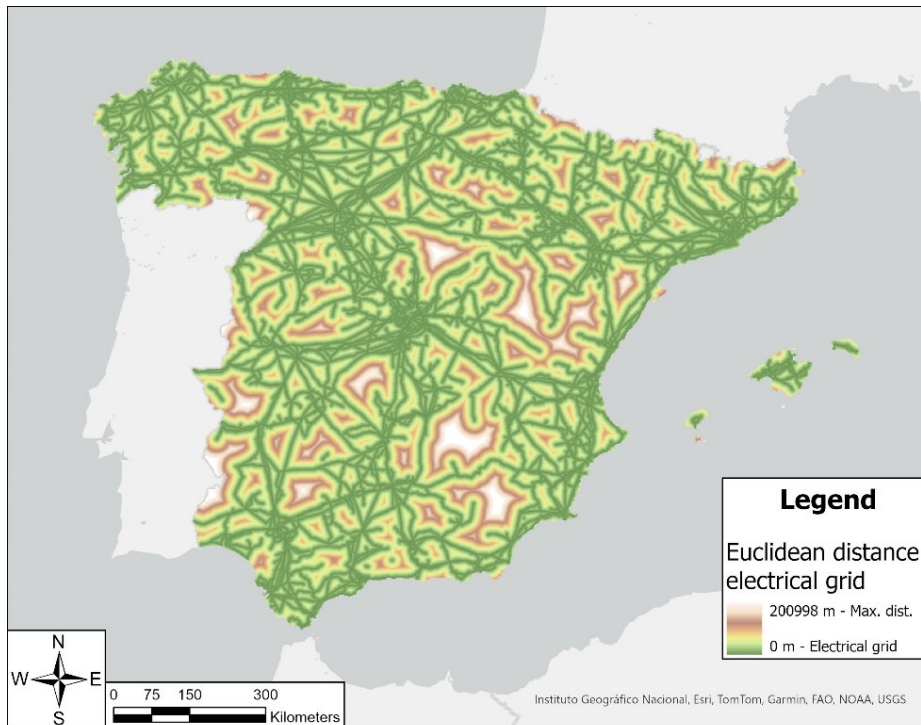
Figure 2.13 - Example of Euclidean Distance from the electrical grid (own elaboration based on data from [5]).

As shown, each point in the figure is classified based on the distance from the closest part of the electrical network, in order to generate a continuous scale of values that goes from zero distance on the electrical grid branches (green colour), to maximum distance from the line (red and white colour).

Moreover, another important aspect to be considered regards the implementation of the methodology of this thesis in the software, that requires the use of map algebra; to employ it, it is more convenient to represent the layers in the form of raster, rather than polygon, in order to allow the use of the map algebra tools cited in the next sections. Thus, the Euclidean distance tool allows to perform this conversion.

As can be noted, the parameters of the distance from urban and rural areas are already comprised in the analysis of the MITECO explained in *section 2.2.2*; however, in that methodology they are considered only as "exclusion" layers; as explained in this section however, the layers elaborated in [5] concerning these parameters will be used as "ponderation" layers as well.

Eventually, in the polygon layer corresponding to the land cover each polygon is associated with different land covers or land uses; the latter are indicated through a codex that refers to the original classes identified to build the original CORINE land cover 2018, used as input data in the research work in [5][6].

2.3 Reclassification

The goal of the reclassification is to express all the chosen parameters according to the same scale of values. Indeed, every parameter is associated in the corresponding layer with a unit of measurement. However, in the final suitability map of this thesis, the suitability of a site is expressed through a Suitability Index, associated to a scale of values that stretches from "0" – Not Suitable, to "1" – Completely Suitable. The reclassification process allows to transform the scale associated with each parameter into one with values between "0" and "1". In this way, all the parameters will be represented in the layers according to a common scale that corresponds to the one employed in the final suitability map. In this prospect, exclusion and ponderation parameters are defined; these categorization is needed in order to identify which factors provide a limitation for the installation of RES, establishing exclusion zones where a hypothetical plant is not recommended to be installed or cannot be installed due to regulations or territorial constraints; and which parameters are employed to have a scale of suitability for the sites where a RES installation is permitted. The reclassification is then based on two types of methodology that can be found in the scientific literature mentioned in *section 1.2.3,* in particular in [27], [23], [28], [29]. [30], [31] : Boolean logic, for the exclusion parameters, and Fuzzy logic, for the ponderation ones. By consulting the scientific literature, other methods are appropriate to conduct a suitability analysis; establishing which method is the most appropriate one is beyond the scope of this thesis work. Therefore, the identification of the exclusion and ponderation parameters coincides with the choice of following an approach similar to the one employed by MITECO. Moreover, in the operation of reclassification, ranges with different arbitrary widths can be defined for the same parameter, following different sources of information. In the absence of a widely accepted criteria for the reclassification of each factor, the fuzzy logic provides a way of dealing with these kinds of problems [35]. In the following paragraphs an explanation of the methodology for the reclassification is provided.

---

[6] In [5] more information about the sources for each employed layer can be found as well. To have a better understanding of the classes used for the land cover layer, see *Appendix 1* and [54].

2.3.1 Boolean logic

The Boolean algebra is a branch of algebra where the values of the variables are the truth values "true" and "false"; in this work the latter are denoted with "1" for "truth" and "0" for "false". Taking into account a raster layer, the value of every cell of the map will be therefore reclassified as "1" or "0", aside from the cells which no value is assigned to (referred as NO-DATA cells). In particular, "1" will be assigned if the cell is suitable for a RES installation according to the considered parameter, while "0" will be assigned if the cell should be excluded from the suitability analysis. Since in a raster layer the parameters are represented in a continuous scale of values, it is necessary to identify ranges of values associated with "1" and "0", in such a way that each cell will be reassigned to a reclassified value. The parameters that are reclassified according to the Boolean logic are:

> ➢ Ground elevation: This parameter is represented in the layer of the Digital Elevation Model (DEM); the values of ground elevation lower than 1500 m are reclassified as "1", while the ones higher than 1500 m as "0".
> ➢ Ground inclination: the values of ground inclination lower than 15° are reclassified as "1", while the ones higher than 15° as "0".
> ➢ Distance from airports: Considering the layer of the Euclidean distance from airports, the values of distance lower than 7000 m are reclassified as "0", while the ones higher than 7000 m as "1".
> ➢ Sensibility exclusion layer for PV: The excluded values are the result of the analysis conducted by MITECO.
> ➢ Sensibility exclusion layer for wind: As for PV systems, the excluded values are the result of the analysis conducted by MITECO.

This reclassification is valid both for PV systems and wind systems. To obtain this reclassification, the ArcGIS tool "Reclassify" is employed; the values representing the limit of each range are the ones resulting from the research work carried out in [5]. In addition, the exclusion layers produced by the research work in [34] are employed.

Concerning the parameter of the ground inclination, two different correlated layers are used in the creation of the suitability map, one with exclusion values and one with ponderation values. This is due to the nature of the parameter: increasing the inclination indeed, the complexity of the infrastructure increases, and consequently the cost increases. Over 15°, the inclination is not recommendable anymore; therefore, all the values higher than that are excluded.

2.3.2 Fuzzy logic

Fuzzy logic is a form of logic in which the truth value of variable can be any real number between "0" and "1"; thus, this logic differs from the Boolean one since it takes into account the concept of "partial truth", according to which the values can be only partially "true" or partially "false". Again, considering a raster layer, the value of each cell of the map, aside from the NO-DATA cells, will be reclassified as a value ranging between "0" and "1"; Since in a raster layer the parameters are represented in a continuous scale of values, it is necessary to identify a relationship that relates each value with a reclassified one, inside the range that stretches from "0" to "1". As for the exclusion layers, "0" is associate with a site unsuitable for a RES installation, while "1" with a site completely suitable; instead, all the values in between are associated with a different level of suitability, that increases moving from 0 to 1. The relationships that allow this type of reclassification, from the continuous scale of the parameter to the continuous scale from "0" to "1", also called "fuzzification", belong to the family of the "fuzzy memberships". In this work, the only two fuzzy memberships employed are the "linear increasing" and the "linear decreasing". In the first one, given a scale of continuous values, "0" is assigned to the lowest value of the scale, while "1" to the highest one; all the values in between will be reclassified as real number between "0" and "1" that increases as the parameter value increases. In an opposite way, with a "linear decreasing", "0" will be assigned to the highest value of the scale, "1" to the lowest one, while all the others will be reclassified as a real number within "0" and "1" that decreases as the parameter values increase. Linear increasing and decreasing memberships and the relative analytical expressions are represented in *Figure 2.14*, where $\mu(x)$ represents the value of the fuzzy set resulting from the fuzzy membership function, x represents the value of the parameter, and a and b represent the extremes of the range of values considered for the association. The parameters reclassified according to the Fuzzy logic and their correspondent fuzzy membership are listed in *Table 2.2*.
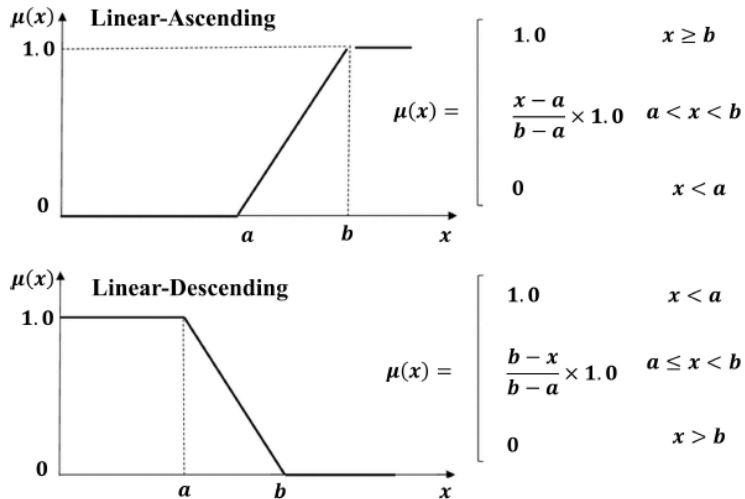
Figure 2.14 - Linear increasing and decreasing membership and respective analytical expression [31].

Table 2.2 - List of fuzzy parameters and associated fuzzy membership or categorization (own elaboration).

Parameter	Fuzzy Logic
Sensitivity ponderation layer for PV	Result of MITECO analysis
Sensitivity ponderation layer for wind	Result of MITECO analysis
Ground Inclination	[< 15 °] → Linear decreasing membership
Land Cover	Linear increasing membership
Electric Power Plant	Linear decreasing membership
Urban residential areas	Linear increasing membership
Rural residential areas	Linear increasing membership
Transport Network	Linear decreasing membership
Coastline	Linear increasing membership
Electrical grid	Linear decreasing membership
Electrical substation	Linear decreasing membership
Annual average daily solar irradiation	Linear increasing membership
Annual average wind speed	Linear increasing membership

This reclassification is valid both for PV systems and wind systems. The association with a particular membership is carried out through the tool "Fuzzy membership". Concerning distance from urban and rural residential areas and distance from coastline, the linear increasing membership is chosen, since the suitability of a site for a hybrid power plant increases with the increase of the distance from human settlements and from the coastline; indeed, this aspect allows to avoid inconveniences related to interference with human activities, environmental problems, and problems with the plant components life and efficiency. The same relationship is chosen for solar irradiation and wind speed: indeed, increasing the renewable resources available in one site, the level of suitability of the latter increases as well. Concerning ground inclination, distance from already existing power plant and substations, and distance from electrical and transport network, a relationship of linear decreasing is chosen; indeed, if these quantities increase, the complexity of hybrid power plant increases and new infrastructure are needed; therefore, the cost of construction and operation increases and the level of suitability of the considered site decreases.

Among these parameters, the layer corresponding to the land cover features a reclassification that is the result of the analysis carried out in [5]; in this analysis, the original layer represents a partition of the territory in polygons shown in *Appendix 1*.

According to the reclassification, a value among "0" and "5" was assigned to each polygon, providing a measure of how suitable the land is for a PV-Wind HPP, according to the natural or man-made element that occupies the land. In general, according to the most frequent type of partition used in the scientific literature concerning the land cover, the highest value of suitability is associated with lands presenting scarce or no vegetation. With the increase of complexity and dimension of the vegetation, the suitability level of a land decreases. Areas already employed for agriculture or human activities, or lands occupied by natural elements other than vegetation as glaciers or marshes are associated with a low or null value of suitability.

To be associated to a fuzzy membership, which is more appropriate to reclassify continuous variables and not categories, the following scale of value is employed, in order to recreate a linear increasing membership:

Table 2.3 - Categorization of land use parameter to represent it as a fuzzy parameter (own elaboration).

Category	Fuzzy membership value
0	0
1	0.2
2	0.4
3	0.6
4	0.8
5	1

Finally, the ponderation layers produced by the analysis carried out in [34] are employed.

2.4 Creation of the suitability map

To create the final suitability map, the available layers must be superimposed to obtain a single raster layer. In this thesis, no MCDM method is performed and no weights are assigned to the parameters; therefore, in the process of superimposing, the layers have the same weight, so that they will have the same importance, differently from the methodology followed in [5] and [34]. The general procedure, represented by means of the "Model builder" function of ArcGIS pro in *Figure 2.15*, consists in following two equals path for PV and wind, to obtain two final suitability maps for PV plants and for wind plants; then, the two layers are superimposed to generate the final hybrid suitability map.
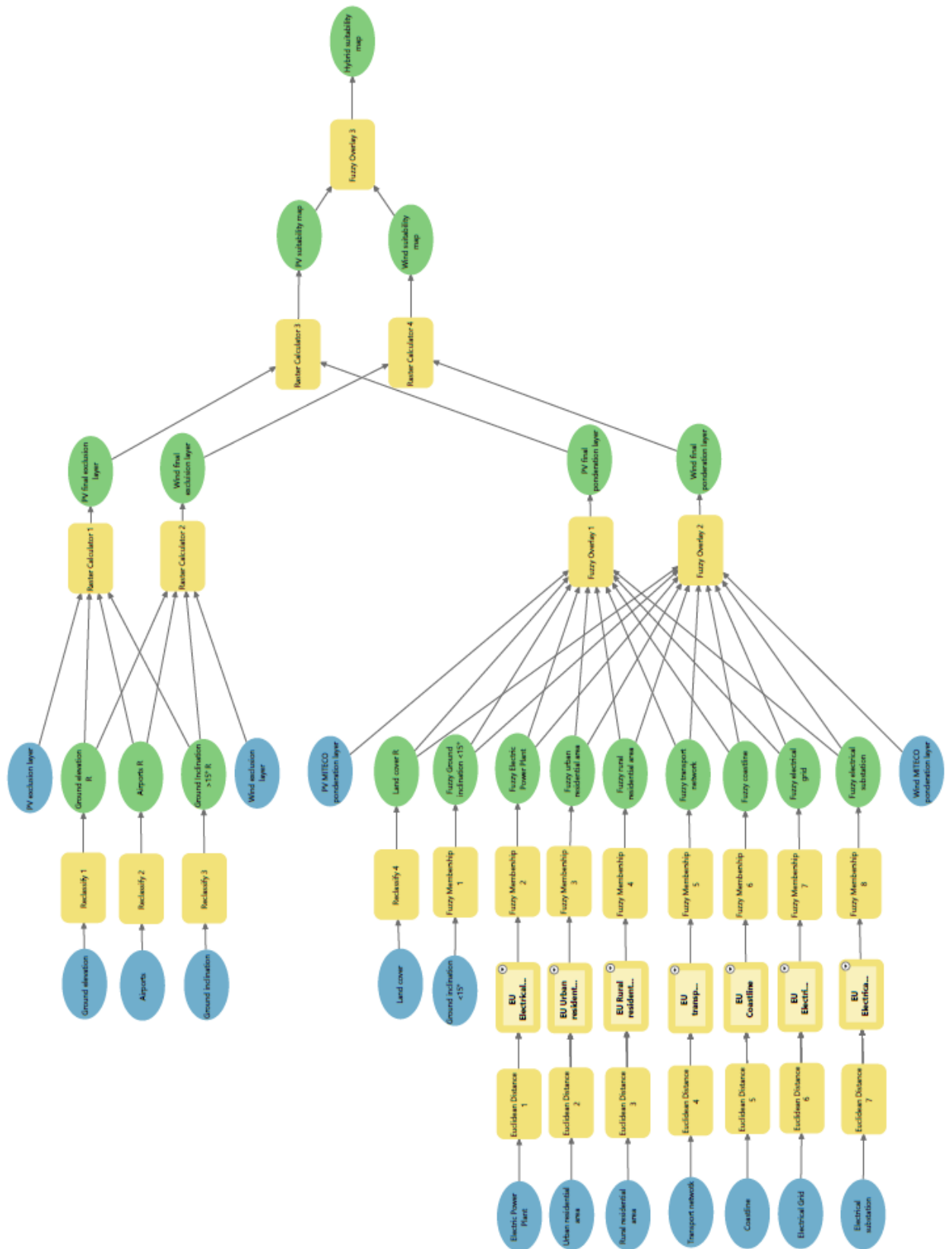
Figure 2.15 - Followed methodology to create a suitability map represented through the ArcGIS Pro Model Builder (own elaboration).

According to the methodology, in the first place, exclusion layers are overlapped performing a product executed with the tool "Raster calculator" of ArcGIS Pro; in this way, two final exclusion layers for PV and wind, consisting in cells with "0" and "1" values, are obtained. Then, considering the ponderation layers, they are superimposed through the tool "Fuzzy overlay"; the fuzzy operators and the corresponding expressions that can be used for the overlay are represented in *Figure 2.16* ([23]).

Type of function	Expression
AND	$\mu_x = Min(\mu_1, \mu_2, \mu_3, \cdots)$
OR	$\mu_x = Max(\mu_1, \mu_2, \mu_3, \cdots)$
PRODUCT	$\mu_{Product} = \prod_{i=1}^{n} \mu_i$
SUM	$\mu_{SUM} = 1 - \prod_{i=1}^{n}(1 - \mu_i)$
GAMMA	$\mu_\gamma = \prod_{i=1}^{n} \mu_i^{1-\gamma} \cdot (1 - \prod_{i=1}^{n}(1 - \mu_i))^\gamma$

Figure 2.16 - Fuzzy overlay functions and associated expressions [23].

In this work, the fuzzy GAMMA operator is chosen, corresponding to the expression:

$$\mu_\gamma = \prod_{i=1}^{n} \mu_i^{1-\gamma} \cdot \left(1 - \prod_{i=1}^{n}(1 - \mu_i)\right)^\gamma \qquad (2.5)$$

Where μ are the fuzzy membership functions, while n is the number of fuzzy membership functions. In the *equation 2.4.1*, γ can have a value between "0" and "1"; if γ = 1, the operation corresponds to the fuzzy "SUM", while if γ = 0, the operation corresponds to the fuzzy "PRODUCT". Fuzzy "AND" and "OR" correspond to intermediate values between the one that gives the SUM and the one that gives the PRODUCT. As stated in [23] and [36], the GAMMA function enables to balance multiple input criteria, in particular assuming γ = 0.9. Thus, using this operator with γ = 0.9, the ponderation layers are overlapped to obtain two final ponderation layers, one for PV plant and one for wind plant, consisting in cells with values in the range that stretches from "0" to "1". Final exclusion and ponderation layers are represented in *Appendix 2, Appendix 3, Appendix 4, Appendix 5.*

The exclusion and the ponderation layers are then multiplied by means of the tool "Raster calculator", and two final suitability layers for PV and wind systems are created (*Figure 2.17* and *Figure 2.18*).
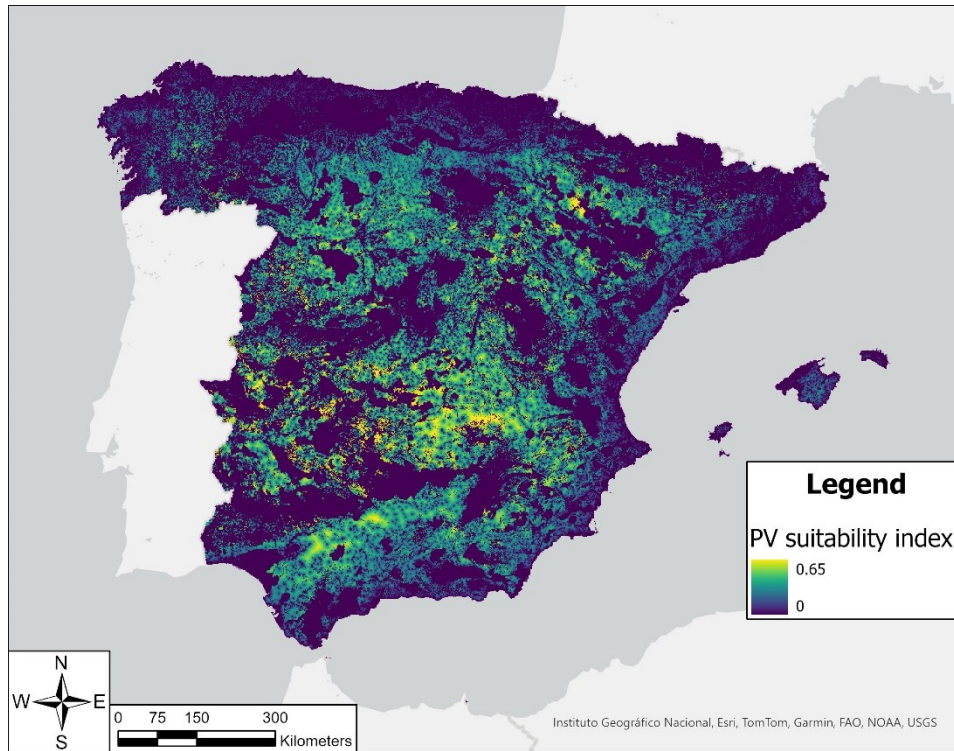
Figure 2.17 - Suitability map for PV systems (own elaboration).
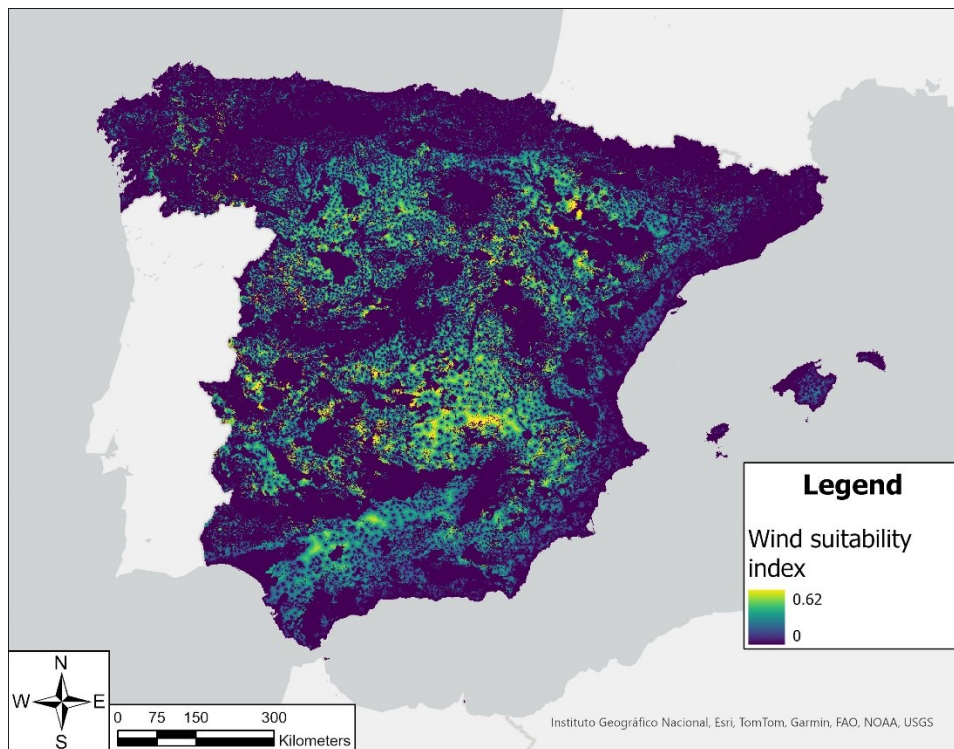
Figure 2.18 - Suitability map for wind systems (own elaboration).

These layers represent a suitability index employing a scale that stretches from "0 – Not Suitable" to "1 – Completely Suitable", equal to the scale of ponderation layers. As shown in *Figure 2.17* and *Figure 2.18*, however, the maximum value of the scale "1" is not

reached; instead, a maximum value of 0.65 for PV and 0.62 for wind systems are obtained. Thus, even for the most suitable sites, not all the parameters are favourable for RES installation.

To generate the hybrid suitability map, the PV suitability map and the Wind suitability map must be superimposed; to perform this operation, the tool "Fuzzy overlay" and the GAMMA operator with γ = 0.9 are used. The final result is represented in *Figure 2.19*.
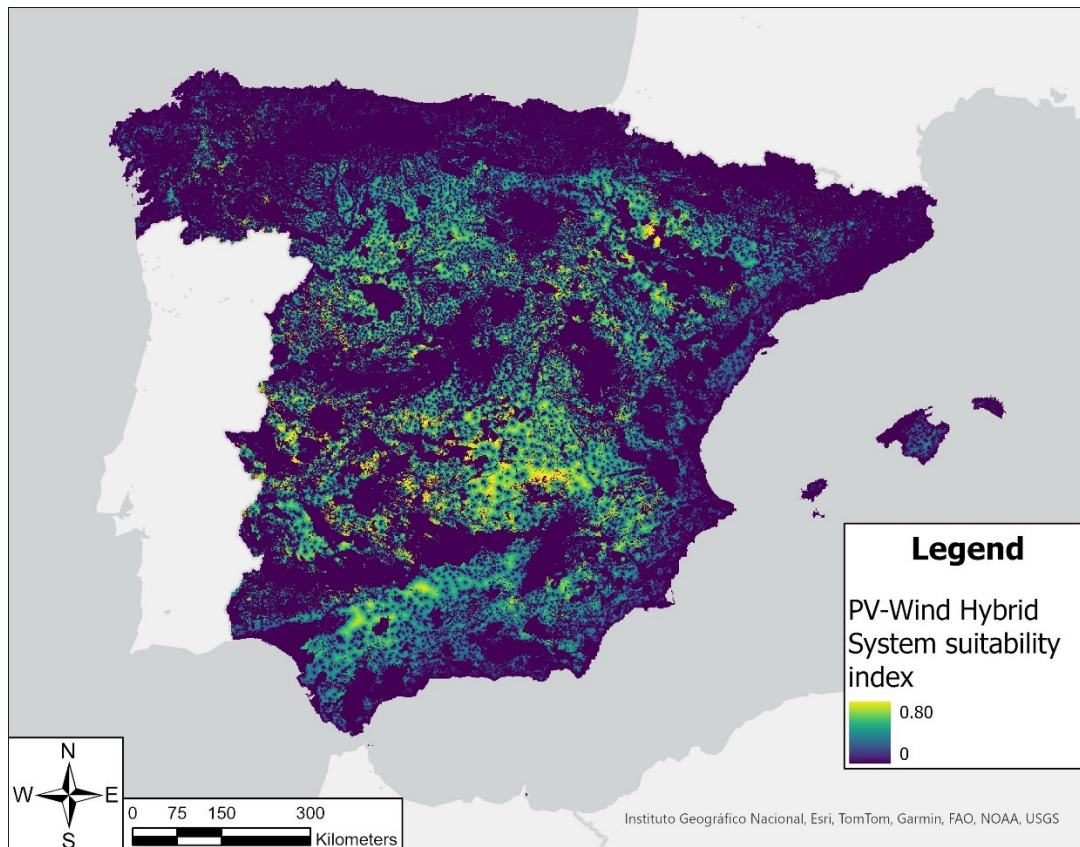
Figure 2.19 - Suitability map for PV-Wind Hybrid systems (own elaboration).

As demonstrated for PV and wind systems, the suitability index for PV-Wind HPP systems stretches from a "0" value (not suitable) to a maximum value of 0.80, lower than the maximum value of the suitability scale "1" (completely suitable). Thus, suitable sites can be characterized by not favourable values of some of the parameters of the analysis. Moreover, it is important to point out how all the parameters employed have the same weight; in the analysis of the profitability carried out in Chapter 3 and 4 however, solar irradiation and wind speed will be crucial for the evaluation of the available renewable sources, and ultimately of the profitability of a site. As a consequence, suitable sites can be characterized by different values of renewable sources availability, leading to different values of profitability for a hypothetical hybrid installation.

In addition, not all the study area is considered in the profitability analysis carried out in Chapter 3; indeed, the territory selected for the latter analysis corresponds only to the obtained suitable area where the suitability index is higher than 0.5, in absence of a more precise criteria to select the area for the analysis. This value is chosen arbitrarily, to make sure that the points chosen for the profitability analysis will have a higher chance of being characterized by a high profitability. Since a more precise criteria to individuate which sites can be considered for a profitability analysis is missing, a possible following development of this thesis could be focussed on this aspect. A comment on this choice according to results will be given in the conclusions. The territory with a suitability index higher than 0.5 is represented in *Figure 2.20*.
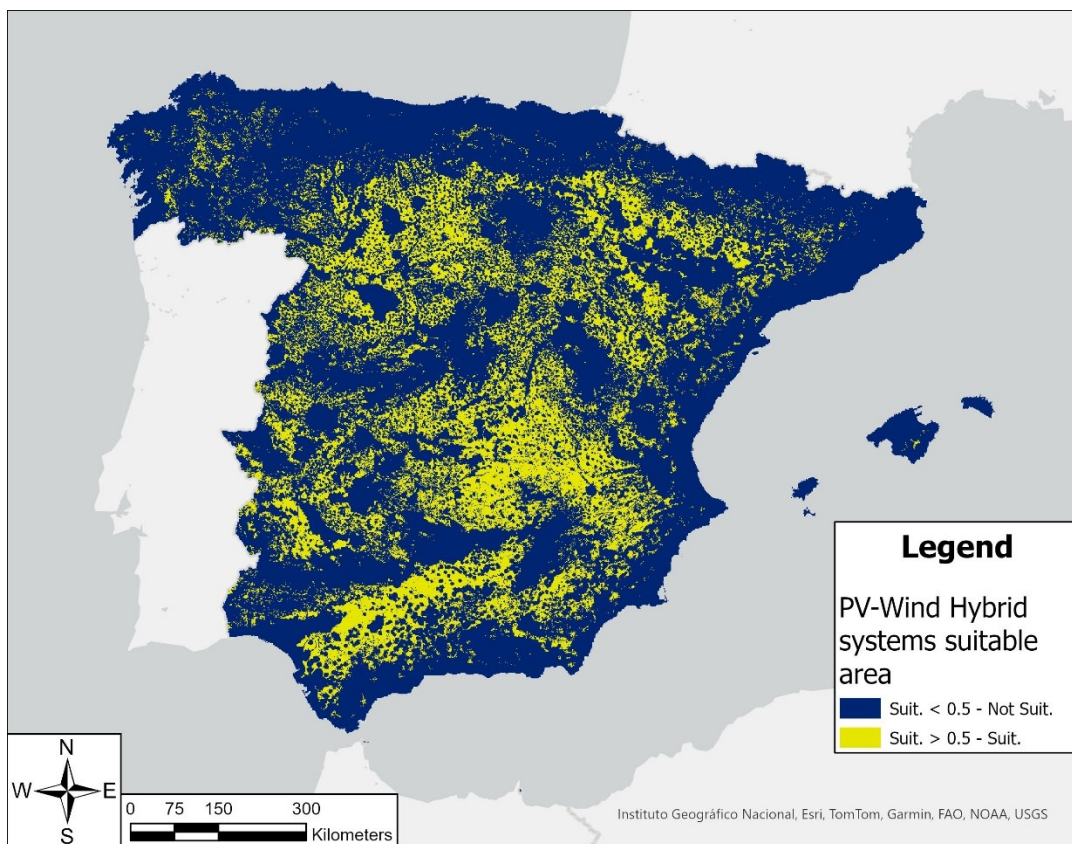
Figure 2.20 - PV-Wind HPP Suitable area map; in yellow, the area selected for the following profitability analysis; in blue the area excluded (own elaboration).

Considering the number of pixels that form the final raster layer, the percentage of the suitable area is calculated, and it is equal to 24.35% of the total considered area. Considering the spatial distribution, the percentage of suitable sites in each Autonomous Community of Spain included in the study area on the total study area is shown in *Table 3*; along with it, the relative land use in each Community is calculated, so that it is possible to identify which are the most suitable regions for hybrid installations.

Table 2.4 - Percentage of suitable area on the total study area and on the total Community area for each Autonomous Community (own elaboration).

Suitability index > 0.5		
Comunidad autónoma	% of suitable area on the total study area	% of suitable area on the total Community area
Andalusia	4.13	25.58
Aragon	2.65	26.70
Asturias	0.05	2.00
Balearic Islands	0.01	1.14
Basque Country	0.02	1.25
Cantabria	0.01	1.15
Castile and León	5.69	28.90
Castile–La Mancha	6.77	43.48
Catalonia	0.48	7.10
Extremadura	2.20	27.28
Galicia	0.50	7.88
La Rioja	0.20	18.83
Madrid	0.26	16.41
Murcia	0.56	26.28
Navarre	0.43	19.27
Valencia	0.40	8.77
Ceuta	0	0
Melilla	0	0

As shown in the table above, the Communities of Spain with the highest percentage of suitable area with respect to the total area considered are Andalusia (4.1%), Castile and León (5.7%) and Castilla–La Mancha (6.8%), where a consistent part of the sites with an index higher than 0.5 are located. In addition, it is important to take into account the extension of each Community: Andalusia (25.6%), Castile and León (28.9%) and Castilla–La Mancha (43.48%) are still among the Communities with the highest percentage of suitable area to the total Community area; however, considering the Communities with a percentage higher than 25%, Aragon (26.7%), Extremadura (27.28%), and Murcia (26.28%) represent Communities with an high presence of suitable sites. This high presence is due in general to favourable values of almost all the parameters in these Communities; concerning the renewable resources, in particular, high values of wind speed can be found in the South part of Andalusia and Castile-La Mancha, and in Aragon, while high values of solar radiation can be found in Andalusia and Murcia. Moreover, in Communities as Andalusia, Castile-La Mancha and Extremadura, numerous areas far from urban and rural

nucleus can be found. Finally, large sites regarded as suitable by MITECO according to the environmental sensitivity index are set in these regions.

Concerning the Communities with a low number of suitable sites, Ceuta, Melilla, Balearic Islands, Asturias, Basque Country and Cantabria are the ones less suitable for PV-Wind hybrid installations, having a percentage of suitable sites over the total suitable area and over the total Community area that is lower or equal than 0.1% and 2% respectively. Considering Ceuta and Melilla, the fact that their surfaces characterized by a small extension face the Mediterranean Sea leads to null values of the suitability index. Considering the Balearic Islands, the low number of suitable sites is due in particular to the parameters of the distance from the coastline and distance from urban areas, that present low values in the whole archipelago; instead, the north side of Mallorca possesses low values of suitability index due to the areas regarded as not recommendable by MITECO taking into account the parameters composing the environmental sensitivity index. Considering the Communities of Asturias, Cantabria, and Basque Country, in the North of Spain, they present a low number of suitable sites due in particular to the low values of the parameter of solar radiation, and to the low values of the parameters of distance from the coastline and distance from urban areas, especially in their North side. In addition, large areas of these Communities are regarded as not recommendable by MITECO, taking into account the environmental sensitivity index for wind plants.

Once the suitability map is created, a revision of the results is needed to check the consistency of the latter; this is performed in the next section.

2.5 Revision of the results

One of the main advantages of GIS software as ArcGIS Pro is the possibility of carrying out analysis "pixel by pixel", or "polygon by polygon", depending on the use of raster layers or polygon layers respectively. This allows to compare different sites, and to revise in each site which are the parameters with favourable or unfavourable values for the suitability. The reasons why a certain site is classified as not suitable can be therefore identified and discussed; this allows to check the consistency of the model, referring to the chosen area.

In this regard, to validate the results of the preliminary suitability analysis, four locations, correspondent to real world wind plant sites, are analysed; the choice of considering wind plant sites derives from the observation that one common practice to develop a PV-Wind HPP plant is by adding solar PV (and eventually a storage system) to already existent wind plants, overplanting or with a repowering; a particular contribution to the optimal design of this kind of systems is given in [37]. The chosen sites for the revision are shown in

Figure 2.21, Figure 2.22, Figure 2.23, Figure 2.24; all these sites are set in the suitable area resulting from the analysis:

a) Almonacid de la Cubilla, Zaragoza: 41.33° N; 0.85° W

The first site corresponds to one of the PV-Wind plant operating in Spain, placed in Aragon; in *Figure 2.21* on the left, the foundations of two wind turbines can be seen (the PV system is not shown). The whole area is placed in a suitable site, as shown in *Figure 2.21* on the right. In this area, the consistency of the model is demonstrated.
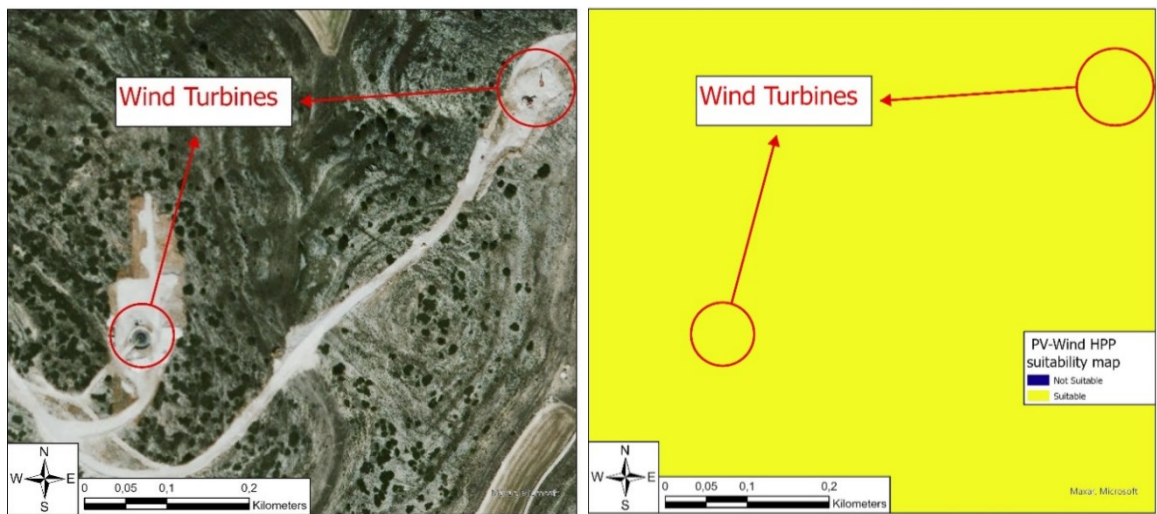
Figure 2.21 - Almonacid de la Cubilla, Zaragoza; first site considered to review the results of the suitability analysis (own elaboration).

b) Las Loras, Burgos: 42.75° N; 4.07° W

The second site analysed is a wind system in Castile and León. As shown in *Figure 2.22*, the rows of wind turbines (on the left) are placed almost completely in suitable areas (on the right). The model is therefore mostly consistent even on large scales, given the extent of the surface occupied by the wind plant. The few turbines placed in not suitable areas demonstrate however how in some cases the choice of the parameters of the model might penalise some areas that are actually profitable for renewable installations. This shows that even though the model is consistent for a preliminary evaluation of the suitability of an area, in a following step it is necessary to perform in-site measurements and observations in order to declare a site as a recommendable one.
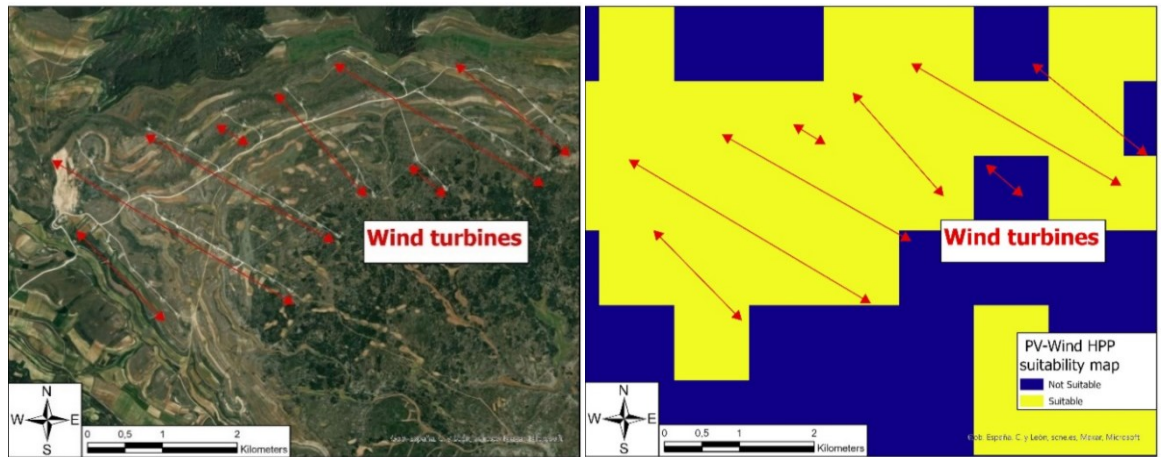
Figure 2.22 - Las Loras, Burgos; second site considered to review the results of the suitability analysis (own elaboration).

c) Molar del Molinar, Albacete: 38.69° N; 2.05° W

The third site represents another Wind-PV HPP operating in Castilla–La Mancha. In the *Figure* 2.23 four wind turbines are represented (the PV system is not shown); two of them result to be placed in a suitable area, while the other two in a not recommendable one; in this case, considering a small scale, another observation can be done: as stated, the resolution of the raster layers considered in the analysis is 1 km X 1 km. However, inside each pixel of 1 km^2, the values of the parameters can be different from the one associated with the pixel itself: an example is represented by the variations in the slope of the terrain, that can consistently vary locally. These local variations are not considered in the analysis due to the chosen resolution. Again, performing on-site measurements results determinant in the eligibility of a site.
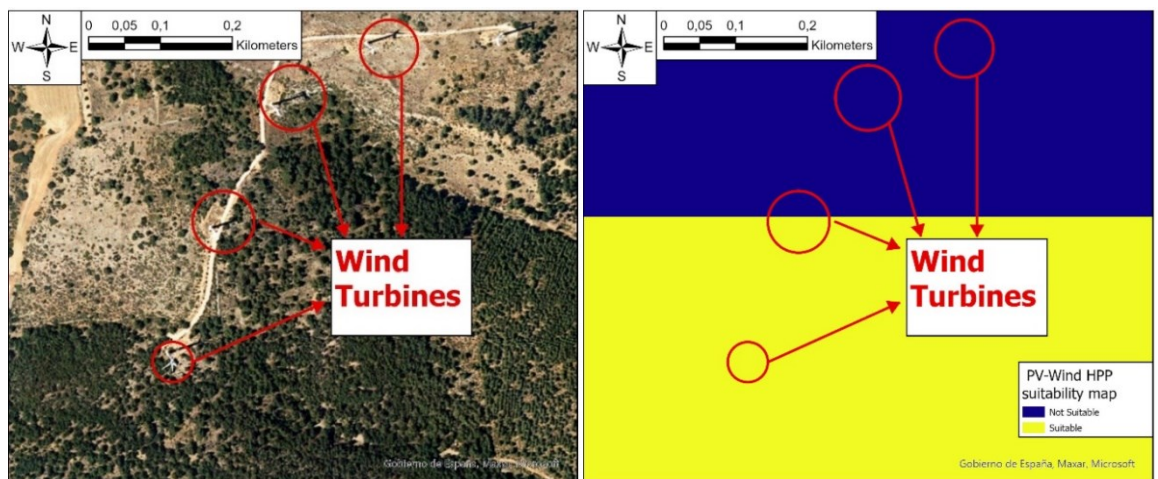
Figure 2.23 - Molar del Molinar, Albacete; third site considered to review the results of the suitability analysis (own elaboration).

d) La Herrería, Cádiz: 36.15° N; 5.72° W

The last site analysed in the revision is represented by a wind farm in Andalucia. In this case, the plant is completely located in a not suitable area (*Figure 2.24*). The model is therefore in contradiction with what can be observed in the real world, where the area has been considered both suitable and profitable for a renewable plant. The reasons why this area is excluded by the model can be investigated: indeed, one of the great advantages of the model built through a GIS software is the possibility of checking every parameter to identify which ones are the most unfavourable for an HPP installation. In this case, according to the classification assumed to perform the analysis, the site is excluded because it is placed too close to urban and rural residential areas and to the coast; this determines a value of the suitability index of 0.4, lower than the threshold value of 0.5, even if the nature of solar and wind sources results favourable for a PV-Wind system. This fact demonstrates the importance of choosing a consistent criterion to select the suitable lands.
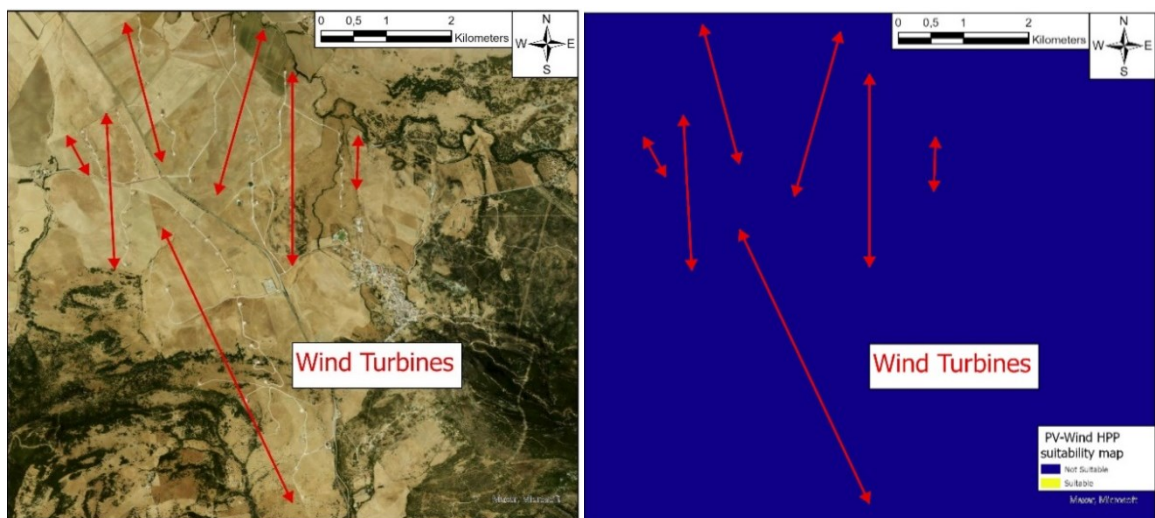
Figure 2.24 - La Herrería, Cádiz; fourth site considered to review the results of the suitability analysis (own elaboration).

In conclusion, this revision shows that the model is consistent; however, to avoid cases in which a site profitable for a hybrid installation is excluded in a preliminary suitability analysis, it is necessary to perform a more in-deep analysis of the type of parameters and of the reclassification range or relationship employed to carry out the creation of the suitability map. For example, considering the parameters of the slope and the elevation, the values over 15° and 1500 m respectively are excluded from the analysis; however, even if the construction complexity and the cost increase, the excluded area can still be available for a hybrid installation, and if it is characterized by a favourable presence of renewable resources, the HPP can still be profitable. Moreover, the land cover layer is composed of many types of elements, as it is shown in *Appendix 1*. A more detailed discussion must be

carried out on each element, to identify which can be suitable or not, and the level of suitability associated with the suitable ones.

Finally, the choice of selecting only the areas with a suitability index higher than 0.5 results in a conservative choice, eliminating from the selection hypothetical profitable areas. However, the extension of the available surface of a site affects the installable capacity of a hybrid plant; therefore, the study of the profitability of a hybrid system depends on the extension of the suitable area as well, and on the way this area is aggregated to form a potential installation site. Consequently, a more consistent selection criterion must be identified in a future research work.

3. Profitability assessment model

In the third chapter of the thesis work, a model for the sizing of a PV-Wind HPP and for the evaluation of its profitability is developed. This model will be employed in the next Chapter for the generation of a profitability map, where the areas suitable for the installation of hybrid systems are evaluated according to an economical index, the Internal Rate of Return (IRR). Indeed, the preliminary analysis carried out in Chapter 2 provides the areas where it is recommendable to install a PV-Wind system; however, as it will be demonstrated in the following sections, not all the sites are equally profitable. The profitability of a utility-scale PV-Wind HPP, measured through the IRR, depends indeed on revenues and costs of the system, that in turn depend on capacity of the plant, economical parameters, and produced energy according to the available solar and wind sources and to the energy injected in the electrical grid. Therefore, it is necessary to develop an approach that enables a) to find the "optimal" capacity of a hypothetical hybrid plant in each suitable site; and b) to compare each plant to find the most profitable sites.

The model created, based on a simple numerical sizing method applied for each suitable site, consists in: a) evaluating the available solar and wind resources; b) evaluating with a numerical method the energy produced by different combinations of PV power production and wind power production that comply with some initial assumptions; c) evaluating the total cost of each combination; d) evaluating the LCOE associated with the production of each combination and identifying the one characterized by the minimum LCOE; e) evaluating the cash flows of each year of useful life of the optimal combination and calculating its IRR. The general scheme of the methodology is represented below in *Figure 3.1*.

52
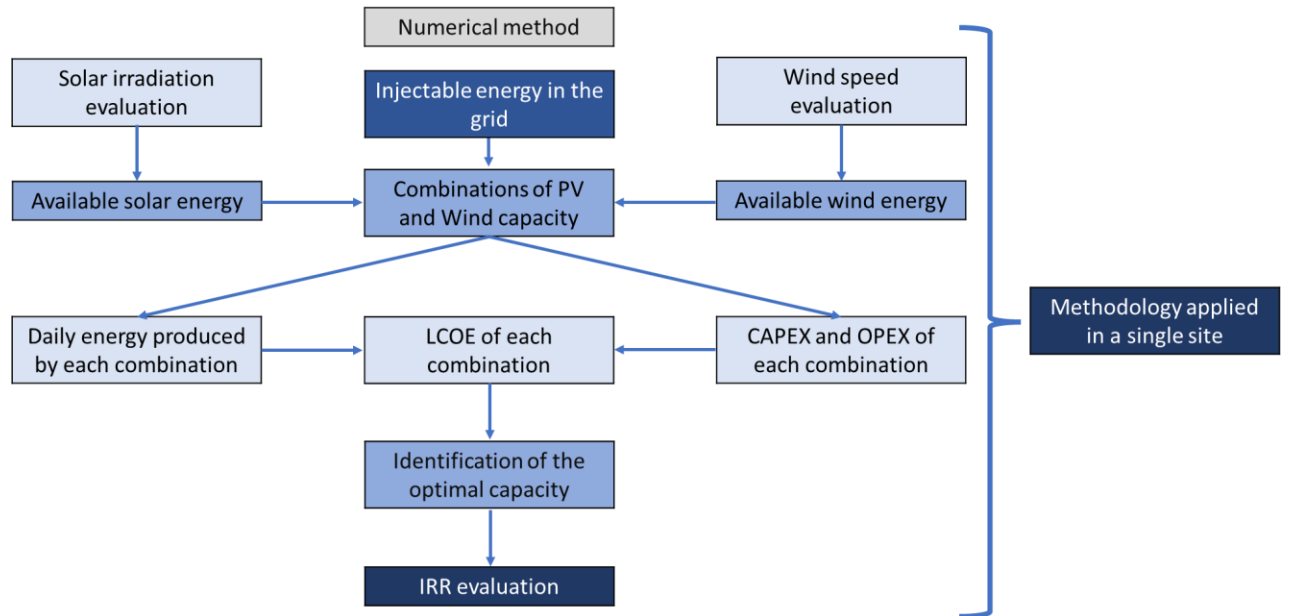
Figure 3.1 - Scheme of the profitability assessment model (own elaboration).

3.1 Evaluation of the available solar energy production

The available solar resource is evaluated in terms of Peak Sun Hours (PSH); in this thesis, PSH are defined as the equivalent number of hours needed to obtain, as a consequence of a solar irradiance of 1 kW/m^2, a quantity of energy equal to the daily one resulting from the average in-plane solar irradiance in a given site. Peak Sun Hours, expressed in [h/day], can be calculated as the ratio between the in-plane daily global irradiation in a given site [kWh/m^2] and a solar irradiance of 1 kW/m^2, that corresponds to the solar irradiance in standard condition (STC):

$$PSH = \frac{in-plane\ daily\ global\ irradiation}{STC\ irradiance} \tag{3.1}$$

As stated, to obtain the value of PSH of a given site, the daily global irradiation on the plane of the panels must be evaluated. As stated in the previous sections, the available data provided by CIEMAT regards the monthly average daily global irradiation on a horizontal plane in the study area. To calculate the monthly average daily global irradiation on an inclined plane, the table in *Appendix 6* is employed. This table is provided by CIEMAT and allows a quick evaluation of the solar resource without employing the use of any other model regarding the monthly solar irradiation. Indeed, the table concerns a factor K$_\beta$, defined as the ratio between the monthly average daily global irradiation on an inclined

plane and the one on a horizontal plane. This factor, resulting from data collected in the study area, is defined for a tilt angle β of an inclined PV panel equal to 30° and for different latitudes. As stated in *section 2.1,* the study area, that coincides with the Spanish peninsular territory, Balearic Islands, Ceuta and Melilla, extends from a latitude of about 35° N of Melilla to a one of about 43° N of the north end of the Iberian Peninsula; since Ceuta and Melilla are excluded by the suitability analysis carried out in Chapter 2, the lower extreme for the latitude range is represented by the south end of the Peninsula, at 36°00'08" N [32]. In addition, the available data regard a latitude range that stretches from 37° N to 43° N; therefore, for a given value x inside a range of given latitudes, the following values of latitude are assumed, so that the values of factor K_β can be associated to each value x of latitude inside the interval defined by the latitude extremes of the study area:

Table 3.1 - Latitude ranges and associated latitude for the model implementation (own elaboration).

LATITUDE RANGE IN THE MODEL	ASSOCIATED TABLE LATITUDE
$36 \leq x < 37.5$	37
$37.5 \leq x < 38.5$	38
$38.5 \leq x < 39.5$	39
$39.5 \leq x < 40.5$	40
$40.5 \leq x < 41.5$	41
$41.5 \leq x < 42.5$	42
$42.5 \leq x \leq 44$	43

In this thesis work, the assumed PV system composing the PV-Wind HPP consists of modules with a dual axis solar tracking system: this system allows to follow the sun path during the day, so that the tilt angle of the inclined module is always the optimal one, maximising the daily production of energy of the system. Thanks to this assumption, it is possible to consider for each latitude *l* and for each month *k* of the year the tilt angle that maximizes K_β as the one of the PV modules, to maximize the energy received in the inclined plane with respect to the one received on the horizontal one, simulating the effect of a dual axis solar tracking system. Thus, for a given site with a latitude correspondent to the range of latitudes *l* and for a given month *k*, $K_{\beta,l,k,max}$ is selected in the table, and the monthly average daily global irradiation $H_{\beta,l,k}$ [kWh/m^2/day] incident on the PV system is calculated as:

$$H_{\beta,l,k} = K_{\beta,l,k,max} \cdot H_{l,k} \tag{3.2}$$

With $H_{l,k}$ horizontal monthly average daily global irradiation for the latitude in the range l and the month k [kWh/m^2/day]. Subsequently, the PSH are expressed as:

$$PSH = \frac{H_{\beta,l,k}}{G_{STC}} \tag{3.3}$$

With G_{stc} global irradiance at the Standard Condition (1 kW/m^2)

Moreover, the energy received by the module is not the one actually produced by the system, due to thermal losses, conduction losses and energy consumption for operation. To take into account these energy losses, the Performance Ratio (PR) can be included in the analysis. As stated in [38], the performance ratio can be defined as the ratio of final PV system yield Y_f to that of reference yield Y_r:

$$PR = \frac{Y_f}{Y_r} \tag{3.4}$$

The final yield of the system Y_f is defined as the ratio of the final or actual energy output of the system [kWh] to the nominal output DC power [kW]:

$$Y_f = \frac{Final\ energy\ output}{Nominal\ DC\ power} \tag{3.5}$$

Meanwhile, the reference yield Y_r is the ratio between total in-plane irradiance [kWh/m^2] to the reference irradiance:

$$Y_r = \frac{Total\ in-plane\ irradiance}{STC\ irradiance} \tag{3.6}$$

The PV reference irradiance at Standard Condition (STC) is equal to 1 kW/m^2. The reference yield depends on the location where the evaluation is carried out. It can be noted that the reference yield coincides with the quantity of the Peak Sun Hours if it is expressed in daily terms; therefore, the daily final yield of a PV system, expressed as [h/day], can be expressed as:

$$PR = \frac{Y_f}{PSH} \rightarrow Y_f = PR \cdot PSH \qquad\qquad (3.7)$$

Following this methodology it is possible to evaluate the available solar source of the PV system composing the PV-Wind HPP in terms of PSH and the energy produced by the plant itself Y_f; another methodology for the calculation of the in-plane daily global irradiation on a month basis starting from values of global irradiation on an horizontal plane is the one consisting of decomposing the global irradiation in direct, diffuse and albedo irradiation. However, methodology as the latter requires computational efforts that lead to increase of the computational time associated with the execution of the model in a GIS software, an increase that might be consistent in some cases.

In addition, a dual axis solar tracking system is assumed to be employed in the PV system; however, this type of system is expensive and might lead to a considerable increase of cost of installation, maintenance, and operations. Other types of systems are available in the market, such as the one axis solar tracking system; it is opportune that future development of this research explores these possibilities, studying the effects on the overall costs and energy production, which affect the final result of the profitability analysis.

3.2 Evaluation of the available wind energy production

The available wind energy is dependent on the wind speed in each location, represented as monthly averages in twelve monthly layers, as already exposed in *section 2.2.1*. To calculate the wind energy production starting from these data it is possible to exploit the research work in [39]. Indeed, as demonstrated, the relationship between wind speed and energy production can be reasonably assumed as linear at monthly timescale, involving a simplification with respect to other procedures that require finer temporal resolution data. To exploit this relationship, the yearly average energy production curve of a V150- 6 MW – IEC S Vestas wind turbine [40], represented in *Figure 3.2*, is taken as reference.
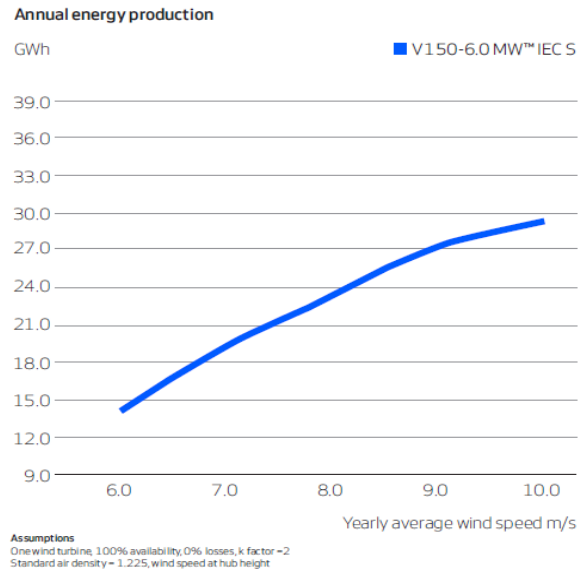
Figure 3.2 - *Annual energy production as a function of the yearly average wind speed for the wind turbine chosen as reference in the model [40].*

This curve is approximated for annual average values by a linear curve, represented by the extrapolated relationship:

$$E_w = 4.5 \cdot v - 12.9 \tag{3.8}$$

Where E_w [GWh] is the annual average energy produced by the wind turbine and v [m/s] is the yearly average wind speed at hub height. In a single site however, the actual production of energy depends on the number of turbines in the area and on their power, i.e. on the capacity of the wind plant hypothetically installed; therefore, the *equation 3.8* must be corrected. Since the raster layers considered have a resolution of 1 km^2, the parameter taken as reference to evaluate the hypothetical wind installed capacity is the wind power installable in 1 km^2. In addition, since the solar irradiation is expressed in monthly average daily values, the wind energy produced is expressed with the same unit of measurement, to be compared with the available solar irradiation expressed in monthly average daily values as well. This is possible considering monthly average values for the wind speed. Thus, the expression of the monthly average daily wind energy production $E_{w,k}$, expressed in [MWh/km^2/day], is:

$$E_{w,k} = \left(1000 \cdot \frac{P_{eol}}{365 \cdot P_{turb}}\right) \cdot (4.5 \cdot v_k - 12.9) \tag{3.9}$$

57

Where P_{eol} is the wind power installable in 1 km^2 [MW/km^2], while P_{turb} is the power of a single turbine [MW]. In the case considered in this thesis, P_{turb} will be assumed equal to 6 MW; instead, as shown in Chapter 4, P_{eol} will be assumed equal to the maximum wind capacity installable in 1 km^2 $P_{eol,max}$.

As can be pointed out, solar irradiation and wind speed are considered both in the suitability analysis and in the profitability evaluation model; however, while in Chapter 2 the annual average daily values (one per site) of the quantities are considered, in the model of this Chapter the monthly average daily values (twelve per site) are used to calculate the solar and wind energy potential. In this thesis, the average annual values of the two variables, obtained as average of the monthly values, are employed to exclude in advance all the sites where the renewable resources are not sufficient to guarantee a profitable exploitation by means of a power plant; this leads to a reduction of the number of sites considered in profitability calculation, reducing the computational cost and time of the Python algorithm that will be discussed in Chapter 4.

3.3 Numerical method for the evaluation of the hybrid system size

To evaluate the capacity of a hypothetical hybrid system in each location, a numerical method is employed. In this thesis, the considered utility-scale hybrid system consists of two components: a wind plant and a PV plant. To evaluate the size of this type of HPP, the capacity of each component must be calculated. In the literature various studies deal with the sizing and optimization of a hybrid plant, both stand-alone and utility-scale; a comprehensive review of design technologies for hybrid power systems for off-grid location can be found in [41]; meanwhile, a review of sizing methods and optimization techniques focused on PV-Wind HPP can be found in [42]. The tools and methodologies that can be employed for the sizing and optimization of an HPP are many; it is important to differentiate between the approaches delineated for off-grid stand-alone systems and the ones concerning grid-connected HPP, due to the differences between the two types of systems. In the following *section 3.3.1*, a sizing method based on a previous research work on stand-alone systems is presented; this method represents the foundation of the numerical method of *section 3.3.2*, that will be implemented in ArcGIS Pro for the profitability analysis, as discussed in Chapter 4.

3.3.1 Analytical method based on the energy demand

The first method considered for the sizing of a PV-Wind HPP is developed starting from the research work carried out in [43] and [44], that concerns an approach to size an isolated PV-Wind installation. The approach employed in this previous work is based on simple equations between parameters that characterize an off-grid hybrid plant, with the aim of providing a simple method for a preliminary feasibility study. The method consists of:

a) Evaluating the average energy consumption of the load E_{load} [kWh/day].
   The stand-alone HPP is assumed to be connected to loads that are characterized by a daily average consumption of energy; the goal of the HPP plant is to satisfy them in every month of the year. The demand of energy is estimated, taking into account also the losses through the efficiency of the installations by means of a coefficient defined as "performance ratio" of the load PR_{load}.

b) Evaluating the available solar resource.
   The available solar resource is evaluated in terms of Peak Sun Hours PSH [h/day], as for the evaluation of this thesis work presented in *section 3.1*. Indeed, this evaluation involves the collection of data on the horizontal daily global irradiation in the site where the PV system is installed and the calculation of the in-plane daily global irradiation taking into account the characteristics of the modules.

c) Evaluating the available wind resource.
   The available wind resource is evaluated in terms of Daily Eolic Density (DED) [kWh/m^2/day], i.e. the energy that can be extracted from the wind on a unit of swept surface, in the site where the wind turbine is installed. The efficiency of the wind turbine is taken into account by means of a coefficient η_{eol}.

d) Evaluating the relationship between the area of the wind turbine rotor A_{eol} and the peak power of the photovoltaic plant P_{pv} for each month of the year *i*.
   Considering a PV-Wind HPP, the average daily energy produced in each month must be higher than the average daily energy consumed by the load. In this way, it is possible to represent this condition for each month of the year by means of twelve inequalities representing the wind turbine area in function of the peak power of the PV system:

$$\frac{E_{load}}{PR_{load}} \leq A_{eol} \cdot DED_i \cdot \eta_{eol} + P_{pv} \cdot PSH_i, \forall 1 < i < 12 \qquad (3.10)$$

These expressions, considering the equal sign in the inequality, are represented in the plane A_{eol}-P_{pv} as twelve straight lines (an example can be found in *Figure 3.3*).

Figure 3.3 - Monthly relationship between the swept surface of a wind turbine and the associated PV system capacity for each month of the year, to satisfy a determined demand of energy (own elaboration).

e) Evaluating the combinations of wind turbine surface and PV power that comply with the energy condition expressed in *equation 3.10.*

It is possible to point out that, in the plane A_{eol}-P_{pv}, the curve of solutions that complies with the condition concerning the average daily energy produced by the system higher than the average daily energy consumed by the load in every month is determined by the branches of the lines that occupy an higher position (in the example *Figure 3.3*, these lines correspond to the months of August and January). The reason is the fact that if the condition is respected in the "worst" months with the highest request of wind power (related to the turbine surface) and PV power, then the system is capable of satisfying the demand even in the other months. Therefore, selecting a hybrid solution, for the worst months every value of A_{eol} corresponds to a value of P_{pv} capable of complying with the assumed energy condition.

f) Evaluating the solution with the minimum cost.

Starting from the costs per unit of peak power for PV systems and per unit of rotor surface for wind systems, the total costs of each suitable solution is calculated. Among all the possible solutions identified in point e), the one with the minimum total cost is selected as the optimal one for the Hybrid systems. For some sites, it is possible to find an optimal solution that coincides either with a wind system alone, or with a PV system alone; in those cases, the hybrid solution is not the most convenient one for the given site.

As stated, this method is developed for stand-alone systems; however, the hybrid system considered in the thesis is a utility-scale system connected to the grid. Generally, in sizing a stand-alone system, the aim of the process is satisfying a determined demand of energy, depending on the user. To find the optimal size it is therefore necessary to identify the minimum size that on one hand allows to satisfy the load demand and on the other corresponds to the minimum employment of economic resources. In sizing a utility-scale grid-connected hybrid system however, as stated in [37], the process aims at maximizing profits deriving from the electric energy sale. As explained in the following sections, in this thesis it is assumed that the electrical energy is sold to an off-taker through a PPA contract; therefore, in this case, the demand of energy to satisfy corresponds to the amount of energy that the supplier must provide as stated in contracts. Trivially, the greater the quantity of energy sold, the greater the profit. Additionally, the quantity of energy that can be injected in the grid is considered to be limited by its maximum evacuation capacity. As a consequence, to maximize the profits and enhance the value of an HPP, the supplier must generate a maximum power close to the maximum evacuation capacity. This concept is at the foundation of the sizing procedure employed in this work.

Taking the methodology developed in [43] and [44] as reference, a first method to find the optimal size of a hybrid plant in a given site is developed. In summary, the aim of the method is to identify a relationship between the capacity of the PV plant P_{pv} [MW] and the one of the wind plant P_{eol} composing the HPP for each month of the year; the fundamental assumption of the method is that the relationship between the two capacities enables to find for each capacity of the wind plant a capacity of the PV plant, so that the combination of the two composes an hybrid system capable of satisfying a given demand of energy in each month of the year. In the method for the stand-alone system, this demand is the energy requested by loads connected to the hybrid system E_{load} [kWh/day]. Similarly, in the case studied in this thesis, concerning a system connected to the grid, a value of energy effectively injected in the grid E_{in} [MWh/day] can be assumed at the beginning of the analysis as the demand the HPP plant has to satisfy. The value of E_{in} can be fixed referring to the energy that is sold to an off-taker according to a contract, and it is limited by the maximum energy that can be injected in the grid $E_{in,max}$ [MWh/day], depending on the maximum evacuation capacity. Therefore, in each month of the year the HPP must produce a quantity of energy equal or greater than E_{in}. To assure this, a linear relationship between the capacity of the PV plant and the capacity of the wind plant is assumed. The relationship $P_{eol} = f(P_{pv})$ can be represented in a plane P_{eol}-P_{pv}; for each month of the year, a linear curve is represented once two points of the curve itself are found. To calculate these two points, the cases in which either P_{eol} or P_{pv} are equal to zero are taken into account; the conceptual meaning of this two points are respectively the power of the PV plant needed to satisfy the demand of energy in a particular month assuming that the power of the wind plant is null, and the power of the wind plant needed to satisfy the same demand in the same month assuming that the power of the PV plant is null. In this way, the two points correspond to

the intersection between a linear curve and the y-axis and the x-axis respectively. Therefore, two points for each month of the year are calculated, and twelve linear curves can be represented in the plane P_{eol}-P_{pv}. An example of the resulting representation is shown below in *Figure 3.4*.
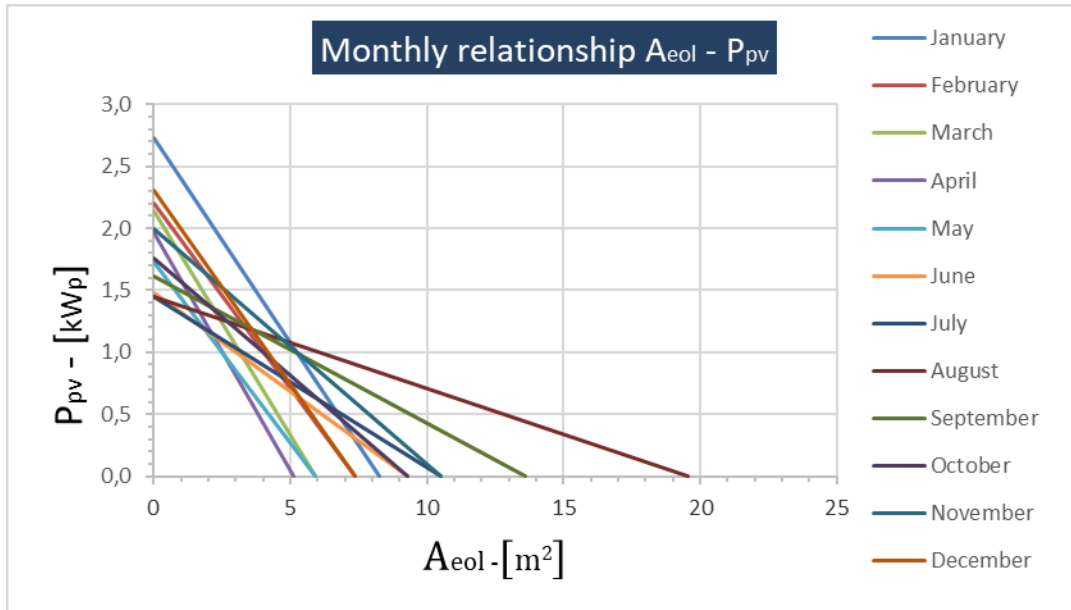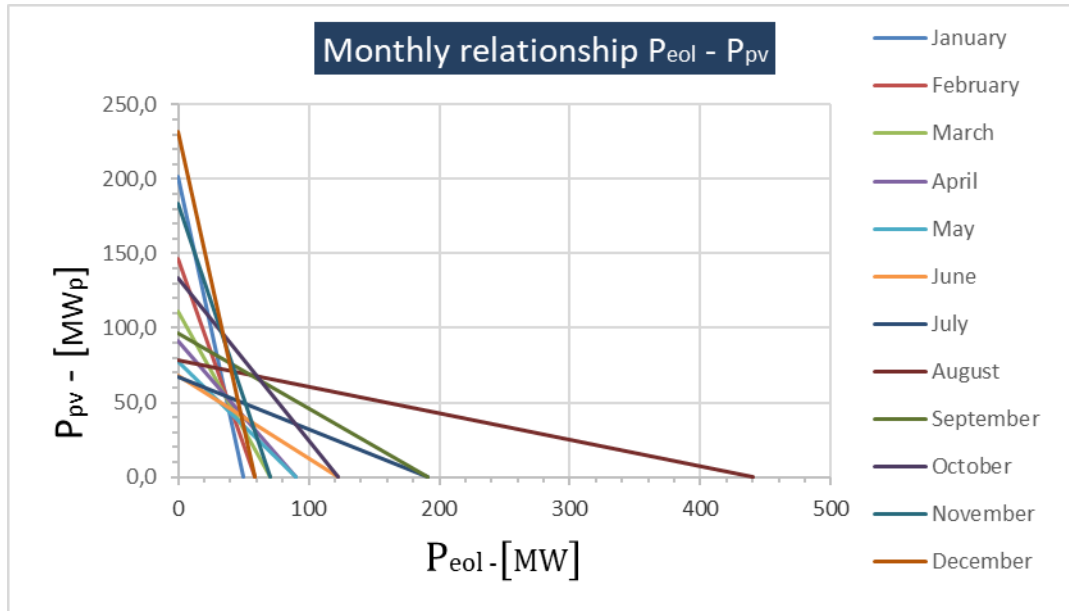

Figure 3.4 - Monthly relationship between the wind system capacity and the associated PV system capacity for each month of the year, to satisfy a determined demand of energy (own elaboration).

The two points needed for the representations are calculated for each month of the year k as follows:

a) The wind power $P_{eol,k,0}$ needed when the PV power $P_{pv,k}$ is null to satisfy the demand E_{in} is calculated through a proportion, considering the energy $E_{w,k}$ produced by the maximum wind power installable in 1 km² $P_{eol,max}$ [MWh/km²]:

$$\frac{P_{eol,k,0}}{E_{in}} = \frac{P_{eol,max}}{E_{w,k}} \rightarrow P_{eol,k,0} = \frac{P_{eol,max}}{E_{w,k}} \cdot E_{in} \qquad (3.11)$$

b) The PV power $P_{pv,k,0}$ needed when the wind power $P_{eol,k}$ is null to satisfy the demand E_{in} is calculated considering the Peak Sun Hours PSH_k:

$$P_{pv,k,0} = \frac{E_{in}}{PSH_k} \qquad (3.12)$$

With these points ($P_{eol,k,0}$, 0) and (0, $P_{pv,k,0}$) in the plant P_{eol} - P_{pv} it is possible to find the equation of the linear curves, expressed as:

$$y = mx + b \tag{3.13}$$

Indeed:

$$m_k = -\frac{P_{pv,k,0}}{P_{eol,k,0}}; \tag{3.14}$$

$$b_k = P_{pv,k,0} \tag{3.15}$$

The linear relationship $P_{eol} = f(P_{pv})$ corresponding to the month k is therefore:

$$P_{pv,k} = m_k P_{eol,k} + b_k \tag{3.16}$$

Represented the linear curves, the next step is considering which is the "worst wind month": this corresponds to the month in which, given the capacity of the PV plant equal to zero, the capacity of the wind plant $P_{eol,k,0}$ requested to satisfy the demand is the highest among all the months. In this way, if such a capacity is installed, it will be enough to satisfy the demand of energy in all the other months, where $P_{eol,k,0}$ will be lower. The highest among all the $P_{eol,k,0}$, that will be renamed $P_{eol,max}$, represents the reference for the numerical method employed for the sizing process. Indeed, the latter is performed by subdividing this quantity $P_{eol,max}$ in equal intervals; the length and the number of the intervals are arbitrary (*Figure 3.5*).
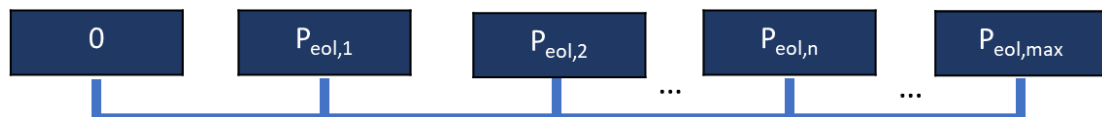
Figure 3.5 - Subdivision of Peol,max in equal intervals (own elaboration).

Then, for each $P_{eol,i}$, identified as upper extreme of the interval i, (the lower extreme of the first interval will be 0, while the upper extreme of the last interval will be $P_{eol,max}$), the capacity of the PV plant $P_{pv,i,k}$ needed to satisfy the demand in each month k is calculated through the *equation 3.16* (*Figure 3.6*).

	0	$P_{eol,1}$	$P_{eol,2}$	$P_{eol,n}$	$P_{eol,max}$
January	$P_{pv,0,1}$	$P_{pv,1,1}$	$P_{pv,2,1}$	$P_{pv,n,1}$	$P_{pv,max,1}$
February	$P_{pv,0,2}$	$P_{pv,1,2}$	$P_{pv,2,2}$	$P_{pv,n,2}$	$P_{pv,max,2}$
...	...	...	...	...	...
k-month	$P_{pv,0,k}$	$P_{pv,1,k}$	$P_{pv,2,k}$	$P_{pv,n,k}$	$P_{pv,max,k}$
...	...	...	...	...	...
December	$P_{pv,0,12}$	$P_{pv,1,12}$	$P_{pv,2,12}$	$P_{pv,n,12}$	$P_{pv,max,12}$
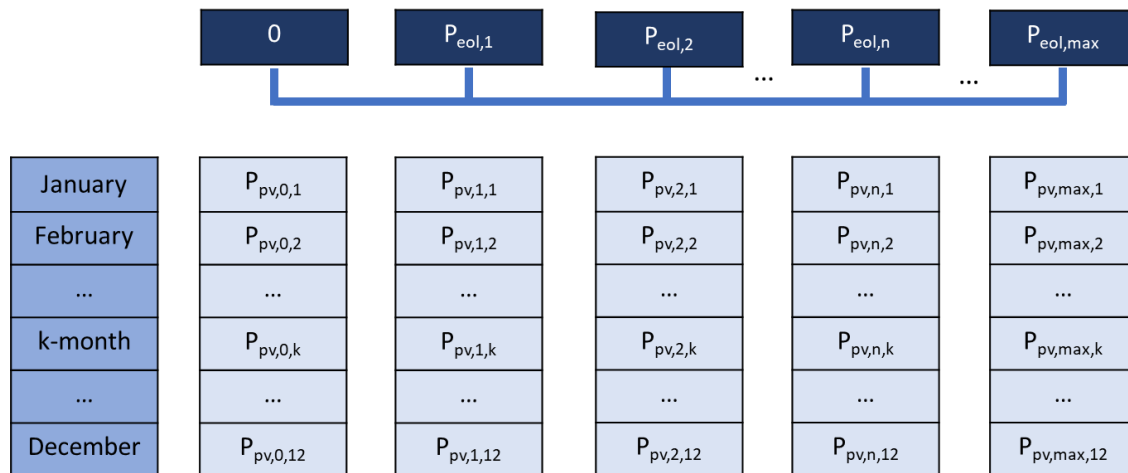
Figure 3.6 - Calculation of the PV system capacity to satisfy the demand of energy for each wind system capacity and for each month of the year (own elaboration).

To identify a combination of capacity of the PV plant and capacity of the wind plant to install to satisfy the demand of each month, each $P_{eol,i}$ can be coupled only with the maximum capacity $P_{pv,i,k}$, related to $P_{eol,i}$ itself. Indeed, if the demand of energy is satisfied for the month in which the capacity of the PV plant requested is the highest, the capacity will be enough to satisfy the demand in every other month. The maximum among each list of $P_{pv,i,k}$ related to $P_{eol,i}$ will be renominated $P_{pv,i}$ (*Figure 3.7*).

	0	$P_{eol,1}$	$P_{eol,2}$	$P_{eol,n}$	$P_{eol,max}$
January	$P_{pv,0,1}$	$P_{pv,1,1}$	$P_{pv,2,1}$	$P_{pv,n,1}$	$P_{pv,max,1}$
February	$P_{pv,0,2}$	$P_{pv,1,2}$	$P_{pv,2,2}$	$P_{pv,n,2}$	$P_{pv,max,2}$
...	...	...	...	...	...
k-month	$P_{pv,0,k}$	$P_{pv,1,k}$	$P_{pv,2,k}$	$P_{pv,n,k}$	$P_{pv,max,k}$
...	...	...	...	...	...
December	$P_{pv,0,12}$	$P_{pv,1,12}$	$P_{pv,2,12}$	$P_{pv,n,12}$	$P_{pv,max,12}$
	$P_{pv,max}$	$P_{pv,1}$	$P_{pv,2}$	$P_{pv,n}$	0
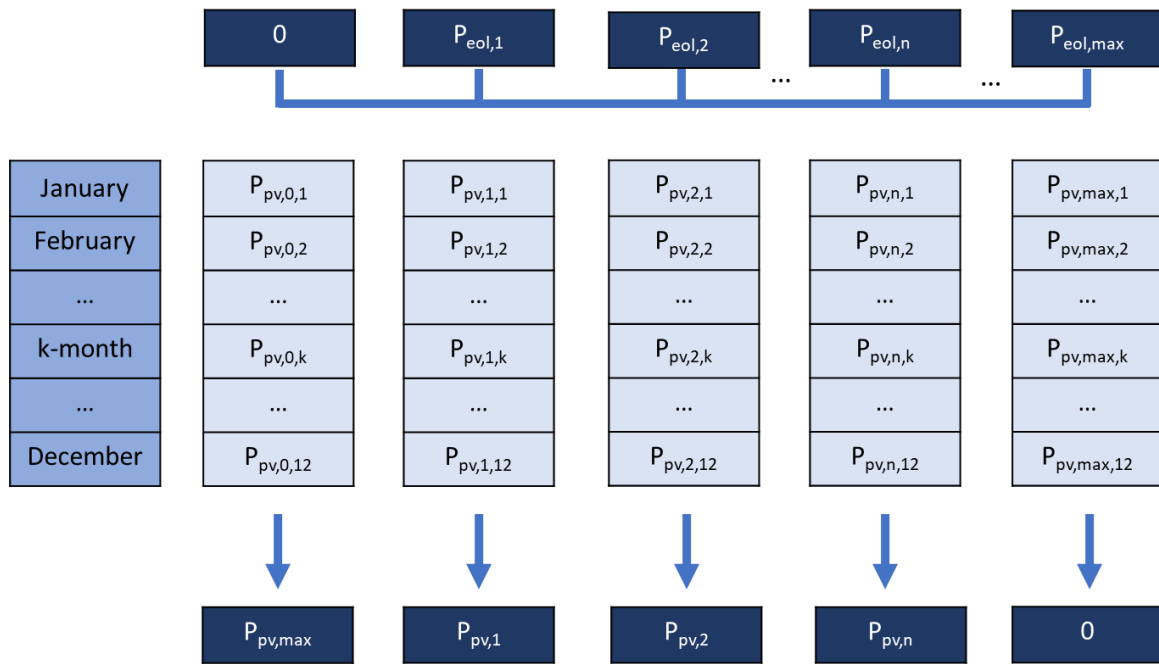
Figure 3.7 - Calculation of the highest PV system capacity to satisfy the demand of energy for each wind system capacity (own elaboration).

At this point, what is available is a number of i+1 combinations of PV and wind capacities, starting from the couple $(0, P_{pv,k,0})$, till the couple $(P_{eol,max}, 0)$; thus, it is necessary to define a criterion to select the optimal one, as it will be discussed in *section 3.5*.

The approach discussed above is not the only one that could be employed; in particular, another "pure" numerical method can be developed. This method will be discussed in the following section.

3.3.2 Numerical method based on the maximum energy injectable in the grid

As already discussed in *section 3.3.1,* the electrical grid is characterized by a value of maximum energy injectable; this value can be considered to develop another numerical method. As the previous method, the PV-Wind HPP is considered as connected to the grid, and it must produce a quantity of energy that is contracted with an off-taker.

Considering a national electrical network, the maximum evacuation capacity of the grid varies from point to point; consequently, to perform an analysis on the energy that a utility-scale RES system can produce, data regarding the evacuation capacity of the grid and of its substations are needed. However, at the time when this research work was carried out, the investigation on this type of data was not performed. Thus, a constant value of maximum evacuation capacity is assumed for the totality of the area considered. This value of power

is subsequently translated in terms of daily maximum energy injectable in the grid, as indicated below:

$$E_{in,max} = P_{in,max} \cdot 24 \qquad (3.17)$$

With $E_{in,max}$ [MWh/day] as maximum energy injectable in the grid and $P_{in,max}$ [MW] as maximum evacuation capacity. Moreover, a range of "flexibility" in the energy production is assumed, to take into account the possibility of injecting in the grid less than the maximum value of energy injectable. As a consequence, the daily energy E_{in} [MWh/day] that the hybrid system inject effectively in the grid will be:

$$E_{in} = f \cdot P_{in,max} \cdot 24 \qquad (3.18)$$

With f [%] as fraction of energy that the producer commits to sell to an off-taker. So, once $P_{in,max}$ and f are set, the capacity of the PV and wind plant composing the HPP have to produce together a quantity of energy that is greater or equal to a constant value E_{in} to maximize profits.

From this point on, the sizing procedure follows a pure numerical method, starting from the maximum values of capacity of PV systems and wind systems that can be installed in 1 km². First, $P_{eol,max}$ [MW/km²] and $P_{pv,max}$ [MW/km²] are subdivided into equal intervals; the number and length of each interval is arbitrary and affects the time of execution of the simulations that will be carried out during the implementation of the model (*Figure 3.8*).
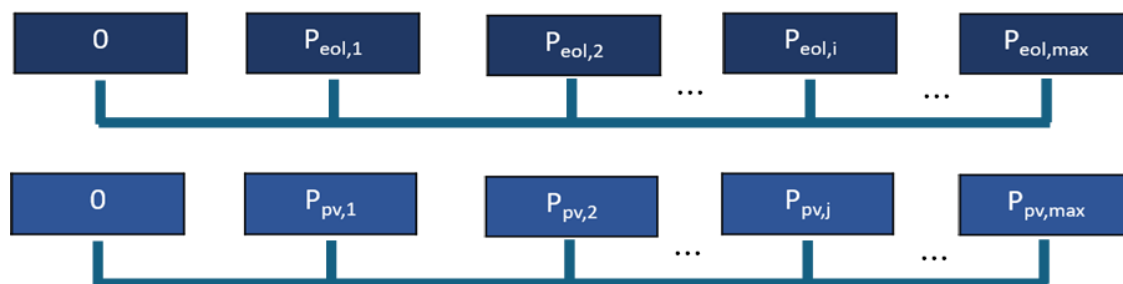
Figure 3.8 - Subdivision of Peol,max and Ppv,max in equal intervals (own elaboration).

Every combination of $P_{w,i}$ and $P_{pv,j}$ is considered as the hypothetical size of the PV plant and wind plant composing the HPP. Then, the monthly average daily total production of energy $E_{i,j,k}$ related to each combination of capacities *(i,j)* and related to each month *k* of

the year is calculated as sum of the monthly average daily production of energy deriving from the PV plant $E_{pv,j,k}$ and the one deriving from the wind plant $E_{eol,i,k}$ (*Figure 3.9*):

$$E_{i,j,k} = E_{eol,i,k} + E_{pv,j,k} \tag{3.19}$$

$E_{eol,i,k}$ is calculated with a proportion, considering the energy $E_{w,k}$ related to the month k produced by a capacity equal to the maximum installable capacity in 1 km^2 $P_{eol,max}$, calculated as in *section 3.2*, and the power of the wind plant $P_{eol,i}$ of the correspondent combination i:

$$\frac{E_{eol,i,k}}{P_{eol,i}} = \frac{E_{w,k}}{P_{eol,max}} \rightarrow E_{eol,i,k} = \frac{E_{w,k}}{P_{eol,max}} \cdot P_{eol,i} \tag{3.20}$$

Instead, $E_{pv,j}$ is calculated as the product of the Peak Sun Hours PSH_k of the correspondent month k [h/day], evaluated as in *section 3.1*, and the power of the PV plant $P_{pv,j}$ of the correspondent combination *(i,j)*:

$$E_{PV,j,k} = PSH_k \cdot P_{pv,j} \tag{3.21}$$

The *equation 3.19* for the total energy produced during month k becomes:

$$E_{i,j,k} = \frac{E_{w,k}}{P_{eol,max}} \cdot P_{eol,i} + PSH_k \cdot P_{pv,j} \tag{3.22}$$

Figure 3.9 - Calculation of the produced energy for each combination of wind system capacity and Solar system capacity (own elaboration).

In order to compare the different combinations of capacities, the yearly average daily total energy production $E_{prod,i,j}$ of each combination *(i,j)* is calculated as the average of the monthly average daily total energy production $E_{i,j,k}$ previously evaluated:

$$E_{prod,i,j} = \frac{\sum_{k=1}^{12} E_{i,j,k}}{12} \qquad (3.23)$$
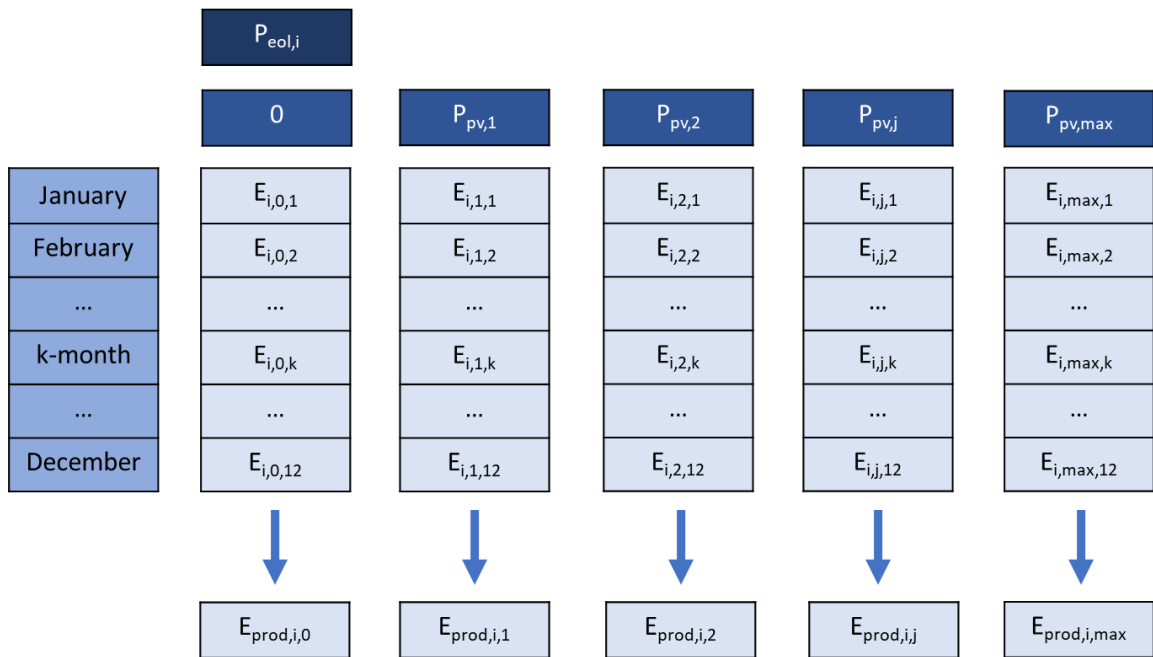
Figure 3.10 - Calculation of the annual average energy produced by the hybrid system (own elaboration).

Once $E_{prod,i,j}$ for each combination *(i,j)* is available, only the combinations related to a daily energy production higher than energy that the producer commits to sell to an off-taker are considered; the remaining combinations do not satisfy the initial assumption, and therefore they do not represent a suitable size for the HPP. Moreover, due to the constraints of the electrical grid, if the produced energy is higher than the maximum energy injectable, the excess of energy produced is curtailed; therefore, the combinations of capacities that are included in this case are considered as producing a value of daily energy equal to the maximum injectable one.

As valid for the previous numerical method, a criterion for the evaluation of the optimal combination of capacities must be identified; in this regard, the values of the average annual daily produced energy can be employed in combination with the values of the total costs for each combination to perform the evaluation, as it will be discussed in *section 3.5*.

3.4 Evaluation of the total cost of the hybrid plant

Once the combinations of capacities of PV and wind plants are calculated to comply with the energy constraints of both the energy that the producer commits to sell to an off-taker and the maximum injectable energy, the optimal capacity of the HPP must be identified; this is evaluated by analysing the economic aspects related to the HPP. Therefore, an analysis of the total cost of each combination must be performed. The total cost of a hybrid system can be defined as the sum of the capital expenditures (CAPEX) and operating expenditures (OPEX) related to both the PV and the wind plant.

The CAPEX [M€], also called overnight costs, refers to the initial investment required to establish a power plant; it includes costs related to: system components, structural components, electrical infrastructure, development, engineering and management, site access and staging, assembly and installation, contingency, construction finance.

The OPEX [M€] instead, refers to ongoing operational expenses involved in running and maintaining the power plant throughout its operational lifetime; it includes the cost related to: operations administration, asset management and security, insurance, property tax, land lease, electrical components replacement, system components replacement, system inspection and monitoring, vegetation management, cleaning.

The CAPEX is evaluated as an "overnight" cost; therefore, the expenditure is concentrated in the year "0", at the beginning of the HPP project. Instead, the OPEX is evaluated as an expenditure that occurs in every year of the operational life of the HPP project; consequently, to evaluate the total cost of the project it is necessary to consider the time value of money, and so the net present value of the OPEX for each year of the project life,

dependent on a discount rate *r*. The expression of the total cost for each combination *(i,j)* is therefore:

$$C_{tot,i,j} = CAPEX_{eol,i} + CAPEX_{pv,j} + \sum_{k=1}^{n} \frac{OPEX_{eol,i,k}}{(1+r)^k} + \sum_{k=1}^{n} \frac{OPEX_{pv,j,k}}{(1+r)^k} \qquad (3.24)$$

With *n* equal to the project lifetime [years].

To evaluate CAPEX and OPEX, values of unitary CAPEX and OPEX for a unit of capacity $CAPEX_{unit,i,j}$ [M€/MW] and $CAPEX_{unit,i,j}$ [M€/MW] are derived from the scientific literature; subsequently, the latter are multiplied by the PV and wind capacities of the combination *(i,j)*:

$$CAPEX_{eol,i} = CAPEX_{eol,unit,i} \cdot P_{eol,i} \qquad (3.25)$$

$$CAPEX_{pv,j} = CAPEX_{pv,unit,j} \cdot P_{pv,j} \qquad (3.26)$$

$$OPEX_{eol,i} = OPEX_{eol,unit,i} \cdot P_{eol,i} \qquad (3.27)$$

$$OPEX_{pv,j} = OPEX_{pv,unit,j} \cdot P_{pv,j} \qquad (3.28)$$

It is interesting to point out that CAPEX and OPEX comprehend some terms that are directly related with the parameters that were chosen to perform the suitability analysis in Chapter 2:

- Distance from electrical power plant, substations, and transmission network.
  These distances directly affect the CAPEX, since the absence of an electrical network or an already existing power plant or substation in the surroundings leads to an increase of the costs to build the necessary electrical infrastructure.
- Distance from transport network.
  As the distance from already existing electrical infrastructure, even the distance from the transport network increases the CAPEX, due to the expenses to make the power plant accessible.

- Land use.
  Different land uses are associated with a different CAPEX and OPEX, due to the expenses to make the land available for a power plant and to property tax and land lease.
- Slope and elevation.
  As stated in *section 2.2*, high slope and elevation are associated with construction difficulties and with more complicated maintenance operations, and therefore to high CAPEX and OPEX.

Therefore, these parameters can be directly included in the profitability analysis, instead of considering them for a preliminary suitability analysis where some arbitrary ranges of values are assumed; in this way, the analysis results more consistent, avoiding cases in which a profitable site is excluded in the first step of the evaluation process for presenting not favourable values of the parameters mentioned above. More information must be collected on which elements compose CAPEX and OPEX and how they affect the costs themselves. In this thesis, in the absence of more precise information, the factors listed above are considered on the suitability analysis only.

3.5 Evaluation of LCOE and hybrid system "optimal" size

The total cost of each combination *(i,j)* represents a first information about what the optimal size of the HPP for each location can be. However, to include in the discussion the quantity of energy that can be produced by the HPP, the Levelized Cost of Electricity (LCOE) is taken into account. This index represents the price at which the generated electricity should be sold for the system to break even at the end of its lifetime; it is evaluated as the ratio between the discounted costs over the lifetime of the HPP divided by a discounted sum of the actual energy amounts delivered (i.e. excluding the curtailed ones), and it is expressed in [€/MWh]:

$$LCOE_i = \frac{\tau \cdot CAPEX_{hyb,i,j} + OPEX_{hyb,i,j}}{E_{prod,i,j} \cdot 365 \cdot 10^{-5}} \tag{3.29}$$

Where:

c) $CAPEX_{hyb,i,j}$ [M€] is the total capital cost of the hybrid plant:

$$CAPEX_{hyb,i,j} = CAPEX_{eol,i} + CAPEX_{pv,j} \tag{3.30}$$

d) OPEX$_{hyb,i,j}$ [M€/year] is the operation and maintenance cost for one year; the OPEX for one year is assumed to be the same for each year k of the project lifetime:

$$OPEX_{hyb,i,j} = OPEX_{eol,i} + OPEX_{pv,j} \qquad (3.31)$$

e) E$_{prod,i,j}$ [MWh/day] is the annual average daily energy produced by the combination of capacities *(i,j)* composing the HPP, calculated as in *section 3.4*.

f) τ [-] is the capital recovery factor; it depends on the discount rate *r* and on the project lifetime *n* [years], and it is defined as:

$$\tau = \frac{r \cdot (1 + r)^n}{(1 + r)^n - 1} \qquad (3.32)$$

Once the LCOE of each combination *(i,j)* of capacities is calculated, the optimal capacities for the PV and wind plant composing the optimal HPP for each location correspond with the ones showing the minimum LCOE among all.

Due to the way the sizing process is developed, in some locations it could be possible to obtain an optimal power plant where either the PV capacity or the wind capacity are equal to zero. For this location, it is not possible to find a combination of PV and wind capacity that leads to an HPP more convenient than a power plant composed only of one of the two technologies. These locations are therefore excluded from the analysis, along with all the sites where no combinations of capacities satisfy the demand of energy from the grid.

3.6 Evaluation of cash flows and IRR

The following and final step consists in evaluating the profitability of the optimal HPP identified for each suitable location. The Internal Rate of Return (IRR) is chosen as index to represent the profitability of the plant; this latter is defined as the discount rate that makes the net present value (NPV) of all cash flows equal to zero and it is derived from the following expression:

$$NPV = \sum_{k=0}^{n} \frac{C_k}{(1 + IRR)^k} = 0 \qquad (3.33)$$

Where NPV [M€] is the Net Present Value of the plant, n [years] is the project lifetime of the plant and C_k [M€] is the cash flow related to year k, composed by the sum of $CAPEX_{hyb,k}$ [M€], $OPEX_{hyb,k}$ [M€/year] and revenues $R_{hyb,k}$ [M€] related to year k for the optimal size in the considered site; in the cashflow calculation, costs are assumed as negative and revenues as positive:

$$C_k = CAPEX_{hyb,k} + OPEX_{hyb,k} + R_{hyb,k} \qquad (3.34)$$

$CAPEX_{hyb,k}$ and $OPEX_{hyb,k}$ are referred to the optimal capacity of the plant, and they are calculated as explained in *section 3.4* as sum of CAPEX and OPEX of the wind and PV system; instead, the energy sold to the grid must be taken into account for the calculation of the revenues. In this thesis, it is assumed that the supplier owner of the HPP in each location sells the energy to an off-taker through a contract of Power Purchase Agreement (PPA). In this contractual agreement, seller and buyer agree to sell and buy an amount of energy generated by a renewable asset (in the thesis case, by a PV-Wind Hybrid System). PPAs are usually signed for a long-term period between 10-20 years and allow renewables projects to increase their level of revenue certainty. Therefore, the energy effectively injected into the grid as stated by the PPA is assumed to be sold at a fixed price. This quantity of energy can be lower or equal to the energy produced by the plant and must be lower than the maximum injectable energy. As a consequence, different cases can be investigated; three examples are represented by:

a) The HPP produces a daily quantity of energy that is equal or higher than the energy effectively injected into the grid, set by the PPA; the quantity of energy injected is sold at a fixed price; the remaining produced energy is curtailed.

b) The HPP produces a quantity of energy higher than the energy that according to the PPA should be injected into the grid; however, the supplier is allowed to sell the quantity of energy in excess with respect to the contracted energy at a price lower than the price set by the PPA; moreover, all the energy produced in excess with respect to the maximum injectable energy is curtailed.

c) The condition regarding the minimum energy that the HPP must produce and inject into the grid according to the PPA contract is removed; the HPP is allowed to sell to the grid all the energy produced at a fixed priced stated in the PPA, independently from the quantity produced, inside the boundary set by the maximum energy injectable.

In this thesis, only the first case is implemented in the model; thus, the revenues related to the year k are calculated as:

$$R_k = p \cdot E_{in} \cdot \frac{365}{1000000} \qquad (3.35)$$

With p [€/MWh] as price contracted in the PPA and E_{in} [MWh/day] daily energy sold by the PV-Wind HPP to the grid.

Regarding the second case, the possibility of selling part of the excess energy leads to an increase of the revenues, and therefore to an improvement of IRR.

Finally, concerning the third case, the possibility of selling any quantity of produced energy makes the installation of an HPP unprofitable. Indeed, in this scenario the most profitable configurations of the system will be just the ones where the cheapest technology between PV and wind is employed. Considering indeed a system where both the technologies are installed, this system, for the same capacity installed, will have a total cost higher than a system composed by the cheapest technology only.

Once the type of PPA contract and the PPA price are set, the revenues and the cashflows for the year k can be calculated, and the IRR for the given site and optimal size of the HPP plant is evaluated.

As discussed in the sections above, the methodology is based on proper assumptions. Starting from this model, it is subsequently possible to increment its complexity, to obtain a better representation of real case scenarios. For instance, more information about the evacuation capacity of the electrical grid can be collected; in addition, a storage system can be added to the system, with important consequences on the available capacity of the hybrid system. Finally, other types of approaches can be studied for the sizing method; for example, the identification of the optimal capacity of the plant can be performed directly choosing the combination of PV and wind capacities with the highest IRR among the possible combinations; however, different approaches as the latter might require more computational power, to reduce the computational time of the execution of algorithms based on the model.

In conclusion, following the methodology explained in this Chapter it is possible to calculate the IRR for each site evaluated as suitable with the implementation of the model in a Python algorithm; executing the script, a map representing the IRR for each site analysed is generated. The generation of this map is the topic of the next chapter and represents a way to perform a profitability analysis on the installation sites in the territory.

4. Profitability assessment

The last Chapter of the thesis focuses on the profitability assessment of the study area, that is carried out generating a profitability map of the territory. Indeed, the suitability map resulting from the suitability analysis in Chapter 2 and the model for the study of the profitability created in Chapter 3 can be employed for a profitability analysis. This analysis is carried out implementing the profitability assessment model in an algorithm written in Python programming language; this algorithm is subsequently executed in the ArcGIS Pro environment, using as base map the area suitable for PV-Wind HPP installation, in order to generate a series of maps that represent the various parameter taken into account by the profitability model; since the economic index IRR is employed to study the profitability of the hybrid systems, as stated in *section 3.7,* a final map reporting the values of this index for each site analysed is created eventually. This map represents the final goal of this master thesis and allows to compare the sites suitable for a PV-Wind HPP in Spain, identifying the most convenient ones.

The algorithm is written in an external environment with respect to ArcGIS Pro, thanks to the use of the code editor VS Code. However, it is also possible to write it through an internal editor, developed with the purpose of creating, modifying and employing ArcGIS Pro tools through Python language. This GIS software indeed provides the ArcPy Python package, that allows the use of functions, modules, and classes so that it is possible to perform geographic data analysis in an alternative way with respect to the tools already implemented in the software. The great advantages of performing an analysis through a Python algorithm are the possibility of automation, that allows to implement complex models composed by different operations on data, and the possibility of employing Python libraries and modules external to the ArcGIS Pro software. In this particular case, the libraries of Numpy and Numpy financial are employed, since they allow the use of functions for the calculations of net present values and the Internal Rate of Return.

To execute the algorithm, it is necessary to base the analysis on some assumptions that concern the values of the parameters taken into account; changing some of these assumptions, it is possible to obtain different results. This allows to perform a sensitivity

analysis on the values of the parameters, identifying different scenarios and pointing out how the various quantities of the model affect the final results.

In this chapter, first a brief description of the Python script is presented; then, the assumptions and the results of a first simulation of the profitability model in ArcGIS Pro are shown; finally, a sensitivity analysis is performed changing the assumptions of the model.

4.1 Brief description of the Python algorithm

The profitability analysis algorithm is structured in a way that all the steps of the profitability model are executed both with raster layers, representing maps in the form of matrices of pixels, and with polygon layers; the latter represent each square kilometre in the form of a point (*Figure 4.1*), so that it is possible to visualize grids of points. The use of polygon layers is essential, because it allows the use of attribute tables (*Figure 1.6*). In these tables, each polygon, represented with a point and related to a site, is associated with data representing different "features" of the polygon itself. For instance, each point can be associated with a value of PV or wind capacity, a value of produced energy, a value of LCOE related to a hypothetical Hybrid system installed in the given site, and so on. In this way, the operations of the profitability model can be performed either with the use of map algebra and spatial analysis tools among raster layers, or with the use of algebraic expressions applied on data organized in a tabular form. In the first case, all the operations are executed pixel by pixel; in the second case the operations are executed polygon by polygon (in the thesis case, point by point). The conversion between raster layers and polygon layers is carried out through conversion functions. Since the calculations must be iterated in a first moment for each month of the year and then for different combinations of parameters, "for loops", "while loops" and "if loops" are employed to automate the iteration.
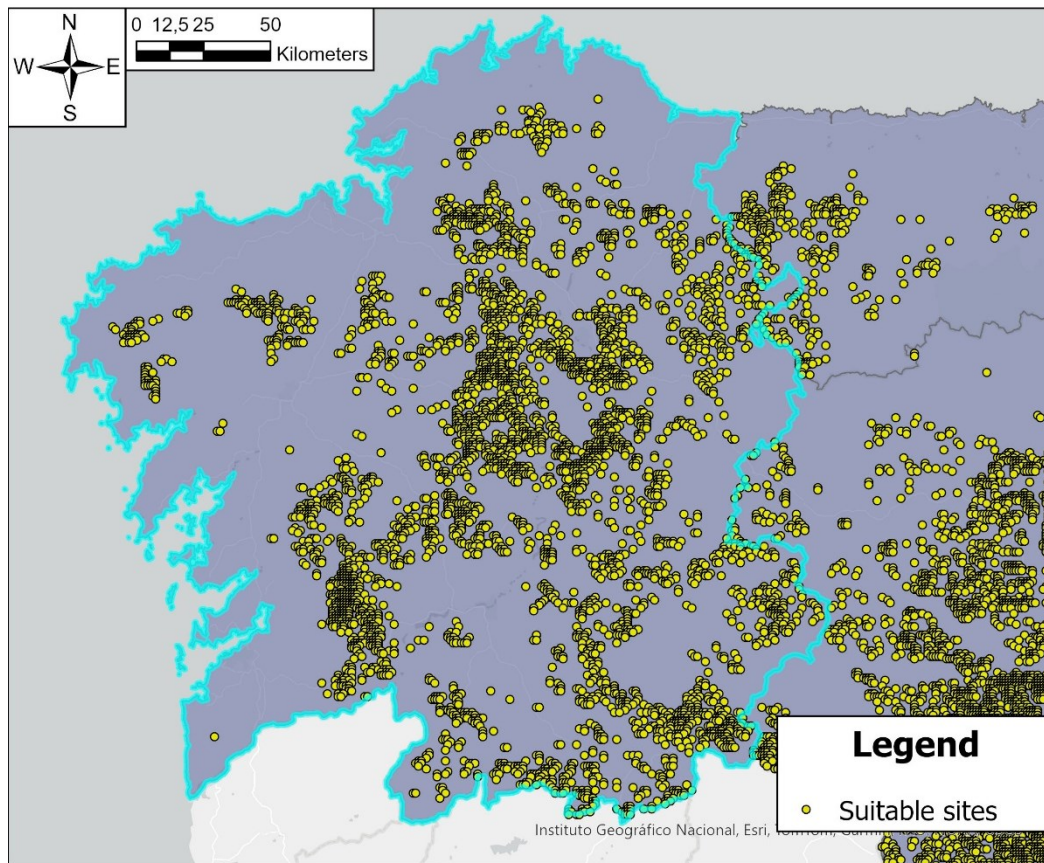
Figure 4.1 - Example of polygon layer of points; the highlighted region is the Community of Galicia; in this case, the points represent suitable sites for PV-Wind hybrid installations (own elaboration).

According to the model of Chapter 3, the analysis follows the following steps:

a) Evaluation of the solar and wind resources.

   This evaluation is carried out on the raster layer of the suitability index generated with the methodology presented in Chapter 2 (*Figure 2.20*). Raster layers representing the wind and solar energy produced are created.

b) Identification of PV and wind capacity.

   Different combinations of PV and wind capacity composing a HPP are identified, and a raster layer is generated for each one of them. Each raster layer is then converted into a polygon layer of points.

c) Evaluation of daily energy produced, costs and LCOE of each combination.

   The daily energy that can be produced by the different combinations of PV and wind capacities and their total cost and LCOE are evaluated; the calculation is iterated for each point of each layer representing a combination.

d) Identification of the optimal capacity.

   Through a tool denominated "cursor", for each point of the study area, the combination of capacities that correspond to the minimum LCOE among all the

combinations is identified; a new polygon layer in which each point is associated to the optimal capacity of the PV and wind plant is created.

e) Calculation of cash flows and IRR

In the new polygon layer, the cash flows associated with every year of the project lifetime are calculated for each point; this allows to evaluate the IRR for the optimal capacity identified for each site. The polygon layer is eventually converted again in a raster layer, representing the final profitability index.

The time needed to execute the Python script is inside a range that stretches between 2 hours and 35 minutes and 2 hours and 45 minutes, using a 12th Gen Intel(R) Core (TM) i5-1235U, 1.30 GHz processor. The execution of this Python script in a relatively acceptable time is an example of the great potentiality of Geographical Information Systems. Indeed, the integration of different types of tools, as a GIS-based software (ArcGIS Pro) and a programming language (Python), allows to manage and analyse a large number of georeferenced data, performing a multitude of calculations and implementing complex models; moreover, this implementation leads to final results that can be easily visualized and interpreted, and that can be employed for decision making and problem solving processes.

4.2 Profitability map

As already stated in Chapter 2, the area selected for the profitability analysis in the one represented in *Figure 2.20*; this territory comprehends all the areas characterized by a suitability index higher than 0.5 over all the study area. In particular, this layer is employed in the form of raster, as requested by the Python algorithm.

It is important to point out that the algorithm proceeds in a way that the mathematical operations are executed pixel by pixel with the layers in the forms of raster, and polygon by polygon (for instance, point by point) with the layers in the form of polygons. Therefore, as a rule of thumb, the execution of the simulation is quicker if layers with a reduced number of pixels or polygons are employed. In this prospect, the choice of selecting only a reduced number of suitable cells results in a lower computational time.

Moreover, the absence of a criterion to classify the suitable cells in the suitability raster layer affects the way in which the results are presented. Indeed, this absence determines the inability, both at the beginning and at the end of the analysis, to gather pixels to form polygons that represent sites with a given surface. Thus, despite the goal of the analysis is selecting profitable sites for PV-Wind HPP, in this thesis each suitable cell with a suitable index higher than 0.5 is considered as a potential site itself; since all the raster layers employed in the analysis present a resolution of 1 X 1 km, the final profitability map will

be a raster layer with pixels of 1 km^2 as well. This means that the resulting IRR will be presented in the final layer as an index associated to a square kilometre. In a real case scenario, however, the extension of the surface of an installation site can be different from one km^2; in addition, the available surface affects the final profitability of a plant since it determines the maximum installable capacity of a PV or a wind plant. All these reasons heighten the importance of continuing this research work along these lines.

In this section, the profitability map generated with a first simulation is presented, along with a discussion on the distribution of the resulting profitable sites. This first simulation is based on the following assumptions:

- Wind maximum installable power: Considering the research work carried out in [45], a range of values between 6.2 MW/km^2 and 46.9 MW/km^2 can be considered; in the simulations of this thesis, an average value of 20 MW/km^2 is assumed.

- Solar maximum installable power: Considering the research work carried out in [46], a range of values between 35.1 MW/km^2 and 117.6 MW/km^2 can be considered; in the performed simulations, an average value of 50 MW/km^2 is assumed.

- Maximum injectable power in the electrical grid: the evacuation capacity of the Spanish electrical grid is not investigated in this thesis work; therefore, a constant value of 10 MW is assumed for the first simulation.

- Maximum injectable energy in the electrical grid: the value of this parameter is a direct consequence of the maximum injectable power; indeed, it is assumed that it is possible to inject 10 MW of power for each hour of the day. Thus, the maximum daily injectable energy is:

$$E_{in,max} = P_{in,max} \cdot 24\ h = 10\ MW \cdot 24\ h = 240\ MWh$$

- Grid injected energy: considering a margin of flexibility for the energy injected in the grid, it is assumed that the energy actually injected and sold to an off-taker is equal to the 90% of the maximum injectable energy.

- Wind turbine power: as already stated, a V150- 6 MW – IEC S Vestas wind turbine [40] with a nominal power of 6 MW is taken as reference for the estimation of the energy generated; to identify the wind plant capacity instead, a wind turbine of 5 MW is considered.

- PV system performance ratio: a value of 0.8 is considered, assuming the system to be a good performing one [38].

- Number of intervals for the values of wind plant capacity to analyse: $P_{eol,max}$ is subdivided in four intervals. Therefore, the analysed wind plant capacities are: 0, 5, 10, 15 and 20 MW.

- Number of intervals for the values of PV plant capacity to analyse: $P_{pv,mac}$ is subdivided into 10 intervals. Therefore, the analysed PV plant capacities are: 0, 5, 10, 15, … 40, 45 and 50 MW.
- Project lifetime: a value of 25 years is assumed.
- Component useful life: a value of 25 years is assumed both for the components of the PV system and the ones of the wind system.
- Discount rate: a general value of 7% is chosen; this value represents the middle value among 3% - 7% - 10%, that correspond to three different assumptions chosen by the International Energy Agency IEA to perform the analysis in [47].
- Unitary costs: the value assumed correspond to the ones reported by the National Renewable Energy Laboratory (NREL) in [48] and [49]:

Table 4.1 - Unitary CAPEX and OPEX for wind and PV plants employed in the profitability analysis (own elaboration based on data from [48] - [49]).

	WIND PLANT	PV PLANT
Unitary CAPEX	1.40 M€/MW	0.92 M€/MW
Unitary OPEX	0.04 M€/MW/year	0.02 M€/MW/year

- PPA price: Considering the range of values reported in [50], a favourable scenario for the provider is chosen in the first place, and a value of 75 €/MWh is assumed.

Performing the simulation with these parameters, the following map of profitability is obtained:
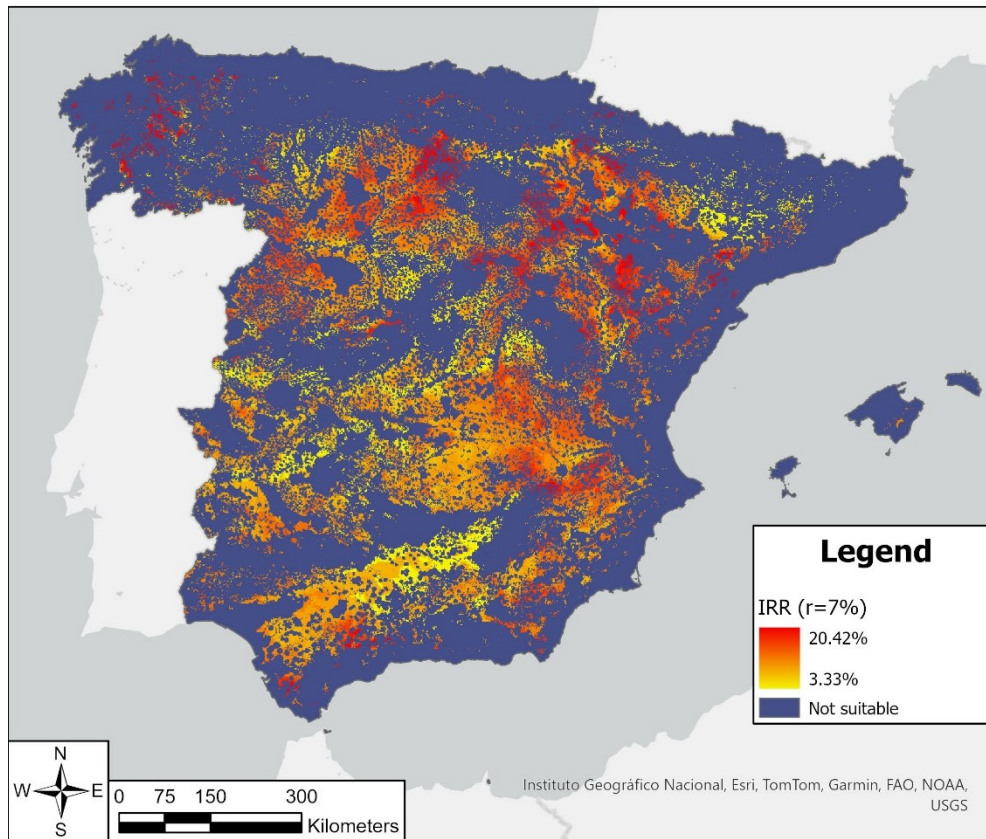
Figure 4.2 - Profitability map obtained with the assumptions of section 4.2 (own elaboration).

As shown in the figure above, the range of IRR values stretches from 3.33% to 20.42%. The maximum values of IRR that can be obtained are therefore relatively high; this is due in particular to the favourable conditions assumed in the sale of electrical energy, that involves a favourable selling price of 75 €/MWh. In addition, the distribution of IRR decimal values inside the range determined by the maximum and minimum IRR values can represented (*Figure 4.3*):
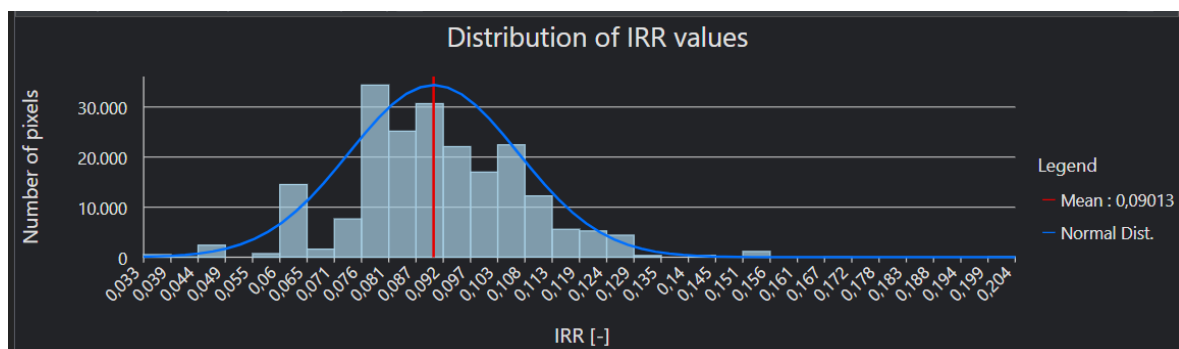
Figure 4.3 - Distribution of IRR values obtained with the assumptions of section 4 (own elaboration).

As can be noted, the mean value is around an IRR of 9%; moreover, it can be calculated that 90.5% of the analysed suitable sites possess a value of IRR higher than 7%, value that is assumed in this thesis as a lower limit for the IRR values of hybrid systems considered profitable. This number corresponds to 21.91% of the total number of sites. Thus, under these assumptions most of the suitable sites are profitable; as already stated, this is due to the high value of price for the PPA chosen in this scenario.

As for the suitability index, the spatial distribution of the profitable sites is calculated, considering the % of profitable sites with an IRR higher than 7% in each Community and the % of profitable sites with an IRR higher than 7% with respect to the Community suitable area; this allows to point out the Communities where an installation of a PV-Hybrid system results in a profitable plant.

Table 4.2 - Percentage of profitable area on the total profitable area and on the Community suitable area for each Community (own elaboration).

IRR > 7%		
Autonomous Community	% of profitable area on the total profitable area	% of profitable area on Community suitable area
Andalusia	15.59	82.66
Aragon	11.32	93.78
Asturias	0.19	87.94
Balearic Islands	0.05	100
Basque Country	0.08	94.67
Cantabria	0.06	100
Castile and León	24.33	93.73
Castile–La Mancha	29.05	94.04
Catalonia	1.25	57.81
Extremadura	8.40	83.69
Galicia	1.92	84.04
La Rioja	0.79	85.54
Madrid	0.75	62.22
Murcia	2.54	99.75
Navarre	1.88	95.81
Valencia	1.81	99.74
Ceuta	0	0
Melilla	0	0

According to the table, the Communities with the highest share of profitable area with an IRR >7% are Andalusia (15.59%), Castile and León (24.33%) and Castile-La Mancha

(29.05%); this result reflects the spatial distribution of the suitable sites with respect to the total study area, and they are due to favourable values of the parameters of wind speed and solar radiation in these regions and to their wide extension. As for the suitable area, the Communities that are characterized by the lowest share of profitable areas are the Balearic Islands, even though the archipelago is characterized by moderate wind speed and solar irradiation, and the northern regions of Cantabria and Basque Country, characterized by high or moderate values of wind speed but low values of irradiation. Considering Ceuta and Melilla instead, as already stated, they do not present a suitable area for hybrid systems; therefore, they are excluded from the profitability analysis.

Another percentage that is interesting to analyse regards the share of profitable areas with an IRR>7% with respect to the total Community suitable area; this allows to find the regions where the territory analysed is characterized by low values of profitability, with sites featuring an IRR lower than 7%. As already stated, since the value of price for the PPA is favourable, most of the sites are considered suitable; however, it can be pointed out that Catalonia and the Community of Madrid present the lowest percentages, 57.8% and 62.22%, showing that a consistent number of sites in these regions are suitable for a hybrid installation that results however in an unprofitable system.

To have a better view of which are the most suitable sites in Spain, the spatial distribution of sites presenting an IRR higher than 10% are studied. These sites represent 24.82% of the suitable sites and 6% of the total study area. Again, the percentage of profitable area on the total profitable area and the % of profitable area on the Community suitable area are calculated and represented in *Table 4.3*:

Table 4.3 - Percentage of profitable area with IRR > 10% on the total profitable area and on the Community suitable area for each Community (own elaboration).

IRR > 10%		
Autonomous Community	% of profitable area on the total profitable area	% of profitable area on Community suitable area
Andalusia	5.98	8.70
Aragon	19.73	44.81
Asturias	0.39	50.50
Balearic Islands	0.004	2.13
Basque Country	0.12	35.50
Cantabria	0.17	77.39
Castile and León	36.12	38.16
Castile–La Mancha	24.60	21.84
Catalonia	1.82	22.95
Extremadura	0.78	2.12
Galicia	5.16	61.99
La Rioja	1.11	33.12
Madrid	0.10	2.24
Murcia	0.44	4.73
Navarre	2.22	31.05
Valencia	1.27	19.20
Ceuta	0	0
Melilla	0	0

As demonstrated, while Castile and León and Castile–La Mancha result another time the Communities with the highest percentage of profitable sites with an IRR>10% with respect to the total profitable area (36.12% and 24.6% respectively), reflecting the spatial distribution of the suitable areas, the sites in Andalucia are not among the most profitable one; indeed, the percentage of profitable sites changes from 15.59% for the ones with an IRR>7% to 5.98% for the ones with an IRR>10%. Instead, a moderate increase in the two percentages can be pointed out taking into account the Community of Aragon, with a change from 11.32% to 19.73%. The Communities with the lowest share are still the Balearic Islands (0.004%), Basque Country (0.12%), Cantabria (0.17%), together with the Community of Madrid, with a percentage that slightly decreases from 0.75% to 0.10%.

Subsequently, the share of profitable area with an IRR>10% on the Community suitable area for each Community is calculated; among all the Communities the ones with the highest percentage are Asturias (50.50%), Cantabria (77.39%), and Galicia (61.99%). It is interesting to point out that the same communities result among the ones with the lowest share of both suitable and profitable sites; however, these Communities present also high

values of average wind speed; this characteristic ensures therefore high profitable installations.

Another parameter that can be taken into account to study the profitability of a hybrid system is the LCOE; as shown in the model discussed in Chapter 3, this parameter is employed to find the optimal capacity of an HPP in each site, finding the PV plant and wind plant capacities that ensure the minimum LCOE among the combinations analysed. In *Figure 4.4*, the resulting minimum LCOE for each site is represented, considering the simulation carried out with the assumptions discussed in this section:
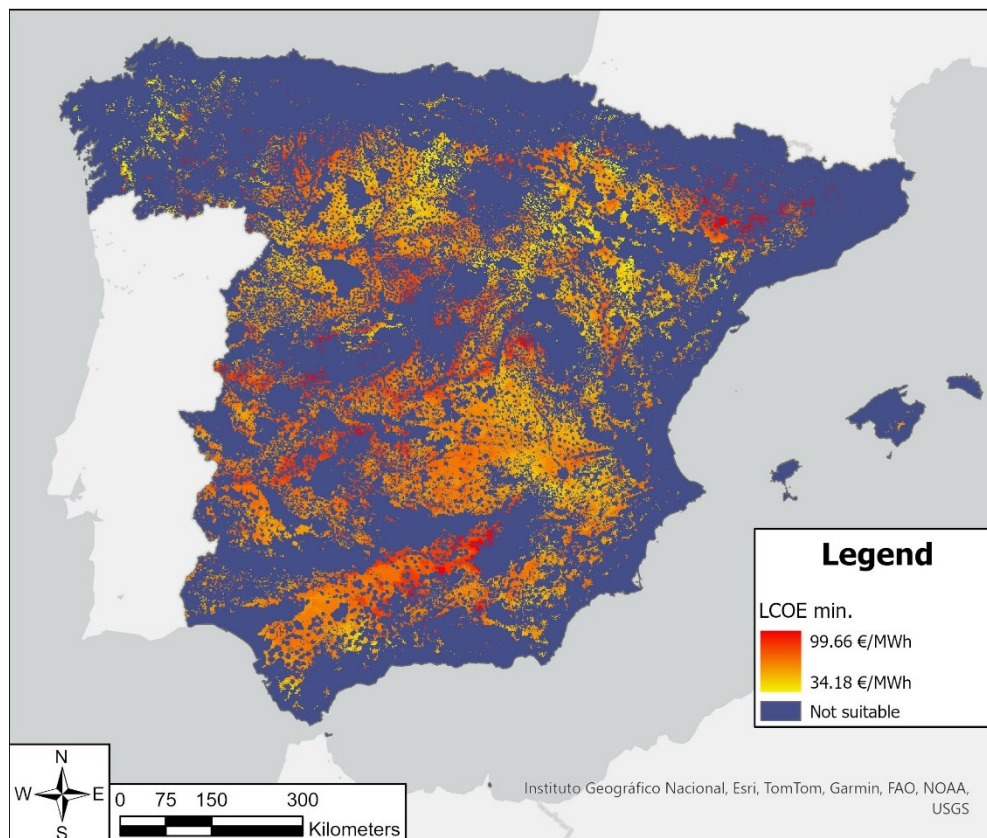
Figure 4.4 - Minimum value of LCOE for each analysed suitable site (own elaboration).

As shown in the figure above, the values of minimum LCOE are represented by means of a scale with a lower extreme represented in yellow and an upper extreme represented in red; the most convenient sites are therefore shown in yellow, presenting low values of minimum LCOE. Observing the map, it is possible to point out that the spatial distribution of convenient sites reflects the distribution of the most profitable sites, presenting the most convenient sites in Communities as Galicia, Castile and León and Aragon, along with Castile–La Mancha and the south part of Andalusia.

Eventually, the distribution of optimal capacities in the study area is analysed, to find the most common ones. The percentages of hybrid systems with a particular combination of

PV and wind plants capacities on the total number of systems analysed are reported in *Table 4.4*:

Table 4.4 - Percentage of hybrid systems with a particular combination of PV and wind plants capacities on the total number of systems for each analysed combination (own elaboration).

		Wind plant capacity				
		0	**5**	**10**	**15**	**20**
	0	0	0	0	0.0005%	0.18%
	5	0	0	0	0.027%	0.55%
	10	0	0	0	0.004%	2.11%
	15	0	0	0	0.17%	5.87%
PV plant capacity	**20**	0	0	0	2.51%	7.92%
	25	0	0	0.15%	10.41%	2.77%
	30	0	0	2.67%	14.72%	0.77%
	35	0	0	8.15%	5.69%	0.047%
	40	0	0.35%	12.08%	2.42%	0.063%
	45	0	2.67%	3.66%	0.30%	0.022%
	50	0.003%	8.03%	4.54%	1.09%	0.24%

As shown in the table above, the most common combination of capacities is composed of a wind plant of 15 MW and a PV plant of 30 MW. It is clear that all the combinations that do not ensure a production of energy capable of satisfying the condition on the injected energy set in advance (as stated in the model discussed in Chapter 3) are not considered suitable for a hybrid installation.

It is important to point out that the capacity of the PV-Wind HPP depends basically on the energy that must be produced to satisfy the demand of energy that has to be injected into the grid; therefore, an increase of the parameter of the maximum evacuation capacity of the grid and, consequently, of the injected energy leads to a progressive increase of the capacity of the hybrid system.

In the context of the thesis, other simulations of the Python model are executed changing the initial assumptions, in order to have a better understanding of the parameters influence; this sensibility analysis is discussed in the next section.

4.3 Sensibility analysis

As stated in the introduction, the context in which renewable systems are developed is changing rapidly. In the first place, this is reflected by rapid changes in the market conditions the renewable systems operators must work in; in the second place, the efforts and commitments assumed by institutional figures lead to adopted policies characterized by a constant evolution of burdens and limitations that affect renewable systems installation and operation. For these reasons, the model and the way in which it is implemented must be flexible and easily editable, to respond to changes that can quickly occur in real-world scenarios, being the model a representation of the real-world itself.

In this regard, another main advantage of GIS is their dynamicity. Indeed, working with GIS software as ArcGIS Pro it is possible to perform relative quick analysis, changing, adding, or removing parameters, as it will be demonstrated by the sensibility analysis carried out in this section. This characteristic demonstrates how GIS are powerful instrument suitable for tackling real-word problems.

In the following, a total of other five simulations are performed, changing some of the assumptions of the model; the results of the latter are reported in the following sections. In *section 4.3.1,* the effect of the variation of the value of the PPA price is discussed; in *section 4.3.2,* the effect of the variation of the maximum injectable power in the grid is considered; finally, in *section 4.3.3*, the effect of the variation of the discount rate is presented.

4.3.1 Variation of PPA price

The first assumption to vary in the sensibility analysis is the price of the Power Purchase Agreement. In the first simulation performed in *section 4.2* the PPA price assumes a value of 75 €/MWh; taking into account the range of PPA prices presented in [50], this value can be considered as a favourable value for the producer that sells energy to an off-taker. For the sensibility analysis two other values of price are considered; in the first place, a simulation with a price of 55 €/MWh is executed; subsequently, a value of 35 €/MWh is assumed. These two values represent scenarios where the price is less favourable for a seller, and they affect the profitability of the hybrid systems. Except the PPA price, the same assumptions and study area reported in *section 4.2* are considered.

The first result, assuming a PPA price of 55 €/MWh, is represented in *Figure 4.5*.
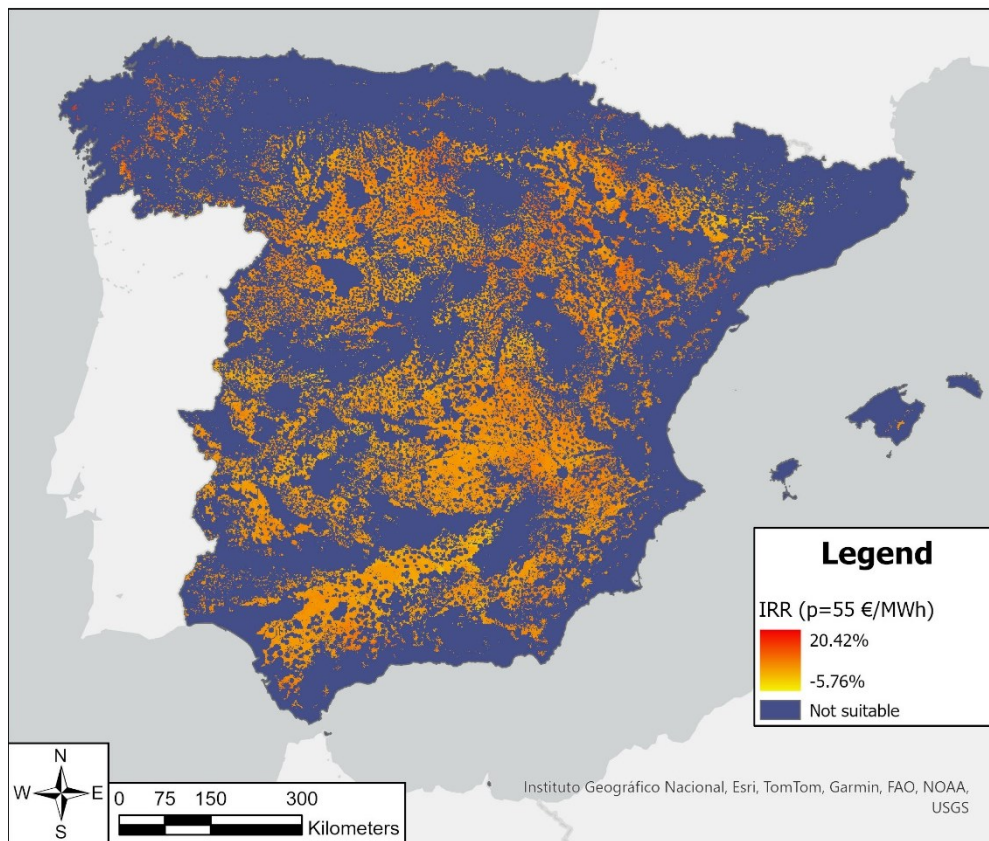
Figure 4.5 - Profitability map obtained assuming a price for the PPA of 55 €/MWh (own elaboration).
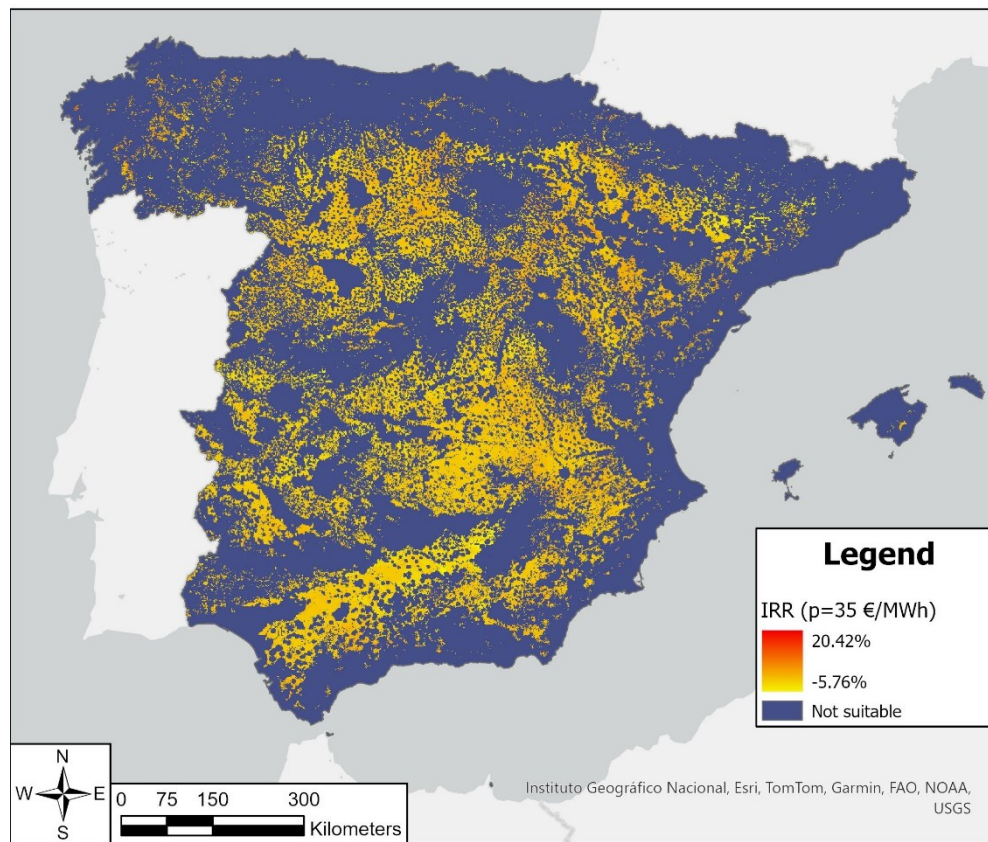
In this simulation, since all the assumptions regarding the sizing numerical model and LCOE model presented in Chapter 3 do not change, the optimal capacity of the plants calculated in each site by means of the Python algorithm reported in *section 4.2* are still valid. Indeed, the change of the PPA price affects only the revenues, and therefore the results of the IRR. In particular, since the value of the maximum evacuation capacity of the grid remains 10 MW, and as a consequence the value of energy that must be injected into the grid according to the PPA (assumed as 90% of the maximum injectable energy) do not change, the sites where the optimal capacity of the hybrid system calculated through the algorithm is capable of satisfying the demand do not change as well; as a consequence, the number of sites, i.e. pixels where the IRR can be calculated is the same of the previous simulation; thus, in F*igure 4.2* and *Figure 4.5* the same number of suitable pixels are analysed.

The main significant difference regards the values of the scale of IRR; indeed, while in *section 4.2* the simulation returns values in a scale that stretches from 3.33% to 20.42%, with a PPA price of 55 €/MWh the scale presents as extremes -0.35% and 13.90%. Thus, it can be noted that in general the values of IRR decrease as expected, since the PPA price is lower than the one in the previous simulation. In particular, some sites present a negative IRR, while in the most profitable ones the IRR is about 7 percentage points lower.

Concerning the distribution of values, it can be calculated that only 5.52% of the analysed suitable sites and 1.34% of the total study area present a value of IRR over the 7%, showing a consistent decrease with respect to the values of 90.5% and 21.91% respectively obtained in the previous simulation.

Eventually, considering the spatial distribution, since the distribution of available renewable resources in the territory does not change, the distribution of the most and less profitable sites do not change considerably.

A second result, assuming a PPA price of 35 €/MWh, is represented in *Figure 4.6*.

Figure 4.6 - Profitability map obtained assuming a price for the PPA of 35 €/MWh (own elaboration).

In this simulation, all the assumptions regarding the sizing numerical model and LCOE model remain the same to the ones of the simulations with 55 €/MWh and 75 €/MWh; therefore, the same statements regarding the effect of the change of the PPA price can be pointed out. In particular, since the value of price is the least favourable, the consequent values of IRR in the scale are lower than the ones in the previous simulations; indeed, in this simulation the scale stretches from a bottom end of -5.76% to an upper extreme of 6.64%. Therefore, it can be noted that, taking as limit an IRR of 7%, no site is profitable for a hybrid installation with this price; only few areas, in Communities as Galicia, Aragon

and the north-eastern part of Castile and León where the sites with the highest profitability can be found, reach values of IRR close to 7%.

Considering the simulation, it is therefore clear that decreasing the value of PPA price, the revenues and consequently the profitability of hybrid systems decreases.

4.3.2 Variation of discount rate

In the second series of simulations for the sensibility analysis, different values of discount rate are considered; two values, equal to 3% and 10%, together with the value of 7% chosen for the simulation in *section 4.2*, are assumed. These values reflect discount rates considered by IEA in the analysis in [47], and they are useful to represent different electricity market scenarios. In the two simulations of this section all the assumptions are equal to the ones chosen in the simulation in *section 4.2.,* except for the value of the discount rate, as stated, and for the value of the PPA price, that is assumed equal to 55 €/MWh, to take into account a middle range scenario of prices.

The results of the first simulation, executed with a discount rate equal to 10%, are represented in *Figure 4.7*.
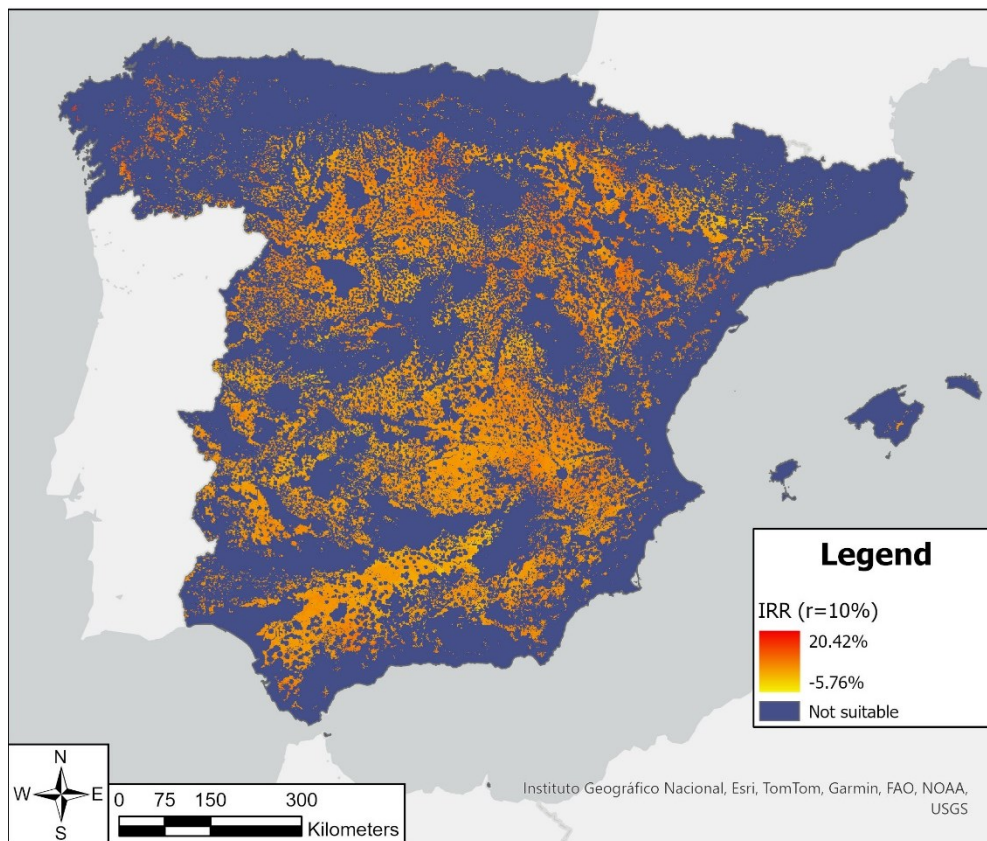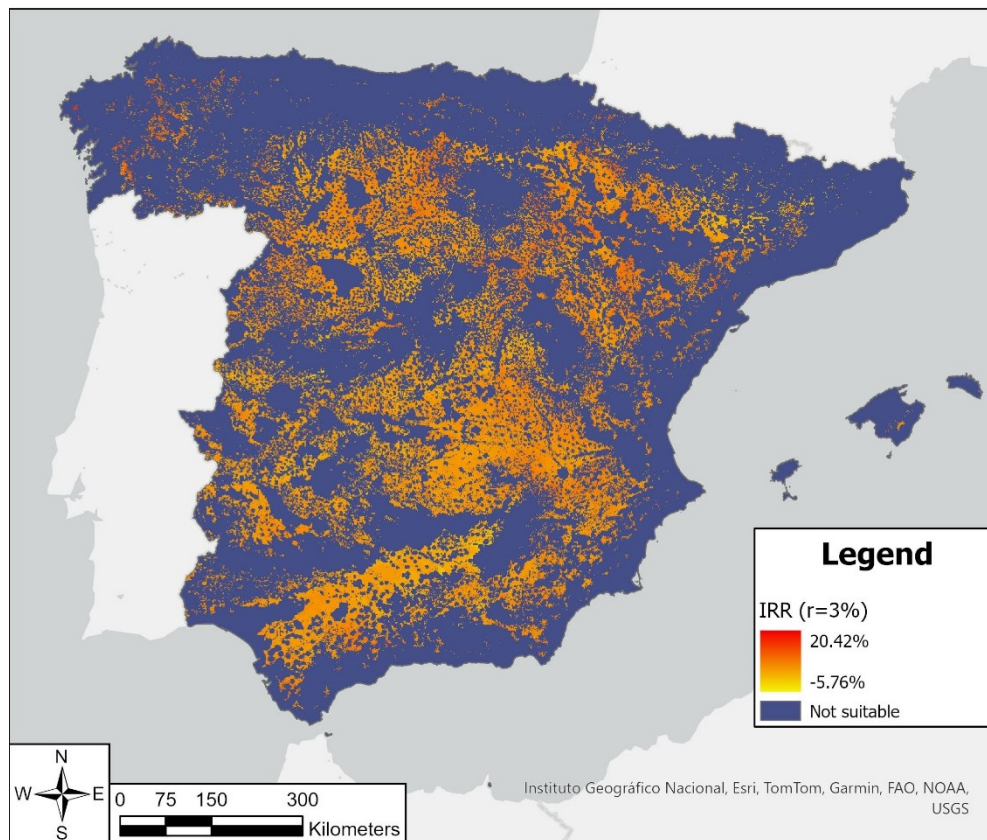

Figure 4.7 - Profitability map obtained assuming a discount rate of 10% (own elaboration).

In this simulation, the discount rate is higher with respect to the value of 7%, chosen for the simulations in *section 4.2* and *section 4.3.1*. However, comparing the results obtained with a 10% discount rate represented in *Figure 4.7* with the ones obtained for values of PPA price equal to 55 €/MWh and discount rate equal to 7%, represented in *Figure 4.5*, no differences can be pointed out. Indeed, the IRR scale presents in both cases an upper extreme of 13.90% and a lower extreme of -0.35%. Moreover, the distributions of values are very similar, with a share of 5.54% of values being over an IRR of 7%. In general, some differences can be found in the value of LCOE minimum employed for the choice of the optimal size of the HPP in each site; indeed, as shown in the model presented in Chapter 3, the discount rate affects the LCOE and the total OPEX of a plant; however, these small differences do not affect the final value of IRR. Eventually, the spatial distribution of IRR values does not change considerably.

In the second place, a simulation with a PPA price of 55 €/MWh and a discount rate of 3% is performed; the results are represented in *Figure 4.9*.

Figure 4.8 - Profitability map obtained assuming a discount rate of 3% (own elaboration).

Considering this simulation, the same considerations regarding the one executed with a discount rate of 10% can be pointed out. Therefore, it can be stated that limited changes in the discount rate do not affect the results in a considerable way.

4.3.3 Variation of evacuation capacity of the electrical grid

The final simulation carried out for the sensibility analysis concerns the effects of the parameter of evacuation capacity of the grid on the results. Indeed, all the previous simulations in *section 4.2*, *section 4.3.1, section 4.3.2* are performed with values of maximum injectable power of 10 MW, value that sets the energy that must be injected according to the PPA to the 90% of 240 MWh, with the latter as the maximum value of energy that can be injected daily. In the simulation of this section instead, a value of maximum injectable power of 15 MW is assumed; consequently, the energy that must be injected according to the PPA is set to 90% of 360 MWh on a daily basis. Thus, the energy that the optimal hybrid system in each site must produce is higher with respect to the other simulations. In this section, the other assumptions are equal to the ones exposed in *section 4.2*, except for the maximum evacuation capacity of the grid, as stated, and for the PPA price, assumed as 55 €/MWh.

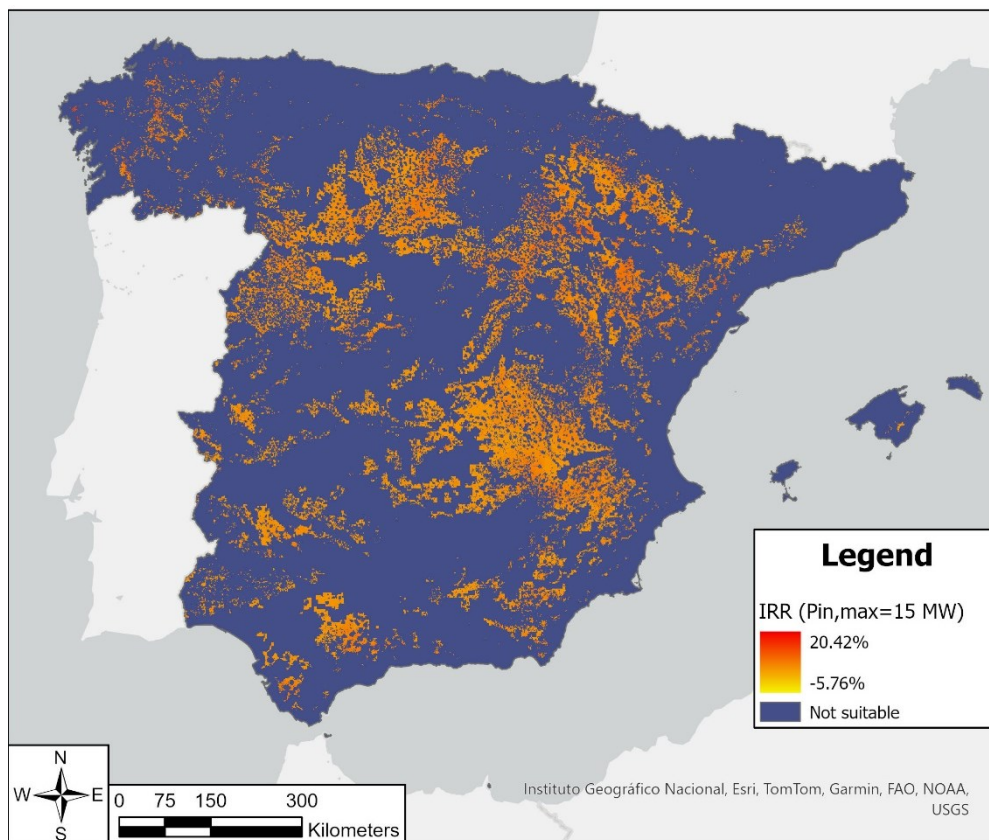The results of the simulation are presented in *Figure 4.11*.

Figure 4.10 - Profitability map obtained assuming a maximum evacuation capacity of the grid of 15 MW (own elaboration).

As it is shown in figure above, the assumption $P_{in,max}$=15 MW leads to a change both in the values of IRR and in the number of profitable sites. Indeed, first of all, comparing the scale of IRR values obtained with this simulation and the one obtained assuming $P_{in,max}$=10 MW and a PPA price equal to 55 €/MWh, represented in *Figure 4.5*, the lower extreme changes from -0.35% to 4.51%, while the upper one changes from 13.90% to 14.57%. Thus, the extremes of the scale are higher, showing that an increase of the quantity of energy that must be injected into the grid produces in general an increase of the revenues, and therefore an increase of the profitability of a hybrid system. However, the increase of the quantity of injected energy leads to the need of increasing the size of the systems, in order to produce more energy daily; consequently, the availability of renewable resources in some sites is not enough to allow the installation of a hybrid system that complies with the demand of energy. These sites are therefore excluded from the analysis, and the number of pixel where the IRR is calculated decreases: while the number of pixels analysed in the simulation with $P_{in,max}$=10 MW is equal to 24.2% of the total study area, in the simulation with $P_{in,max}$=15 MW the number changes to 15.13% of the total study area.

Considering instead the distribution of IRR values, it can be calculated that 10.24% of the analysed suitable sites and 1.55% of the total study area present a IRR value higher than 7%; this represents a slightly increase with respect to the values of 5.52% and 1.34% respectively obtained in the simulation with $P_{in,max}$=10 MW and PPA price equal to 55 €/MWh, due, as stated, to the higher revenues expected from a hybrid system that can inject and sell an higher quantity of energy with respect to the other scenarios.

Finally, regarding the spatial distribution, the Communities with the highest share of sites presenting an IRR higher than 7% are Castile and León (35.52%), Aragon (30.31%) and Galicia (12.94%); therefore, these results do not differ considerably from the results already presented in *section 4.2*.

5. Conclusions

Identifying suitable locations for the installation of hybrid systems based on wind and solar energy that allow a high profitability for a power plant is a key issue for the spread of this new promising technology. In this study, as a first step, a map of sites suitable for PV-Wind installations in Spain is generated, based on climatic, ecological, and economical factors, combined by means of the Boolean and Fuzzy logic. Then, a simple model for the sizing and evaluation of a hybrid power plant, based on proper assumptions, is created. Finally, the model is implemented to produce a map of profitability for suitable sites in Spain.

Considering the suitability analysis, an index of suitability is calculated and represented in the suitability map; the sites with a suitability index higher than 0.5 are chosen to carry out the analysis of the profitability of the hybrid systems. According to this criterion, it results that 24.35% of the Spanish peninsular territory, Balearic Islands and Ceuta and Melilla is suitable for the installation of PV-Wind hybrid systems.

Considering the profitability analysis, the Internal Rate of Return of the hybrid system with the optimal capacity is calculated for each suitable site; a threshold value of 7% is assumed to determine which sites can be considered as profitable. Depending on the values assumed for the parameters of the model different results are obtained. A first simulation, performed with a favourable PPA price of 75 €/MWh, a discount rate of 7% and a grid evacuation capacity of 10 MW, reports that most 90.5% of the suitable sites and 21.91% of the total study area guarantee the installation of profitable hybrid systems, with IRR that peaks at the value of 20.42%.

Performing a sensitivity analysis on the PPA price, lowering the price to 55 €/MWh and 35 €/MWh leads to a decrease of the maximum values of IRR obtained to 13.90% and 6.64% respectively. At the same time, the percentage of suitable sites decreases: considering a PPA price of 55 €/MWh, only 5.52% of the suitable area and 1.34% of the total study area is profitable; considering a PPA price of 35 €/MWh, no site can be considered as profitable.

Subsequently, a sensitivity analysis on the discount rate is carried out, changing its value from a 7% assumed for the previous simulations to a 10% and 3%. The obtained results

show that the variation of this parameter in a small range does not consistently affect the values of IRR. Indeed, setting a grid maximum evacuation capacity of 10 MW and a PPA price of 55 €/MWh, with all the three values of discount rate the maximum value of IRR obtained is 13.90%, with a percentage of sites presenting a profitability higher than 7% around 5.5%. Therefore, a change in the discount rate produces differences that are negligible.

Finally, sensitivity analysis on the grid maximum evacuation capacity is performed, considering a value of 15 MW, different from the value of 10 MW assumed for the previous simulations. Since in this scenario, the quantity of energy that can be injected in the grid is higher, the IRR values increase with respect to the results obtained with evacuation capacity of 10%, with a peak that moves from 13.90% to 14.57%; moreover, on one hand, the percentage of sites where it is possible to install a hybrid system capable of producing a quantity of energy that satisfies the request decreases from 24.20% to 15.13% of the total studied area; on the other hand, the percentage of sites with IRR values higher than 7% increases from 5.52% to the 10.24% of the analysed suitable sites. Thus, according to the model, an increase of the maximum evacuation capacity of the grid leads to an increase of the IRR values and, at the same time, to an increase of the optimal capacity of the hybrid systems needed to satisfy the demand of energy set by the contracts.

In conclusion, a tool has been developed to help in the decision making. Depending on the employed parameters and on their values, different results are obtained; this capability represents a characteristic of this kind of tools. From the review of the results, it can be observed that a more in-deep study on the parameters to perform the analysis must be carried out, to ensure more precise results. In particular, considering the parameters employed for the suitability analysis, the range of values assumed as suitable for a PV-Wind hybrid plant must be reviewed, along with the criterion used to select the suitable sites and aggregate the available surface in a site itself. In addition, the degree of detail of the model can be incremented: a) including the economic factors of the preliminary analysis in the evaluation of the CAPEX and OPEX, to study the influence of the different components; b) considering different models of PPA; c) investigating the way in which wind plant and PV plant may interfere with each other; d) including a storage system, frequently associated with PV-Wind hybrid systems; e) considering hourly averages for the power produced by the plant, for a better evaluation of the optimal size; f) Including georeferenced data regarding the maximum injectable power in the electrical grid; g) investigating a different way to express the profitability of a hybrid plant to highlight its advantages.
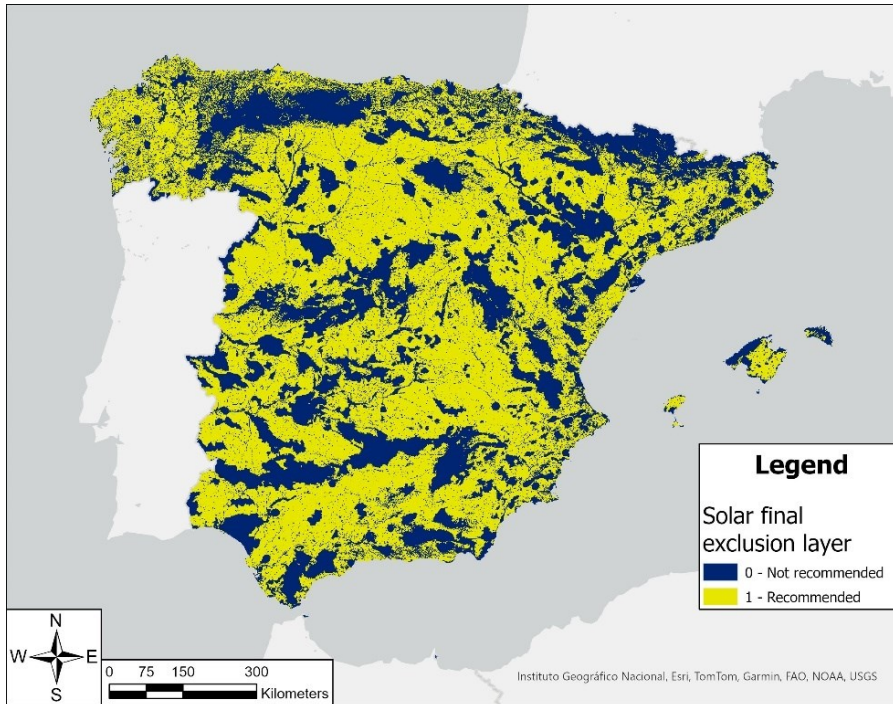
Appendix

Appendix 1. Polygons composing the land cover layer and relative Codex and reclassification value (own elaboration based on data from [5]).

| ELEMENT	CODEX	RECLASSIFICATION VALUE
Continuous urban fabric	111	0
Discontinuous urban fabric	112	0
Industrial or commercial units	121	0
Road and rail networks and associated land	122	0
Port areas	123	0
Airports	124	0
Mineral extraction sites	131	0
Dump sites	132	1
Construction sites	133	0
Green urban areas	141	0
Sport and leisure facilities	142	0
Non irrigated arable land	211	2
Permanently irrigated land	212	2
Rice fields	213	2
Vineyards	221	0
Fruit trees and Berry plantations	222	1
Olive groves	223	1
Pastures	231	4
Annual crops associated with permanent crops	241	1

Complex cultivation patterns	242	2
Land principally occupied by agriculture, with significant areas of natural vegetation	243	0
Agricultural-forestry areas	244	0
Broad-leaved forest	311	0
Coniferous forest	312	0
Mixed forest	313	0
Natural grasslands	321	3
Moors and heathland	322	2
Sclerophyllous vegetation	323	1
Transitional Woodland-shrub	324	0
Beaches, dunes. Sands	331	2
Bare rocks	332	1
Sparsely vegetated areas	333	5
Burnt areas	334	0
Glaciers and perpetual snow	335	0
Inland marshes	411	0
Peat bogs	412	0
Salt marshes	421	0
Salines	422	0
Intertidal flats	423	0
Water courses	511	2
Water bodies	512	0
Coastal lagoons	521	0

| Estuaries | 522 | 0 |
| Sea and ocean | 523 | NO-DATA |

Appendix 2. Solar final exclusion layer resulting from the analysis presented in Chapter 2 (own elaboration).

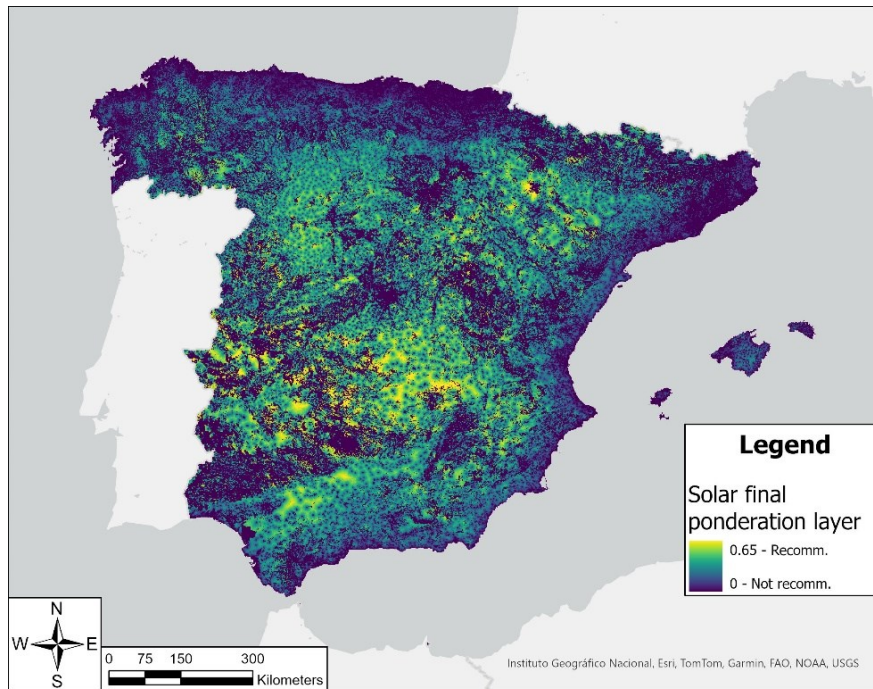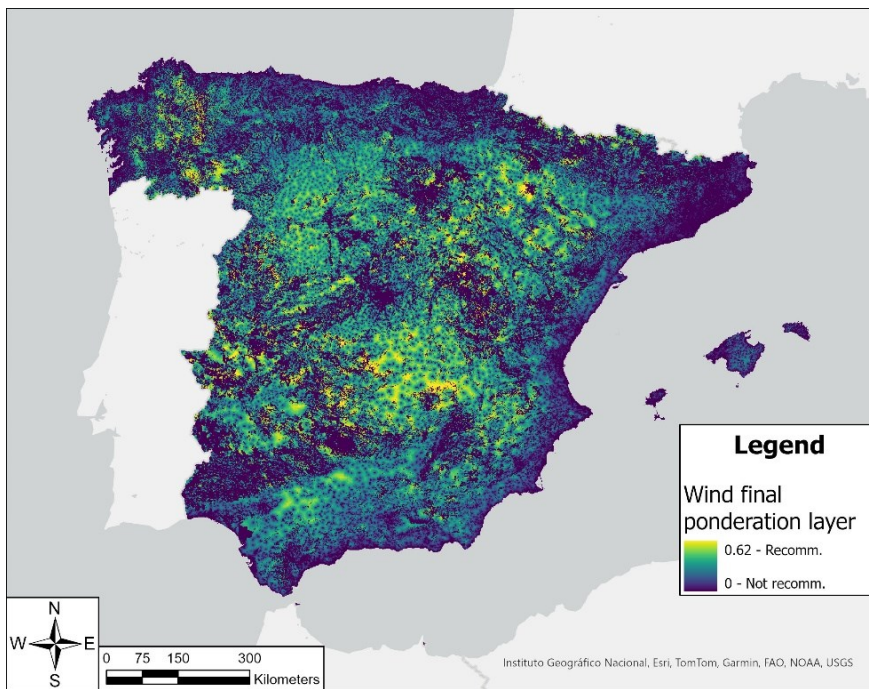*Appendix 3. Wind final exclusion layer resulting from the analysis presented in Chapter 2 (own elaboration).*
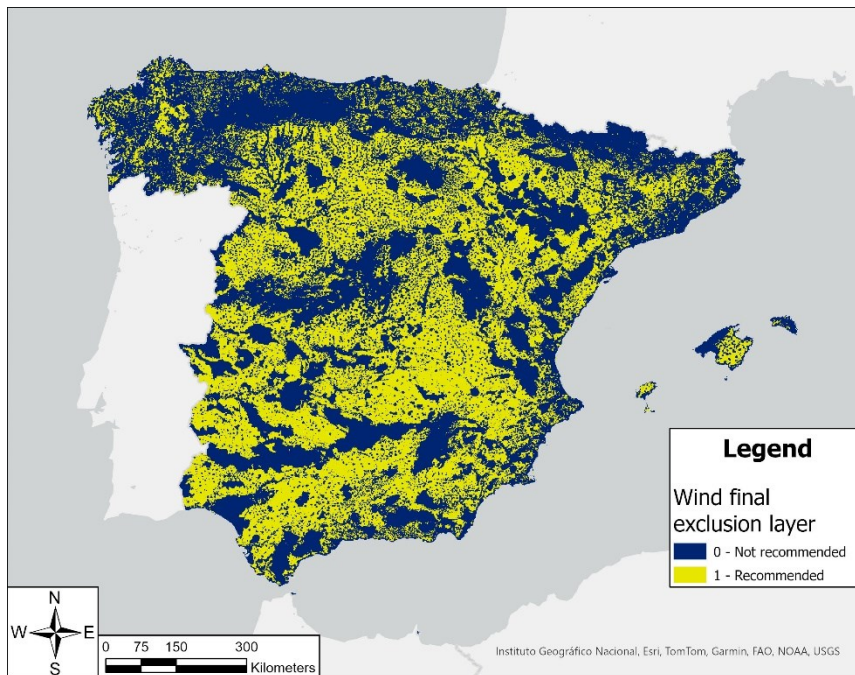
Appendix 4. Solar final ponderation layer resulting from the analysis presented in Chapter 2 (own elaboration).

Appendix 5. Wind final ponderation layer resulting from the analysis presented in Chapter 2 (own elaboration).

Appendix 6. Table for the calculation of K (section 3.1) for a tilt angle of 30° and for different latitudes and months of the year (CIEMAT).

Table for Tilt β = 30°							
Month	*LAT=37°*	*LAT=38°*	*LAT=39°*	*LAT=40°*	*LAT=41°*	*LAT=42°*	*LAT=43°*
January	1.35	1.37	1.39	1.41	1.42	1.44	1.46
February	1.25	1.26	1.27	1.29	1.30	1.32	1.33
March	1.14	1.15	1.16	1.17	1.18	1.19	1.20
April	1.06	1.07	1.07	1.08	1.09	1.09	1.10
May	0.98	1.03	1.03	1.03	1.04	1.04	1.05
June	0.96	1.02	1.02	1.02	1.03	1.03	1.03
July	0.98	1.03	1.03	1.04	1.04	1.05	1.05
August	1.06	1.08	1.08	1.09	1.10	1.10	1.11
September	1.17	1.19	1.20	1.21	1.22	1.24	1.25
October	1.30	1.36	1.37	1.39	1.41	1.44	1.46
November	1.38	1.49	1.51	1.54	1.57	1.59	1.62
December	1.37	1.48	1.50	1.52	1.54	1.57	1.59

References

[1] IEA, "Renewables 2023," International Energy Agency, Paris, 2024.

[2] IRENA, "Tracking COP28 OUTCOMES," International Renewable Energy Agency, Abu Dhabi, 2024.

[3] EI, "Statistical Review of World Energy," Energy Institute, London, 2023.

[4] WindEurope, "Renewable Hybrid Power Plants," WindEurope, Brussels, 2019.

[5] M. J. Ferres González, R. P. Campaña and F. J. Domínguez Bravo, "ELABORACIÓN DEL MAPA DE HIBRIDACIÓN DE ENERGÍA EÓLICA Y SOLAR EN ESPAÑA," Madrid, Spain, 2021.

[6] M. Shao, "A review of multi-criteria decision making applications for renewable energy site selection," *Renewable Energy,* no. 157, pp. 377-403 , 2020.

[7] X. Costoya, "Combining offshore wind and solar photovoltaic energy to stabilize energy supply under climate change scenarios: A case study on the western Iberian Peninsula," *Renewable and Sustainable Energy Reviews,* no. 157, p. 112037, 2022.

[8] L. Arribas, "Review of Data and Data Sources for the Assessment of the Potential of Utility-Scale HybridWind–Solar PV Power Plants Deployment, under a Microgrid Scope," *Energies 2021, 14, 7434,* no. 14, p. 7434, 2021.

[9] L. Petersen, "Vestas Power Plant Solutions Integrating Wind, Solar PV and Energy Storage," in *3rd International Hybrid Power Systems Workshop*, 2018.

[10] Q. Hassan, "A review of hybrid renewable energy systems: Solar and wind-powered solutions: Challenges, opportunities, and policy implications," *Results in Engineering,* no. 20, p. 101621, 2023.

[11] D. Kaushik, "Enhanced Features of Wind-Based Hybrid Power Plants," in *4th International Hybrid Power Systems Workshop*, Crete, Greece, 2019.

[12] R. Antunes Campos, "The complementary nature between wind and photovoltaic generation in Brazil and the role of energy storage in utility-scale hybrid power plants," *Energy Conversion and Management* , no. 221, p. 113160, 2020.

[13] WindEurope, "Database forWind + Storage Co-located Projects.," [Online]. Available: https://windeurope.org/about-wind/database-for-wind-and-storage-colocated-projects/. [Accessed 28 April 2024].

[14] Iberdrola, "Iberdrola completes construction of Spain's first hybrid wind-solar plant," 27 September 2023. [Online]. Available: https://www.iberdrola.com/press-room/news/detail/iberdrola-completes-construction-spain-first-hybrid-wind-solar-plant. [Accessed 5 May 2024].

[15] SolarDuck, "SolarDuck, Green Arrow Capital and New Developments s.r.l. sign collaboration agreement for a grid-scale offshore hybrid wind-solar project in Italy," 29 February 2024. [Online]. Available: https://solarduck.tech/solarduck-green-arrow-capital-and-new-developments-s-r-l-sign-collaboration-agreement-for-a-grid-scale-offshore-hybrid-wind-solar-project-in-italy/. [Accessed 29 April 2024].

[16] Adana Green Energy, "Adani Green Becomes Worlds Largest Wind Solar Hybrid Power Developer," 5 Decemebr 2022. [Online]. Available: https://www.adanigreenenergy.com/newsroom/media-releases/Adani-Green-Becomes-Worlds-Largest-Wind-Solar-Hybrid-Power-Developer. [Accessed 31 May 2024].

[17] Adani Green Energy , "Bitta, Gujarat," Adani Green Energy, [Online]. Available: https://www.adanipower.com/en/operational-power-plants/bitta-gujarat. [Accessed 21 04 2024].

[18] IEA, "National Wind-Solar Hybrid Policy," 12 May 2021. [Online]. Available: https://www.iea.org/policies/6485-national-wind-solar-hybrid-policy. [Accessed 3 May 2024].

[19] Asociación Empresarial Eólica (AEE), "FOMENTO DE LA HIBRIDACIÓN EÓLICA: PROPUESTA REGULATORIA," Madrid, 2019.

[20] J. D. Bravo, "Breve Introducción a la Cartografía," Madrid, 2000.

[21] S. Saraswat, "MCDM and GIS based modelling technique for assessment of solar and wind farm locations in India," *Renewable Energy,* no. 169, pp. 865-884, 2021.

[22] S. Ali, "GIS based site suitability assessment for wind and solar farms in Songkhla, Thailand," *Renewable Energy,* no. 132, pp. 1360-1372, 2019.

[23] K. Aghaloo, "Optimal site selection for the solar-wind hybrid renewable energy systems in Bangladesh using an integrated GIS-based BWM-fuzzy logic method," *Energy Conversion and Management,* no. 283, p. 116899, 2023.

[24] J. C. Osorio-Aravena, "How much solar PV, wind and biomass energy could be implemented in short-term? A multi-criteria GIS-based approach applied to the province of Jaén, Spain," *Journal of Cleaner Production,* no. 366, p. 132920, 2022.

[25] M. A. Raza, "Site suitability for solar and wind energy in developing countries using combination of GIS- AHP; a case study of Pakistan," *Renewable Energy,* no. 206, p. 180–191, 2023.

[26] S. E. A. Sassi Rekik, "Optimal wind-solar site selection using a GIS-AHP based approach: A case of Tunisia," *Energy Conversion and Management,* vol. X, no. 18, p. 100355, 2023.

[27] N. Y. Aydin, "GIS-Based site selection approach for wind and solar energy systems: a case study from Western Turkey," Ankara, Turkey, 2009.

[28] D. Latinopoulos, "A GIS-based multi-criteria evaluation for wind farm site selection. A regional scale application in Greece," *Renewable Energy,* no. 78, pp. 550 - 560, 2015.

[29] A. Sekeroglu and D. Erol, "Site selection modeling of hybrid renewable energy facilities using suitability index in spatial planning," *Renewable Energy,* no. 219, p. 119458, 2023.

[30] M. S. Sachit, "A novel GeoAI-based multidisciplinary model for SpatioTemporal Decision-Making of utility-scale wind–solar installations: To promote green

infrastructure in Iraq," *The Egyptian Journal of Remote Sensing and Space Sciences,* no. 27, pp. 120 - 136, 2024.

[31] R. Tarife, "Integrated GIS and Fuzzy-AHP Framework for Suitability Analysis of Hybrid Renewable Energy Systems: A Case in Southern Philippines," *Sustainability,* no. 15, p. 2372, 2023.

[32] Instituto Geográfico Nacional (IGN), "Datos geográficos y toponimia," 1 January 2011. [Online]. Available: https://www.ign.es/web/ign/portal/ane-datos-geograficos/-/datos-geograficos/datosPoblacion?tipoBusqueda=CCAA. [Accessed 5 May 2024].

[33] L. Qiu, "Systematic potential analysis on renewable energy centralized co-development at high altitude: A case study in Qinghai-Tibet plateau," *Energy Conversion and Management,* no. 267, p. 115879, 2022.

[34] The Ministry for the Ecological Transition and the Demographic Challenge (MITECO), "ZONIFICACIÓN AMBIENTAL PARA LA IMPLANTACIÓN DE ENERGÍAS RENOVABLES: EÓLICA Y FOTOVOLTAICA," Madrid, Spain, 2020.

[35] L. A. Zadeh, "Fuzzy sets," *INFORMATION AND CONTROL,* no. 8, pp. 338-353, 1965.

[36] S. M. Lewis, "A fuzzy logic-based spatial suitability model for drought-tolerant switchgrass in the United States," *Computers and Electronics in Agriculture,* no. 103, pp. 39-47, 2014.

[37] A. R. Silva and A. Estanqueiro, "From Wind to Hybrid: A Contribution to the Optimal Design of Utility-Scale Hybrid Power Plants," *Energies,* no. 15, p. 2560, 2022.

[38] A. M. Khalid, "Performance ratio – Crucial parameter for grid connected PV plants," *Renewable and Sustainable Energy Reviews,* 2016.

[39] E. García-Bustamante, "A Comparison of Methodologies for Monthly Wind Energy Estimation," *Wind Energy. 2009; 12:640–659,* no. 12, pp. 640-659, 2009.

[40] Vestas Wind Systems, *EnVentus platform,* Vestas, 2023.

[41] O. E. Olabode, "Hybrid power systems for off-grid locations: A comprehensive review of design technologies, applications and future trends," *Scientific African,* no. 13, p. e00884, 2021.

[42] K. Anounea, "Sizing methods and optimization techniques for PV-wind based hybrid renewable energy system: A review," *Renewable and Sustainable Energy Reviews,* no. 93, pp. 652-673, 2018.

[43] L. Arribas, "Dimensionamento de una instalación eólico/fotovoltaica aislada (I)," *Era Solar,* no. 136, pp. 102-115, 2007.

[44] L. Arribas, "Dimensionamento de una instalación eólico/fotovoltaica aislada (II)," *Era Solar,* no. 137, pp. 88-97, 2007.

[45] P. Enevoldsen and M. Jacobson, "Data investigation of installed and output power densities of onshore and offshore wind turbines world wide," *Energy for Sustainable Development,* no. 60, pp. 40-51, 2021.

[46] International Renewable Energy Agency (IRENA), "Renewable Technology Innovation Indicators: Mapping progress in costs, patents and standards," Abu Dhabi, United Arab Emirates, 2022.

[47] Internation Energy Agency (IEA), "Electricity Market Report 2023," Paris, France, 2023.

[48] National Renewable Energy Laboratory, "2021 Cost of Wind Energy Review," NREL, 2022.

[49] National Renewable Energy Laboratory, "U.S. Solar Photovoltaic System and Energy Storage Cost Benchmarks, With Minimum Sustainable Price Analysis: Q1 2022," NREL, 2022.

[50] Pexapark, "European Market Outlook 2024," Schlieren, Switzerland, 2023.

[51] T. L. Saaty, "How to make a decision: The analytic hierarchy process," *European Journal of Operational Research,* no. 48, pp. 9 - 26, 1990.

[52] CIEMAT, "Participación del CIEMAT en la elaboración de mapas solares y eólicos para el Banco Mundial," 2013. [Online]. Available: https://www.ciemat.es/cargarAplicacionNoticias.do?identificador=331 https://www.ceta-ciemat.es/images/ficheros/fichas-proyectos/ficha_adrase_F.pdf .

[53] W. C. Skamarock, "A Description of the Advanced Research WRF Model Version 4," National Center for Atmospheric Research (NCAR), Boulder, USA, 2021.

[54] European Enviroment Agency (EEA), , "CORINE Land Cover," [Online]. Available: https://land.copernicus.eu/en/products/corine-land-cover?tab=main. [Accessed 8 May 2024].

Acknowledgments

I would like to express my gratitude to my supervisor, Prof.ssa Anna Stoppato, for agreeing to oversee this interesting thesis work, for her thoughtful advice and feedback, and for the exceptional availability shown during these months.

I would also like to extend my heartfelt thanks to my traineeship tutors, Dr. Javier Dominguez and Luis Arribas, for their guidance on every occasion and for their constant encouragement. Their commitment and willingness to share their knowledge and experience have been pivotal in shaping this work.

Finally, a special thank you goes to everyone who has supported and contributed to this thesis at CIEMAT. The privilege of completing my thesis in such a professional and welcoming environment has been an invaluable experience.